Alternative Sulfur Acquisition Pathways in *Neisseria gonorrhoeae*

A thesis

submitted partial fulfilment

of the requirements for the degree

of

Master of Science (Research) in Cellular and Molecular Biology

at

The University of Waikato

by

Stacy Lyn van Niekerk

THE UNIVERSITY OF
WAIKATO
Te Whare Wānanga o Waikato

2021

Abstract

Neisseria gonorrhoeae is an obligate human pathogen responsible for the sexually transmitted infection, gonorrhoea. Its success as a pathogen is partly due to robust defence mechanisms that provide protection against oxidative stress encountered during infection. Reduced sulfur compounds such as glutathione, cysteine and methionine are integral to this response and pathogenic growth.

Due to a large genomic deletion and pseudogenes, *N. gonorrhoeae* is incapable of sulfur acquisition via traditional routes and therefore cannot grow when sulfate is the sole sulfur source. However, *N. gonorrhoeae* can grow in the presence of thiosulfate but lacks the ability to reduce thiosulfate via the conventional thiosulfate reduction pathway. This raises questions of how *N. gonorrhoeae* acquires sulfur for cysteine biosynthesis?

We have identified two sulfurtransferase enzymes (Str and PspE) in *N. gonorrhoeae* that we hypothesise provide sulfur in the form needed for cysteine synthesis. We show these enzymes have thiosulfate-thiol sulfurtransferase activity and, importantly, produce sulfide that could be utilised for cysteine biosynthesis. Furthermore, we demonstrate that Str is a promiscuous enzyme with respect to thiol acceptor substrates and, intriguingly, is capable of cyanide detoxification. Our *N. gonorrhoeae* sulfurtransferase deletion strain has a reduced ability to grow when thiosulfate is the only available sulfur source, supporting our hypothesis that Str utilises exogenous inorganic thiosulfate. However, due to functional redundancy provided by the presence of the second sulfurtransferase, PspE, construction of a double knockout strain is essential in understanding the full effect of these enzymes in relation to pathogenicity.

Our proposed energetically favourable pathway of thiosulfate reduction via sulfurtransferase enzymes could be pivotal in advancing our understanding of how pathogens fulfil their sulfur requirements. However, much is to be elucidated regarding the role of these ubiquitous enzymes in bacterial pathogens. Herein, this thesis offers insight into the versatility, function, and formal mechanisms of sulfurtransferases within *N. gonorrhoeae.*

Acknowledgments

First and foremost, I would like to express my immense gratitude to my supervisor, Dr Joanna Hicks. Your guidance and wisdom has been invaluable throughout this journey. Thank you for your enthusiasm, it has encouraged and motivated me. I am incredibly grateful to you for the countless opportunities, it is so appreciated.

I would like to extend my gratitude to the entire staff and students of the Proteins and Microbes lab, it takes a village, and you are certainly mine. Thank you for your encouragement and continued willingness to help. You have enriched this experience for me.

To my parents, you have fed, financed, and supported me from the very beginning of my academic career. I am so appreciative of all you have done and continue to do for me. I would like to share this accomplishment with you. To my siblings, thank you for listening and offering me emotional and mental support.

To an amazing network of friends, you have been an overwhelming source of optimism and comfort. My sincerest thanks to Courtney Cook and Hannah Newton, words cannot describe my gratitude for your unwavering support.

Last, but by no means least, thank you to my partner in life, Joel Burgin, for the pep talks and perspective. You have been there through my most trying times, and for that, I will be forever thankful.

Table of Contents

List of Figures

List of Tables

List of Equations

Abbreviations

ABC	ATP-binding cassette
Abs	Absorbance
AMR	Antimicrobial resistance
APS	Adenosine-5’-phosphate
APS	Ammonium persulfate
Arg	Arginine
Asp	Aspartate
ATP	Adenosine 5’-triphosphate
BFS	Bovine fetal serum
bp	Base pair
CDC	US Centers for Disease Control and Prevention
CN	Cyanide
Cys	Cysteine
DNA	Deoxyribonucleic acid
EDTA	Ethylene diamine tetra-acetic acid (disodium salt)
FPLC	Fast performance liquid chromatography
GCB	Giolitti and Cantoni broth
GlpE	Glycerol 3-phsphate protein E
GSH	Glutathione
GSSG	Glutathione disulfide
GSSH	Glutathione persulfide
HGT	Horizontal gene transfer
His	Histidine
His-tag	Poly-histidine tag
HMCYS	Homocysteine
IMAC	Immobilised metal affinity chromatography
IPTG	Isopropyl-β-d-1-thiogalactopyranoside
k_{cat}	Enzyme rate constant
KCN	Potassium Cyanide

kDa	kilo Dalton
K_M	Michaelis constant
KO	Knockout
LB	Luria Bertani
MFS	Major facilitator superfamily
min	Minutes
MPD	2-Methyl-2,4-pentanediol
MQ	MilliQ ultrapure water
MST	3-mercaptopyruvate sulfurtransferase
NADPH	Nicotinamide adenine dinucleotide phosphate
OAS	*O*-acetylserine
OASS	*O*-acetylserine sulfhydrolyase
OD	Optical density
PAGE	Polyacrylamide gel electrophoresis
PAP	Phosphoadenosylphosphate
PAPS	Phosphoadenosylphosphosulfate
PCR	Polymerase chain reaction
PDB	Protein data bank
PEG	Polyethylene glycol
PspE	Phage shoch protein E
ROS	Reactive oxygen species
s	Second(s)
SAM	*S*-adenosyl methionine
Sbp	Sulfate binding protein
SDS	Sodium dodecyl sulfate
SEC	Size exclusion chromatography
SSCS	*S*-sulfo-*L*-cysteine
ST	Sulfurtransferase
STI	Sexually transmitted infection
Str	Sulfurtransferase in *Neisseria gonorrhoeae*
TEMED	Tetramethylethylenediamine
TST	Thiosulfate sulfurtransferase
TTST	Thiosulfate-thiol sulfurtransferase

US	United States
V	Voltage
v/v	Volume per volume
v/w	Volume per weight
V_{max}	Theoretical maximum reaction rate
WHO	World Health Organisation
WT	Wild type

Chapter One

Introduction

1.1 Introduction

Neisseria gonorrhoeae is the causative agent of the stigmatized sexually transmitted infection (STI), gonorrhoea. Gonorrhoea remains a major public health, social and financial burden with an annual global incidence of 87 million cases (World Health Organisation, WHO), of which marginalised population disproportionately bear the burden (Kirkcaldy et al., 2019). Within New Zealand, the incidence of gonorrhoea infection has alarmingly been on the rise, with the number of reported cases in 2019 doubling those reported in 2014 (Ministry of Health, NZ). *N. gonorrhoeae* has demonstrated an extraordinary ability to develop resistance to antimicrobial treatments since their introduction in the 1930's, with the first case of untreatable gonorrhoea being identified in 2018. As such, the threat of global untreatable strains seems imminent, calling for the scientific community to explore novel therapeutic avenues.

Cysteine biosynthesis and sulfate assimilation pathways are absent in mammals and accordingly have gained considerable interest as a potential therapeutic strategy for pathogenic bacteria, such as *Salmonella typhimurium* and *Mycobacterium tuberculosis* (Spyrakis et al., 2013; Benoni et al., 2016; Campanini et al., 2015; Schnell, Sriram, & Schneider, 2015). However, the sulfate assimilation pathway is absent in *N. gonorrhoeae* and the cysteine biosynthesis pathway is currently uncharacterised. Therefore, much is to be elucidated to determine the suitability of the proposed therapeutic strategy to combat *N. gonorrhoeae* infection. How *N. gonorrhoeae* acquires essential sulfur required for the synthesis of cysteine is not understood. This research herein investigates novel sulfurtransferase enzymes that we hypothesise to be involved in an alternative sulfur acquisition pathway within *N. gonorrhoeae*.

1.2 Gonorrhoea: disease and treatment

N. gonorrhoeae (also called gonococcus) is a Gram-negative, diplococci bacterium that predominantly infects the mucosa of the human urogenital tract. Clinical

manifestations of initial gonococcal infections in the lower-urogenital tract are more identifiable in men compared to women where infection symptoms appear non-specific often resulting in mistaken diagnosis. Problematically, gonococcal infection is frequently asymptomatic in both sexes although the prevailing dogma points to asymptomatic infection being disproportionately more common in women (Edwards & Apicella, 2004; Walker & Sweet, 2011). This discrepancy is suggested to reflect the anatomical differences of the urogenital tract in men and women (Quillin & Seifert, 2018). Diagnosis of asymptomatic infection is challenging and heavily reliant on regional screening practices which has implications for our epidemiological understanding of gonococcal incidence, prevalence, and transmission. Asymptomatic infection has further ramifications in pathogenic transmission, long-term health complications, and facilitating the emergence of antibiotic resistant strains. In 45% of infected women, gonococcal infection ascends into the upper-urogenital tract (Edwards & Apicella, 2004) as a result of untreated, inadequately treated, or undetected infection. Long term gonococcal infection has severe implications for reproductive health causing a multitude of reproductive, maternal and new-born complications including chronic pelvic pain, ectopic pregnancy, pelvic inflammatory disease, tubal factor infertility, spontaneous abortion, and neonatal blindness, to name a few. In men, long term infection has less severe repercussions however can lead to reduced fertility. In rare cases, dissemination can occur potentially giving rise to endocarditis, infectious arthritis (Masi & Eisenstein, 1981) and meningitis. Albeit less frequently, but also problematically, the gonococcus is also capable of infecting (typically asymptomatically) other exposed anatomic mucosal sites such as the rectum, pharynx and conjunctivae. Pharyngeal gonorrhoea is of particular concern as it is considered to play a major role in antimicrobial resistance (AMR) via horizontal gene transfer (HGT) with other commensal *Neisseria* species (Adamson & Klausner, 2021).

N. gonorrhoeae has developed resistance to all frontline antibiotics introduced for its treatment since the 1930s including, in chronological order, sulfonamides, penicillin, tetracyclines, aminoglycosides, fluoroquinolones, macrolides (azithromycin) and cephalosporins (ceftriaxone and cefixime). Resistance to treatment occurs rapidly, with resistant strains replacing the sensitive bacterial

populations within two decades (Suay-Garcia & Perez-Gracia, 2017). Following the failure of monotherapy treatments, dual therapy approaches (most commonly azithromycin and ceftriaxone) have more recently been implemented as a response to resistance. The first instances of resistance against this approach emerged in the United Kingdom and Australia early in 2018 giving rise to super-resistant strains. *N. gonorrhoeae* is listed among the top five AMR threats by the United States (US) Centers for Disease Control and Prevention (CDC) and is classified as a "Priority 2" pathogen by the WHO. The CDC currently estimates that approximately half of all new infections are drug resistant in the US. Consequently, the morbidity of gonococcal infection is increasing exponentially (WHO).

Undisputedly, antimicrobial *N. gonorrhoeae* infection is a global crisis and the urgency for novel therapeutic intervention to overcome AMR is evident. Unravelling key pathways essential for pathogenicity, growth and persistence of *N. gonorrhoeae* is crucial for identifying suitable therapeutic targets. Sulfur acquisition and metabolism is important for bacterial growth, pathogenesis, and the synthesis of reduced sulfur compounds that provide protection against oxidative stress inflicted upon the pathogen during infection. Elucidating how *N. gonorrhoeae* acquires sulfur is fundamental in furthering our understanding of how pathogens fulfil their sulfur requirements and how sulfur compounds are involved in pathogenesis and infection.

1.3 Cysteine and defence against oxidative stress

The generation of damaging reactive oxygen species (ROS), such as hydrogen peroxide (H_2O_2), oxide anions (O_2^-) and hydroxy radicals ($^{\cdot}OH$), is an inevitable part of life under aerobic conditions. ROS induced damage interferes with all cellular components including amino acid modifications via oxidation of thiol groups, damage to cell membranes, and DNA chain breaks. Their toxic effects therefore require crucial protection systems even under normal conditions, and mitigation of ROS is an ongoing challenge inflicted upon all organisms. Oxidative stress describes the situation where the generation or the presence of ROS is imbalanced to the rate of their detoxification. The human immune response attempts to combat pathogenic infection via forcing this difference. This is achieved by robust production and high quantity release of ROS by neutrophils, known as

'the respiratory burst' (El-Benna et al., 2016). One of the main challenges for pathogenic species is the ability to survive in the face of oxidative stress encountered during infection.

Cysteine plays a vital role in making environmental sulfur available to cells and is incorporated into important reduced sulfur compounds such as glutathione (GSH) and thioredoxin. In microorganisms, these compounds are components of crucial reducing systems that provide protection against oxidative stress. Glutathione is a low-molecular-weight, tripeptide (L-γ-glutamyl-L-cysteinyl-glycine) and is considered to be the first line of defence against oxidative stress. Glutathione functions to restore oxidised macromolecules via hydrogen donation and is a chemical scavenger of radicals. These actions result in the oxidation of glutathione, forming glutathione disulfide (GSSG). GSSG is, in turn converted back to glutathione via glutathione oxidoreductase (Gor) that works to restore the pool of reduced glutathione. Glutathione is typically present within bacteria in millimolar concentrations, although are reportedly much higher in *N. gonorrhoeae* (5 mM in *Escherichia coli* versus >15 mM in *N. gonorrhoeae*) (Seib et al., 2006), indicative that glutathione constitutes a powerful redox system. In line with this, Gor and glutathione synthase, a key enzyme in glutathione synthesis, are both upregulated within *N. gonorrhoeae* after transient exposure to hydrogen peroxide (Seib et al., 2006). Given that *N. gonorrhoeae* cannot acquire exogenous glutathione due to the absence of glutathione transporters (Seib et al., 2006), synthesis and maintenance of such high glutathione levels is contingent upon cysteine biosynthetic pathways (Hicks and Mullholland., 2018).

1.4 Nutrient sulfur acquisition strategies for cysteine synthesis in bacterial pathogens

In addition to its role in oxidative stress, cysteine acts as a precursor to many essential sulfur-containing biomolecules. The host-pathogen interface is abundant in both organic and inorganic sulfur containing compounds that can be utilised for the acquisition, formation, or synthesis of cysteine. In short, inorganic sulfur molecules, sulfate and thiosulfate, are reduced to sulfur in the form required for *de novo* cysteine biosynthesis (discussed in section 1.3.1) while organic sulfur molecules are generally processed into cysteine, providing pathogens with an

alternative source of sulfur (Figure 1.1). Pathogenic bacteria are capable of coordinating strategies utilising both inorganic sulfur and organic sulfur sources to satisfy cysteine requirements, as demonstrated in *Escherichia coli* and *S. typhimurium* where organic sulfur molecules appear to have a regulatory effect on inorganic sulfate assimilation and cysteine biosynthesis pathways (Ostrowski & Kredich, 1990; Guedon & Martin-Verstraete 2006).

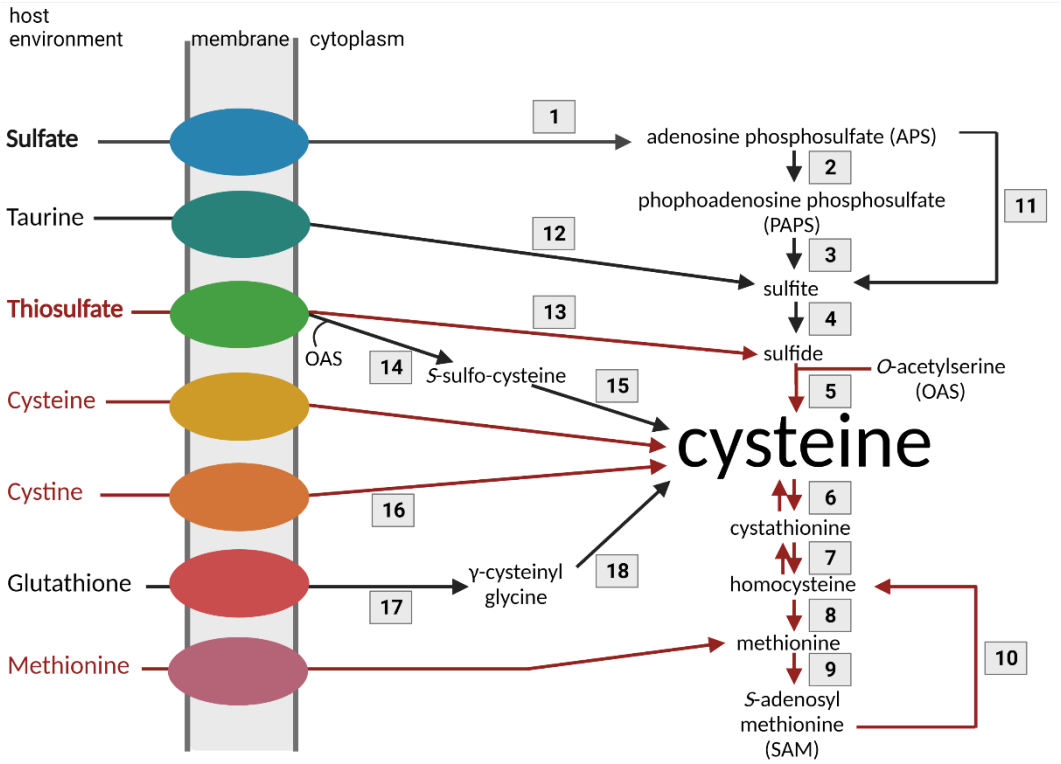

Figure 1.1: Overview of nutrient sulfur acquisition strategies employed by bacterial pathogens and their relevance to cysteine production. Sulfur source in bold are inorganic sulfur sources, the remaining are organic sulfur sources. Pathways in red are present within *N. gonorrhoeae*, those in black are absent. 1: ATP sulfurylase, 2: APS kinase, 3: PAPS Reductase, 4: Sulfite Reductase, 5: *O*-acetylserine sulfhydrolyase-A, 6: Cystathionine-gamma-synthase, 7: Cystathionine beta synthase, 8: Homocysteine S-methyltransferase, 9: *S*-adenosylmethionine synthetase, 10: SAM-dependant methylation forms *S*-adenosyl-homocysteine (SAH) which is degraded to homocysteine via SAH hydrolase, 11: APS reductase, 12: α-ketoglutarate-dependent dioxygenase, 13: thiosulfate-thiol sulfurtransferase, 14: *O*-acetylserine sulfhydrolyase-B, 15: Glutaredoxin or glutaredoxin-like proteins, 16: Unknown reductase that reduces the disulfide bond in cystine, 17: γ-glutamyl-transpeptidase, 18: Dipeptidase. Figure is adapted from Lensmire & Hammer, 2019.

Organic sulfur molecules such as cysteine, cystine, methionine, glutathione, and taurine are abundantly present within the host plasma and serum, although to a lesser extent than inorganic sulfur molecules (Lensmire & Hammer, 2019). Acquisition of these sulfur sources is advantageous as they typically yield cysteine more efficiently than inorganic sulfur sources, requiring fewer enzymes and having a lower cellular energetic cost. Exogeneous cysteine and cystine offer the most effective route of obtaining cysteine, with cysteine only requiring import into the microbial cell and cystine requiring one additional enzymatic reaction to reduce the disulfide bond thereby releasing two cysteine residues (Figure 1.1, # 16). Glutathione liberates cysteine efficiently by breaking the amino bonds in two sequential enzymatic reactions (Figure 1.1, #17 and 18), while methionine comparatively requires a more extensive pathway to yield cysteine which initially requires the transformation of methionine to homocysteine via *S*-adenosyl methionine (SAM) (Figure 1.1, #10). Homocysteine is subsequently converted to cysteine via the reverse transsulfuration pathway (Figure 1.1 #6 and 7). In contrast, taurine acts in a similar service to inorganic sulfur molecules as the product of taurine processing (Figure 1: #12), sulfite, is a substrate for sulfite reductase, the second to last enzyme in the sulfate assimilation pathway.

To establish the efficacy of targeting cysteine biosynthesis as a therapeutic intervention, the relative utility of inorganic versus organic sulfur sources in bacterial pathogenicity, growth and survival needs to be considered. Numerous studies demonstrate that a single organic sulfur source is sufficient to support pathogenic growth *in vitro* (growth in defined media), for example methionine can support growth of *Klebsiella aerogenes, M. tuberculosis,* and *Pseudomonas aeruginosa* (Guédon & Martin-Verstraete, 2007)*;* taurine can support the growth of *Enterobacteriaceae* such as *E. coli* (Cowie, Bolton and Sands, 1951); glutathione can support the growth of *Staphylococcus aureus*, *Clostridium difficile, Bordetella pertussis*, *Neisseria meningitidis*, *E. coli*, *Salmonella enterica*, *Haemophilus influenzae*, and *Streptococcus mutans* (Lithgow et al., 2004; Dubois et al., 2016; Stenson, Patton, & Weiss, 2002; Takahashi, Hirose, & Watanabe, 2004; Suzuki et al., 2005; Wang et al., 2017; Vergauwen et al., 2010; Vergauwen et al., 2013); and cysteine/cystine can support the growth of *S. aureus*, *Campylobacter jejuni, E. coli*, *S. enterica*, and *S. mutans* (Lithgow et al., 2020; Guédon & Martin-Verstraete, 2007;

Vorwerk et al., 2014; Kim et al., 2012). However, the *in vivo* (animal model of infection) evidence regarding the utilisation of the respective sulfur sources for these pathogens during infection is lacking, leaving the significance of these sulfur sources in pathogenesis and virulence ambiguous. Few studies have investigated the *in vivo* utility of exogenous glutathione during infection in mouse models. Mutation of γ-glutamyl transpeptidase (Figure 1.1 #17), the first enzyme involved in liberating cysteine from glutathione, in *Francisella tularensis* results in growth and virulence defects, establishing glutathione as an important sulfur source for this pathogen during infection (Alkuder et al., 2009). Moreover, mutation of the glutathione transporter *Streptococcus pneumoniae*, increases sensitive to oxidative stress and demonstrates an attenuated phenotype during infection (Potter, Trappetti & Paton, 2012), reiterating the importance of glutathione for pathogenic survival within the harsh oxidative environment of the host.

N. gonorrhoeae possess ATP-binding cassette (ABC) transporters that permit the import of cysteine, cystine and methionine (Bulut et al., 2012; Semchenko, Day & Seib, 2016), and therefore can utilise these organic sulfur molecules to obtain cysteine. *N. gonorrhoeae* is incapable of scavenging cysteine from glutathione due to the absence of glutathione transporter systems and the γ-glutamyl transpeptidase enzyme. The absence of glutathione transporter proteins is of particular interest, considering *N. gonorrhoeae's* elevated glutathione concentrations (>15 mM) that provide protection against oxidative stress (as previously outlined in section 1.3). As *N. gonorrhoeae* cannot transport glutathione, the establishment of its high glutathione pool and increased glutathione synthesis during oxidative stress (Seib et al., 2006) is therefore reliant on cysteine as a precursor. In turn, the demand for sulfur must also be increased to support increased cysteine requirements as it is unconvincing that such cysteine requirement is met by exogenous organic sulfur sources alone, given that host serum concentrations for cysteine, methionine, and cystine collectively, are reportedly 136.2 µM (Lensmire & Hammer, 2019). In support of this, cysteine biosynthesis appears essential even in the presence of cysteine in growth media (Remmele et al., 2014). In addition, expression of the transcription factor CysB (a negative regulator of sulfur assimilation and cysteine biosynthesis) is downregulated upon infection of the urogenital tract in woman (McClure et al., 2015) suggesting that cysteine

biosynthesis is active upon pathogenic infection. This finding further highlights the importance of cysteine biosynthesis in the pathogenicity of *N. gonorrhoeae* and, by virtue, the importance of inorganic sulfur assimilation pathways.

1.4.1 Inorganic sulfur assimilation pathways

Pathogenic bacteria have evolved sophisticated mechanisms to acquire essential elements within the host environment. However, compared to the acquisition of other trace elements such as iron, there remains large gaps in our knowledge of how pathogens fulfil their sulfur requirements.

Sulfur is an essential element to all organisms. With a dynamic range of oxidation states (+6 to -2), the redox activity of sulfur supports many aspects of prokaryotic and eukaryotic life. Importantly, sulfur is incorporated into a multitude of essential biological molecules including, but not limited to, co-enzyme A, glutathione, biotin, and mucins. In addition, sulfur is an integral component of proteinogenic amino acids, cysteine, and methionine, and the non-proteinogenic amino acids cystine, homocysteine and taurine. Within cysteine, sulfur plays a crucial role in the formation of disulfide bonds. Disulfide bonds are highly conserved throughout protein evolution due their unique properties and functions in protein structure, regulation of protein activity and catalysis. In contrast to mammals, who metabolise essential methionine for cysteine production, bacteria can acquire sulfide for *de novo* cysteine and methionine synthesis via the reduction of inorganic sulfur sources, thiosulfate and sulfate, obtained from within their environment. Acquisition of sulfur for use in *de novo* cysteine biosynthesis is not only important for pathogenic growth but also plays a crucial role in protection against host defences.

Currently, three pathways for sulfur acquisition for this purpose have been identified in prokaryotes. One pathway utilising sulfate and two pathways utilising thiosulfate; the CysM dependent pathway and, a more recently identified, CysM independent pathway. In all cases, inorganic sulfate assimilation is dependent on active transport of inorganic sulfur into the microbial cell, reduction of the inorganic sulfur source and incorporation into cysteine precursor, *O*-acetylserine (OAS).

The sulfate assimilation pathway is almost exclusively employed by bacteria for the synthesis of cysteine. This involves transport of sulfate into the cell, the successive reduction of sulfate to bisulfide and, finally, the addition of sulfide to an activated form of serine to form cysteine (Figure 1.2). Once imported into the cell, sulfate is activated by ATP sulfurylase (CysDN) to form adenosine-5'-phosphate (APS) and pyrophosphate, in an ATP-dependent reaction. Commonly, the next step in the pathway involves the phosphorylation of APS to form phosphoadenosylphosphosulfate (PAPS) catalysed by APS kinase (CysC) in an ATP dependant reaction. PAPS is then subsequently reduced to sulfite and phosphoadenosylphosphate (PAP) via PAPS reductase (CysH) in an NADPH dependant reaction. Within certain pathogenic bacteria, such as *N. meningitidis* and *M. tuberculosis,* APS is directly reduced to sulfite via a single enzyme, APS reductase (also named CysH) (Rusniok et al., 2009; Palde et al., 2016). In all sulfate assimilation pathways, sulfite is then reduced further to bisulfide by a multi-subunit enzyme sulfite reductase (CysJI), comprised of the two enzymes, CysJ and CysI. This complex operates via a complicated mechanism and is reliant on three NADPH molecules for the successful reduction of sulfite to bisulfide. Bisulfide can then be incorporated into cysteine precursor, *O*-acetylserine (OAS) (or *O*-acyl-L-homocysteine) to generate cysteine (or homocysteine) via the *O*-acetylserine sulfhydrolyase (OASS) enzyme, OASS-A (CysK).

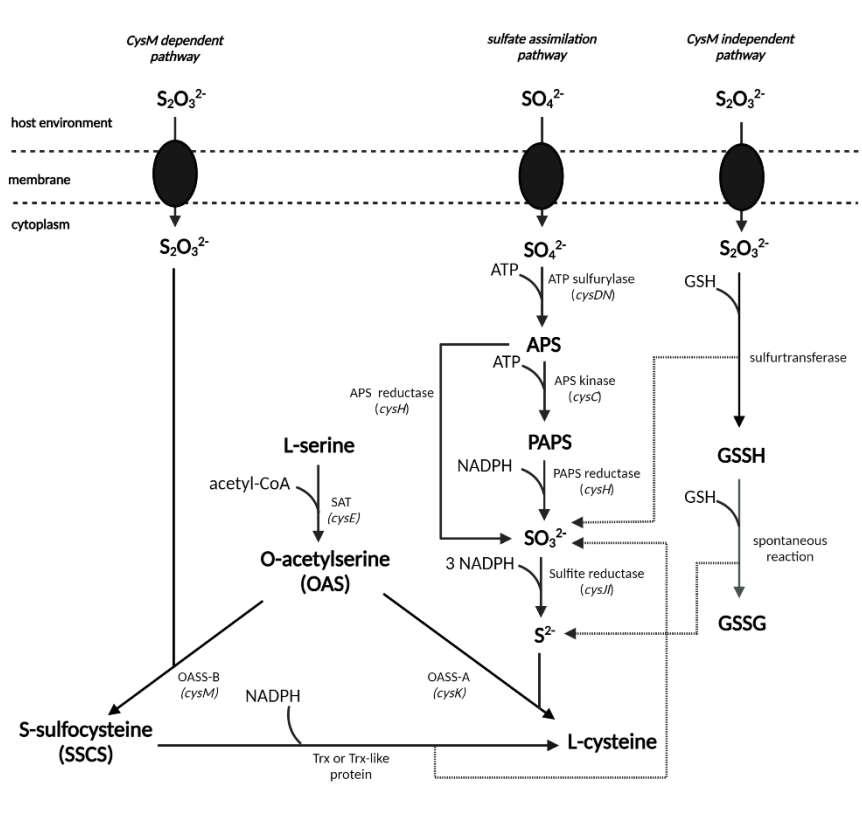

Figure 1.2: Overview of inorganic sulfate assimilation. Dotted lines represent the incorporation of products from one pathway into another. Black circles represent transporter proteins that permit the import of inorganic sulfur sources into the microbial cell.

Alternatively, bacteria can utilise thiosulfate in the pursuit of sulfur for cysteine biosynthesis. Conventionally, this is achieved via the CysM dependent pathway which operates independent of the sulfate assimilation pathway (Figure 1.2). This route relies on two sequential enzymatic reactions. Once imported into the cell, thiosulfate is incorporated into OAS to produce *S*-sulfo-*L*-cysteine (SSCS) via the OASS-B (CysM) enzyme. SSCS is then subsequently reduced to produce cysteine and sulfite via glutaredoxin or glutaredoxin-like proteins in an NADPH dependent reaction.

The recently identified thiosulfate assimilation pathway, named the CysM independent pathway (Figure 1.2), has thus far been characterised in two organisms, *E. coli* (Kawano et al., 2017) and *Saccharomyces cerevisiae* (Chen et al., 2018). The first step of this pathway relies on the reduction of thiosulfate to sulfite and sulfide via a sulfurtransferase enzyme. This is achieved by the enzymatically catalysed reaction of thiosulfate and glutathione to give glutathione persulfide

(GSSH) and sulfite, followed by a spontaneous reaction of GSSH with another glutathione molecule to form glutathione disulfide (GSSG), and bisulfide (Figure 1.2). The two products of the sulfurtransferase reaction, sulfite and sulfide can then feed into sulfate assimilation pathway as previously described (Kawano, Suzuki & Ohtsu., 2018).

The thiosulfate assimilation pathways are remarkably efficient compared to sulfate assimilation, demonstrating significant cellular energy conservations. This is consistent with the physiochemical properties of thiosulfate versus sulfate. Thiosulfate contains a sulfane sulfur, which exists in a more reduced state than the fully oxidised state of the sulfur atom in sulfate (Toohey and Cooper 2014). In support of such principle, prokaryotes such as *E. coli* and *S. cerevisiae* have demonstrated faster growth rates when cultured with thiosulfate as the sole sulfur source compared to when sulfate is the only available source of sulfur (Chen et al., 2018; Kawano, Suzuki & Ohtsu, 2018). Furthermore, the bioenergetic favourability of the thiosulfate pathway is even more dramatic when considering the enzyme requirement to complete these pathways, with the thiosulfate assimilation pathways requiring less than half the number of enzymes compared to sulfate assimilation.

Sulfate is a well-established *in vivo* source of sulfur for numerous pathogenic bacteria including *M. tuberculosis, Acinteobacter baumanii,* and *N. meningitidis* (Gebhardt et al., 2015; Ren et al., 2017; Pinto et al., 2013; Hatzios & Betozzi, 2011), yet other human pathogens such as *Listeria monocytogenes, S. aureus,* and *N. gonorrhoeae* are cysteine auxotrophs due to incomplete sulfate assimilation pathways (Xayarath et al., 2009; Lithgow et al., 2004; Hicks and Mullholland, 2018). However, sulfur requirements can be fulfilled by thiosulfate for *S. aureus* (Lithgow et al., 2004) and *N. gonorrhoeae* (Le Faou, 1984) in the absence of cysteine. *S. aureus* can utilise thiosulfate for synthesising cysteine via the CysM dependent pathway and mutation of this enzyme in *S. aureus* has been associated with increased sensitivity to oxidative stress, supportive of the role of cysteine in survival mechanisms and stress response. How *N. gonorrhoeae* utilises thiosulfate for cysteine synthesis is currently uncharacterised.

1.5 A hypothesised sulfur acquisition pathway in *N. gonorrhoeae*

The active transport of inorganic sulfur sources into the microbial cell is a prerequisite for all assimilation pathways. To investigate the sulfur acquisition pathway in *N. gonorrhoeae*, we must first consider this. Two main transporter systems belonging to the ABC superfamily and the major facilitator superfamily (MFS), have been identified in bacteria for active transport of inorganic sulfur sources. *Neisseria* species harbour the transport system belonging to the ABC transporters superfamily which is comprised of a periplasmic sulfate binding protein (Sbp), two permeases (CysU and CysW) and an ATP binding subunit (CysA) (Kertesz & Wietek, 2001). Sbp may also facilitate the import of thiosulfate, although with reduced efficiency. An alternative periplasmic binding protein, CysP, in lieu of Sbp, has been identified as being more efficient and specific for thiosulfate uptake. No CysP homologs have not been identified in *Neisseria* species, and as such the Sbp ABC transporters are hypothesised to be the only transport system for sulfate and thiosulfate in *Neisseria* species (Hicks & Mullholland, 2018).

N. gonorrhoeae is the only obligate human pathogen among the *Neisseria* species and, in contrast to other *Neisseria* species, demonstrates an inability to grow on sulfate as the sole source of sulfur (Le Faou, 1984). Consistent with this, genetic analysis of the *N. gonorrhoeae* genome reveals a 3.5 kb genomic deletion between the CysG and CysN genes, causing both genes to be truncated and eliminating the CysD and CysH genes (Hicks and Mullholland., 2018, Rusniok et al., 2009), as seen in Figure 1.3. Additionally, the CysJI genes are pseudogenes due to premature stop codons present in their coding sequences (Hicks and Mullholland., 2018). This incomplete pathway has seen *N. gonorrhoeae* previously been classified as a cysteine auxotroph however, cysteine requirements can be fulfilled by thiosulfate (Le Faou, 1984).

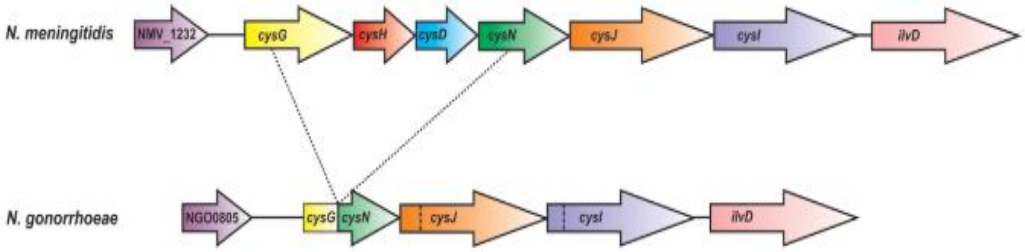

Figure 1.3: Sulfate reduction operon of *N. meningitidis* compared to *N. gonorrhoeae*. Dotted lines represent the 3.5 kb genomic deletion in *N. gonorrhoeae,* truncating CysG and CysN genes while eliminating CysH and CysD. Dashed lines seen in *N. gonorrhoeae* CysJ and CysI genes represent premature stop codons. Figure from Hicks & Mullholland, 2018.

In contrast to many other bacteria who have two isoforms of the *O*-acetylserine sulfhydrylase (OASS) enzyme; OASS-A (CysK) that uses bisulfide and OASS-B (CysM) that uses thiosulfate, *N. gonorrhoeae* only contains a single OASS enzyme (as with all *Neisseria* species). The OASS enzyme in *N. gonorrhoeae* unequivocally demonstrates exclusive substrate specificity for bisulfide and cannot use thiosulfate as a substrate (unpublished results from the Hicks Lab), and as such belongs to the OASS-A (CysK) enzyme family. As *N. gonorrhoeae* cannot acquire sulfide for use by CysK via sulfate assimilation, this then suggests that the CysM independent pathway is operative within *N. gonorrhoeae.* Indeed, two sulfurtransferase enzymes, Str and PspE, have recently been identified within the *N. gonorrhoeae* genome. We therefore propose that sulfur acquisition for the synthesis of cysteine in *N. gonorrhoeae* is achieved by a sulfurtransferase enzyme, thiosulfate, and glutathione (Figure 1.4). We propose that the sulfide product of this reaction is used as a substrate for CysK. Adding weight to this hypothesis, it has long been observed that sulfite accumulates in the growth media of *N. gonorrhoeae* in contrast to other *Neisseria* species (Le Faou, 1984). Our hypothesis explains this observation as sulfite is a by-product of sulfurtransferase catalysed thiosulfate reduction, which accumulates as the result of non-functional CysJI proteins to reduce sulfite.

Notably, the proposed pathway herein is highly advantageous as it, (1) presents the most efficient route for sulfur acquisition of the inorganic sulfur assimilation pathways with respect to bioenergetics, (2) is comparable in efficiency to organic sulfur utilisation, and (3) thiosulfate is a more abundantly available sulfur source in the host-pathogen interface than organic sulfur sources (Lensmire & Hammer,

2018). Defining this proposed pathway within *N. gonorrhoeae* could be pivotal in advancing our understanding of how pathogens fulfil their sulfur requirements. However, much is to be elucidated regarding the role of sulfurtransferases in bacterial pathogens.

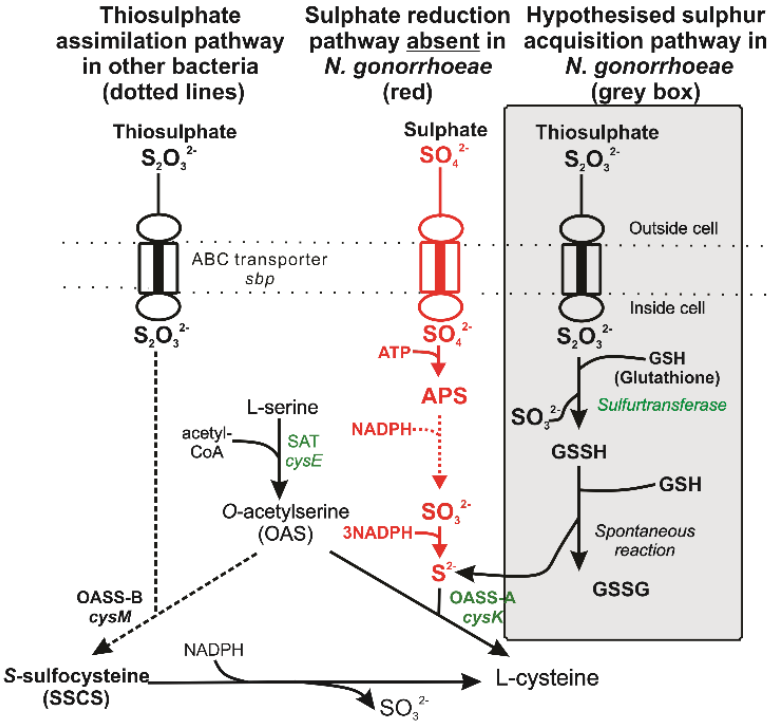

Figure 1.4: Sulfate and thiosulfate transport and reduction pathways. The sulfate reduction pathway absent in *N. gonorrhoeae* is shown in red. The newly hypothesised thiosulfate reduction pathway in *N. gonorrhoeae* is shown in the grey box on the right. Enzymes shown in green are present in *N. gonorrhoeae*. Figure adapted from Hicks & Mullholland, 2018 which now includes the hypothesised sulfur acquisition pathway in *N. gonorrhoeae*.

1.6 Sulfurtransferases

The sulfurtransferases (EC 2.8.1.X) encompass a superfamily of ubiquitously distributed, multifunctional enzymes that catalyse reactions involving the transfer of a sulfur atom from a thiol donor substrate to a thiol acceptor substrate. Members of the sulfurtransferase (ST) family, thiosulfate sulfurtransferase, TST, (EC 2.8.1.1), 3-mercaptopyruvate sulfurtransferase, MST (EC 2.8.1.2), and thiosulfate-thiol sulfurtransferase, TTST (EC 2.8.1.3), are closely related but distinguishable by the reactions they catalyse.

The thiosulfate sulfurtransferases, commonly referred to as rhodaneses, are renowned for catalysing the transfer of sulfur from thiosulfate to cyanide, a strong electron transport chain inhibitor, to produce the less-toxic metabolite, thiocyanate and sulfite (reaction 1).

(1) $S_2O_3^{2-} + CN^- \longrightarrow SO_3^{2-} + SCN^-$

The thiosulfate-thiol sulfurtransferases catalyse the reduction of thiosulfate in the presence of glutathione to sulfite and sulfide in a two-step reaction. The first step involves the enzymatically catalysed transfer of sulfur from thiosulfate to glutathione forming glutathione persulfide (GSSH) and sulfite (reaction 2a). Glutathione persulfide subsequently reacts spontaneously with a second molecule of glutathione forming glutathione disulfide (GSSG) and hydrogen sulfide (reaction 2b).

(2) $S_2O_3^{2-} + GSH \xrightarrow{(a)} GSSH \xrightarrow[(b)]{GSH} GSSG + H_2S$, with SO_3^{2-} as the other product of (a)

On the other hand, the 3-mercaptopyruvate sulfurtransferases utilise 3-mercaptopyruvute as the thiol donor substrate, yet similar to rhodaneses and TTST, transfers sulfur to low molecular thiols (cysteine, glutathione, and dihydrolipoic acid), dithiols (thioredoxin,), and cyanide (Pedre & Dick, 2021). Reactions with cyanide as the thiol acceptor substrate produces thiocyanate and pyruvate (reaction 3) while activity with the thiol or dithiol acceptor substrates ultimately leads to the generation of a persulfide and hydrogen sulfide in a similar

reaction (reaction 4) to the thiosulfate-thiol sulfurtransferase.

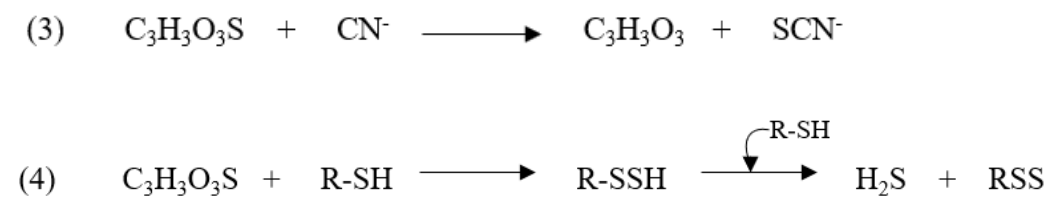

While these reactions are characteristic of the respective sulfurtransferase members, there appears to be overlap in the catalytic activity. For example, rhodaneses exhibit activity with thiols (glutathione, cysteine, and co-enzyme-A) reminiscent of the thiosulfate-thiol sulfurtransferases (Libiad et al., 2018; Aird, Heinrikson & Westley et al., 1983), and dithiols, such as thioredoxin 1 (Ray et al., 2000), in which the products of the reaction are ultimately a persulfide and hydrogen sulfide. The notion that some rhodaneses demonstrate both typical rhodanese activity and TTST activity has previously promoted researchers to suggest the broader enzymatic name for these group of proteins to be sulfane sulfurtransferase (Aird, Heinrikson & Westley, 1987) but perhaps what continues to set rhodaneses and TTSTs apart is that while rhodaneses are capable of TTST activity, TTST cannot directly catalyse cyanide detoxification. Adding to the functional overlap of sulfurtransferases, dual-functioning enzymes have been identified capable of using both thiol donor substrates 3-mercaptopyruvate and thiosulfate (Papenbrock & Schmidt, 2000; Meza et al., 2019), although this currently appears rare. The full extent of substrate promiscuity of these sulfurtransferase members is relatively unclear as testing of various thiols and dithiols as the acceptors substrates has not been habitually assessed in biochemical characterisation studies. Although the imbricate nature of these three sulfurtransferase members regarding substrate activity has been demonstrated *in vitro*, the corresponding physiological relevance is often elusive.

1.6.1 Sulfurtransferases: Structural characterisation

The first, and most well characterised, rhodanese was discovered in *Bos taurus* over 80 years ago (Lang, 1933). Structural analysis of the *Bos taurus* rhodanese (commonly referred to as Rhobov) reveals that the 293 amino acids long protein is comprised of two similar in size (~120 amino acids each) and structure globular domains; a catalytic (Carboxy-terminal) and inactive (N-terminal) domain with the highly conserved respective rhodanese signatures, ([A/V]-X2-[F/Y]-[D/E/A/P]-G-[G/S/A]-[W/F]-X-E-[F/Y/W]) and ([F/Y]-X3-H-[L/I/V]-P-G-A-X2-[L/I/V/F])**.** The C-terminal and N-terminal domains maintain a high degree of three-dimensional structural similarity despite exhibiting low sequence similarity (Ploegman et al., 1978). These domains are comprised of an α/β topology in which a central five-stranded β-sheet core is surrounded by α-helices as seen in Figure 1.5. Importantly, the C-terminal domain contains a redox-active cysteine residue (shown in black stick format in Figure 1.5) which is essential for catalysis while its counterpart in the N-terminal domain, an Asp residue, is not involved in catalysis. The catalytic cysteine residue signifies the start of the highly conserved active site motif (loop) and forms a cradle-like structure which defines the catalytic pocket of the enzyme.

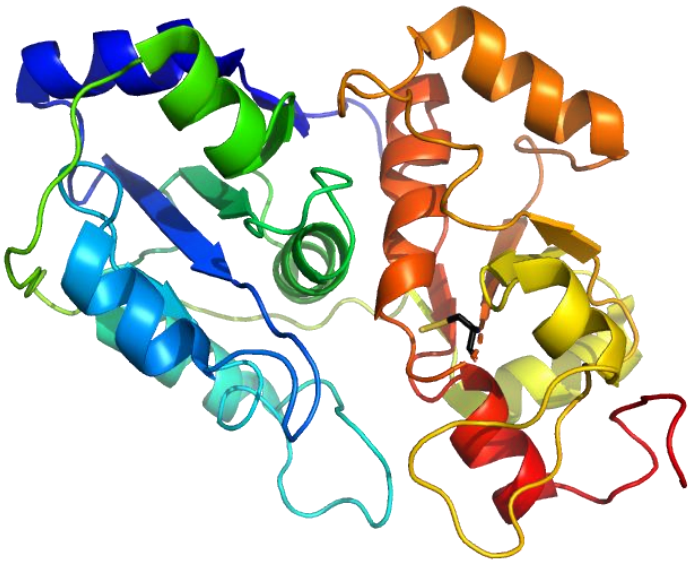

Figure 1.5: Three-dimensional structure of Rhobov (1RHD). The three-dimensional rhodanese structure from *Bos Taurus* was recovered from the Protein Data Bank (www.rcsb.org). The structure is coloured as a gradient from the N-terminus (blue) to the C-terminus (red). The catalytic cysteine residue is shown in stick format in black.

The C-terminal and N-terminal (or catalytic and inactive) rhodanese domains are referred to as the rhodanese structural modules and are highly conversed, distinguishing the sulfurtransferase superfamily. Based on the architecture of these modules, sulfurtransferases can be characterised into four groupings; (I) single domain proteins, (II) tandem domain proteins, (III) multidomain proteins and, (IV) elongated active site loop (Cipollone, Ascenzi & Visca, 2007).

Structural and functional studies on single domain catalytic rhodanese modules confirm that these enzymes are functionally active in the absence of an N-terminal domain, proving that the N-terminal domain is not involved in catalysis and supportive of the hypothesis that tandem-domain rhodanese arose due to the duplication of an ancestral rhodanese gene. The single domain protein, GlpE from *E. coli* is considered the prototype structure for the single domain catalytic rhodanese module (Figure 1.6a) which matches the catalytic domain of eukaryotic and prokaryotic tandem-domain rhodaneses (Spallarossa et al., 2001). Crystal structures obtained from other single domain proteins, such as, PspE from *E. coli*, Rdl2 from *S. cerevisiae* and TSTD1 from humans, reveal that, like the tandem domain proteins, these proteins demonstrate highly conserved three-dimensional structures (Figure 1.5b-d).

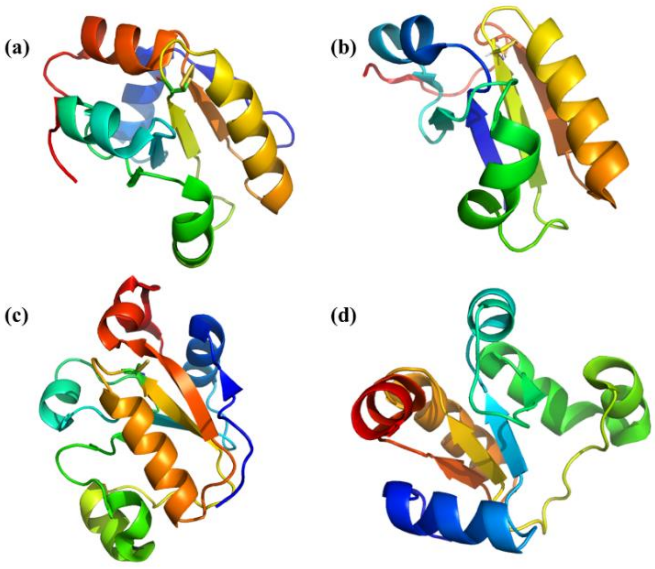

Figure 1.6: Three-dimensional structures of various single domain rhodaneses. All three-dimensional rhodanese structures were recovered from the Protein Data Bank (www.rcsb.org). The structures are coloured from N-terminus (blue) to C-terminus (red). (a) GlpE (1GMX) from *E. coli*, the protype structure for single domain rhodaneses, (b) PspE (2JTQ) from *E. coli*, (c) Rdl2 (6K62) from *S. cerevisiae*, and (d) TSTD1 (6BEV) from *Homo sapiens*.

Single domain proteins appear to be restricted to the rhodanese sulfurtransferase family members and, as with all rhodaneses, carry the highly conserved active motif, CRXGX[R/T] which begins with the redox active catalytic cysteine residue. Single domain catalytic rhodaneses are ubiquitously encoded for by both prokaryotic and eukaryotic genomes while proteins solely containing the inactive rhodanese module (ie. no catalytic cysteine residue) have been identified and characterised in recent years however these are far less common.

The tandem domain sulfurtransferases are highly common and include the double - domain rhodaneses and, closely related, MST. Tandem domain rhodaneses and MST are structurally homologous enzymes and share up to 66% sequence similarly. The main distinguishing difference of the two sulfurtransferase members is the active site motif of the catalytic domain, which is CRXGX[R/T] and CG[S/T]GVT, for rhodanese and MST respectively. This difference corresponds to the distinct ionic charge of thiol donor substrate utilised, thiosulfate (2-) and 3-mercaptopyruvate (1-). Notably, it is possible to convert thiol donor specificity of MST to rhodanese (and vice versa) via site directed mutagenesis, highlighting the high degree of structural similarity (Nagahara, Okazaki & Nishino, 1995).

1.6.2 Sulfurtransferases: Physiological function

Intriguingly, genomic sequence analysis reveals the coexistence of several sulfurtransferase proteins within the overwhelming majority of organisms. For example, the opportunistic pathogen *P. aeruginosa* genome has ten annotated rhodanese (or rhodanese-related) proteins (Cipollone, Ascenzi & Visca, 2007), the *E. coli* genome has nine (Cheng et al., 2008), the *S. cerevisiae* (single celled fungus) and human genomes have five (Chen et al., 2018; Libiad et al., 2018), and the *Arabidopsis thaliana* genome has 18 (Bauer & Papenbrock, 2002). This suggests an assortment of physiological functions are supported by the sulfurtransferase superfamily within organisms. However, despite their omnipresence, a considerable proportion of sulfurtransferase predicted genes are yet to be functionally characterised contributing to the ambiguity surrounding their physiological function.

1.6.2.1 3-Mercaptopyruvate sulfurtransferase

The MST's members are less ubiquitously observed compared to rhodaneses, occurring in most phyla belonging to eukaryotes, occasionally in prokaryotes and appear to be absent in archaea. MST catalyse the transfer of sulfur from 3-mercaptopyruvute to low molecular thiols (cysteine, glutathione, and dihydrolipoic acid), thiol containing proteins (thioredoxin, Mocs3), or cyanide (Pedre & Dick, 2021). However, which thiol acceptor substrates are physiologically relevant and under what conditions is yet to be revealed. Reactions catalysed by MST (with the exception of cyanide) ultimately lead to the generation of hydrogen sulfide, a physiologically relevant signal transmitter (Shibuya et al., 2009; Wang, 2012). In addition to hydrogen sulfide generation, MST activity has been linked to cellular processes such as protection against oxidative stress (Williams et al., 2003), cyanide detoxification, fatty acid metabolism and mitochondrial bioenergetics (Pedre & Dick, 2021). Notably, within pathogenic bacteria such as *E. coli*, mutation of MST and the subsequent reduction of hydrogen sulfide generation has been linked to increased sensitivity to numerous antibiotics (Shatalin et al., 2011). However, this notion has been recently challenged by Wang et al. (2019) who dispute that MST is not the primary source for hydrogen sulfide in *E. coli* under anaerobic conditions.

1.6.2.2 Thiosulfate sulfurtransferase (Rhodanese)

Rhodaneses are defined by the catalytic conversion of cyanide to thiocyanate leading to the long withstanding proposed physiological role in cyanide detoxification which has been demonstrated for tandem domain rhodaneses in eukaryotes (Cipollone et al., 2007; Westley et al., 1983) and prokaryotes (Cipollone et al., 2020; Cipollone et al., 2007; Cipollone et al., 2006) alike. Similar to the MST, rhodaneses also demonstrate activity with different dithiols (such as thioredoxin 1) as acceptor substrates, utilising thiosulfate as the thiol donor substrate, in which case the products of the reaction are oxidised disulfide and sulfide. Interestingly, biochemical characterisation of the single domain rhodaneses, GlpE from *E. coli* and TSTD1 in humans reveal that activity with dithiols are comparable to, or far greater than, activity with cyanide (Ray et al., 2000; Libiad et al., 2018). Thus, dithiols are likely, if not more, relevant substrates for these rhodaneses. While the exact role of dithiol reactions in a physiological context is yet to be unequivocally

clarified, numerous functional roles have been postulated including cellular redox homeostasis (Henne et al., 2015), sulfide based signalling (Libiad et al., 2018) and the formation and repair of iron-sulfide clusters (Nandi & Westley, 1998).

Of particular interest to the research herein, is the functional role of bacterial rhodaneses. To date, the most well characterised bacterial rhodaneses are the single domain rhodaneses, PspE and GlpE from *E. coli*. PspE (phage shock protein E) is the fifth and final gene encoded for within the *psp* (phage-shock protein) operon (*psp*ABCDE) which is induced under various stress conditions (Brissette et al., 1990). Interestingly, PspE is transcribed as part of the operon in addition to having its own promoter (Brissette et al., 1991), allowing transcription under normal conditions. This suggests that PspE offers an alternative or additional functional role distinct from the other Psp proteins within the operon. In support of this, some bacterial genomes, such as in *Yersinia enterocolitica*, the *pspE* gene is absent in the *psp* operon, while in other cases such as in *N. meningitis*, the *pspE* homolog is unaccompanied by the *pspA-D* genes which are apparently absent entirely (Adams et al., 2002). GlpE is the first gene encoded in the *glpEGR* operon (Ray et al., 2000) which belongs to the *glp* regulon responsible for the metabolism of *sn*-glycerol-3-phosphate. A comprehensive study of GlpE in *E. coli* conducted by Chen et al., (2008) involving *in vivo* characterisation of a Δ*glpE* mutant strain together with *in vitro* biochemical characterisation determine that GlpE has seemingly no physiological relevance within the context of the operon of which it found (*glpEGR)* leaving their exact physiological role a matter of further investigation.

While GlpE and PspE both demonstrate cyanide detoxification activity *in vitro* which, together with structural analysis, distinctly classifies them as rhodaneses, their physiological role as cyanide detoxifiers is doubtful due to a low affinity for cyanide. Consistently, Δ*pspE*, Δ*glpE* and Δ*pspE*Δ*glpE E. coli* strains are not more sensitive to cyanide compared to the wild type strain nor does overexpression of either enzyme confer cyanide resistance (Cheng et al., 2008). In the pathogenic bacterium, *S. typhimurium*, expression of *pspE* is highly induced during infection of eukaryotic cells, indicative of an important functional role in host-pathogen interaction, supported by *in vivo* characterisation of a Δ*pspE*Δ*glpE* mutant strain which resulted in reduced virulence compared to wild type (Wallrodt et al., 2013), although the exact nature of this role is yet to be revealed.

Recently, thiosulfate-thiol sulfurtransferase activity (ie. glutathione as the thiol acceptor substrate) for rhodaneses in prokaryotes has been implicated as having a functional role in *de novo* cysteine biosynthesis by reducing thiosulfate to sulfite and bisulfide, which is ultimately incorporated into cysteine (Kawano, Suzuki & Ohtsu, 2018). Thus far, this physiological role has been elucidated for GlpE in *E. coli* (Kawano et al., 2017), and single domain rhodaneses, Rdl1 and Rdl2, in *S. cerevisiae* (Chen et al., 2018). The discovery of this physiological function is significant for two main reasons. Firstly, thiosulfate-thiol sulfurtransferase activity of rhodaneses has been previously deemed physiologically irrelevant based on the assumption that rhodaneses are a poor catalyst for these substrates (Westley et al., 1983) to which, this discovery disputes this proposition, thereby expanding the repertoire of physiologically relevant reactions catalysed by rhodaneses. Secondly, it reveals an alternative pathway for the acquisition of essential sulfur in bacteria which is feasibly operative in a magnitude of other bacterial species, given that rhodaneses are ubiquitously encountered. In accordance with this, deletion of the rhodanese, *cysA*, in *Saccharopolyspora erythraea* results in cysteine auxotrophy (Donadio, Shafiee & Hutchinson, 1989). In addition, phenotypic growth defects observed in *S. cerevisiae* Δ*rd1*Δ*rdl2* mutation strains grown with thiosulfate as the sole sulfur source are restored by the introduction of several bacterial rhodaneses including PspE and GlpE from *E. coli*, RdhA from *P. aeruginosa*, and Duf442 from *Cupriavidus pinatubonensis* (Chen et al., 2018), suggesting that thiosulfate utilisation is likely a common phenomenon for bacterial rhodaneses. On the other hand, the eukaryotic rhodanese TSTD1 has low affinity for thiosulfate utilisation in this way. Considering rhodanese involvement in the context of the sulfur acquisition for cysteine biosynthesis, the observation that TSTD1 rhodanese activity differs to bacteria in this sense is consistent with the fact that eukaryotic organisms are not capable of *de novo* cysteine synthesis, making this a unique function of bacterial rhodaneses. It is conceivable then, that the physiological role of rhodaneses varies between prokaryotic and eukaryotic organisms.

1.6.3 Sulfurtransferases in *Neisseria gonorrhoeae*

Within the *N. gonorrhoeae*, two single rhodanese catalytic domain proteins, Str and PspE, have been recently identified. The Str gene (NGO_0020/NGFG_0015) is annotated as a thiosulfate sulfurtransferase and exists as a single gene within the genome. Interestingly, inspection of the Str active site motif, [CHHGRI], shows a conserved amino acid change in position two, from arginine, as anticipated by the rhodanese conserved motif, CRXGX[R/T], to histidine, although the ramifications of this residue change is unknown. In contrast the PspE gene (NGO_0369/NGFG_00520) is found within the *psp* (phage-shock protein) operon and has the active site motif, CRSGRR, which obeys the conserved rhodanese active site motif.

Based on the evident absence of conventional inorganic sulfur assimilation pathways in *N. gonorrhoeae* and the recently identified role of sulfurtransferases in thiosulfate assimilation, we propose that single domain sulfurtransferases are the missing link in understanding how *N. gonorrhoeae* fulfils its sulfur requirements. We propose that Str and PspE reduce thiosulfate to sulfide in the form required for cysteine biosynthesis via the reduction of thiosulfate in the most bioenergetically efficient pathway.

1.7 Research Objectives

The aim of the research conducted herein was to characterise the structure and function of the newly identified sulfurtransferase (Str) in *N. gonorrhoeae* to determine its role in sulfur acquisition. Part way through this project commencing, a second sulfurtransferase enzyme in the *N. gonorrhoeae* genome, PspE, was identified. Although full characterisation of this enzyme falls outside of the scope of the current project, an additional aim was set to conduct preliminary characterisation of the PspE enzyme to determine if PspE displays similar sulfurtransferase activity to that of Str. The following objectives were set to achieve these aims:

Sulfurtransferase, Str:

1) Characterise the activity of the sulfurtransferase enzyme *in vitro* using enzyme activity assays.

2) Determine the structure of the sulfurtransferase enzyme using protein crystallography.

3) Construct and phenotypically characterise a *N. gonorrhoeae* sulfurtransferase deletion strain.

Phage shock protein E, PspE:

1) Express and purify the PspE protein.

2) Preliminarily characterise the activity of the PspE enzyme *in vitro* using enzyme activity assays.

Chapter 2

Biochemical Characterisation of Single Domain Sulfurtransferases within *Neisseria gonorrhoeae*

2.1 Introduction

The sulfurtransferases encompass an enzyme superfamily that catalyse reactions involving sulfane sulfur containing substrates or products. Of particular interest to this research are the single domain rhodaneses which utilise the sulfane sulfur containing thiol donor substrate, thiosulfate. Single domain rhodaneses are ubiquitously found across all domains of life, yet despite this, few have been subject to biochemical characterisation contributing to the ambiguity surrounding their physiological function.

To date the most lucid physiological role for rhodaneses is cyanide detoxification which is accomplished via the transfer of sulfur from thiosulfate to cyanide, forming thiocyanate. However, the few single domain rhodaneses that have been subject to biochemical characterisation demonstrate a low affinity for cyanide (Cheng et al., 2008; Hunt, 2004; Motl et al., 2017), making a physiological role as cyanide detoxifiers dubious. Alternatively, rhodaneses can catalyse the transfer of sulfur to other thiol acceptor molecules such as thiols (namely glutathione) in a reaction reminiscent of thiosulfate-thiol sulfurtransferase. However, currently these reactions are understudied leaving the physiological relevance of these reactions largely enigmatic.

Recently, single domain rhodaneses have been implicated in having a functional role in sulfur acquisition for *de novo* cysteine biosynthesis (Kawano et al., 2017; Chen et al., 2018) via the CysM independent pathway. The sulfurtransferase in this pathway catalyses the sulfur transfer from thiosulfate to glutathione producing sulfite and glutathione persulfide. Glutathione persulfide subsequently reacts spontaneously with an additional glutathione molecule forming oxidised glutathione and liberating sulfide. Sulfite and sulfide produced as a result of

sulfurtransferase activity feed into the cysteine biosynthesis pathways, being utilised as substrates for sulfite reductase (CysJI) and OASS-A (CysK), respectively.

Within bacterial genomes, at least two single domain rhodaneses are prominently found. In accordance with this, *Neisseria gonorrhoeae* has two single domain rhodanese (or rhodanese-like) enzymes, Str and PspE, which have not been characterised thus far. In light of the discovery of the CysM independent pathway for sulfur acquisition, and the evident absence of conventional sulfur assimilation pathways, we hypothesise that single domain rhodaneses are the missing link in sulfur acquisition for cysteine biosynthesis in *N. gonorrhoeae*. We anticipate glutathione to be a physiologically relevant acceptor substrate for this reaction due to the extremely high glutathione concentrations found within *N. gonorrhoeae*. To explore this hypothesis, we first aimed to biochemically characterise Str *in vitro*. This chapter investigates the kinetic parameters and substrate promiscuity of the recombinant Str enzyme**.** We additionally endeavour to preliminary characterise the PspE enzyme within *N. gonorrhoeae* to determine if PspE displays similar substrate activity to that of Str. Lastly, we attempt to crystalise the Str protein in pursuit of determining protein structure.

2.2 Materials and Methods

2.2.1 Cloning of *str* and *pspE* for expression in *E. coli*

The *str* and *pspE* genes NGFG_00156 and NGFG_00520 respectively were codon optimised for expression in *E. coli* and ordered from Twist Bioscience in the pET28a plasmid between the NdeI and XhoI restriction sites for expression with an N-terminal His-tag. The *str*-pET28a and *pspE*-pET28a plasmids were transformed with chemically competent *E. coli* BL21 (DE3) for protein expression.

2.2.2 Long term storage of *E. coli* BL21 Str and PspE expression strains

E. coli BL21 (DE3) containing *str*-pET28a and *pspE*-pET28a plasmids respectively were inoculated into 3 ml LB broth containing 50 $\mu g.ml^{-1}$ kanamycin and incubated over night at 37 °C at 180 rpm. For long term storage 0.5 ml of each overnight culture was added to 0.5 ml sterile 50% (v/v) glycerol in three cryovials and stored at –80 °C.

2.2.3 Str and PspE *E. coli* expression cultures

Recombinant Str and PspE proteins were expressed in E. coli BL21 (DE3) with an N-terminal His-tag via the method below. A 10 ml seeder culture of LB broth containing 50 µg.ml^{-1} kanamycin was inoculated with either 50 µl of the glycerol stock or a single colony of *E. coli* BL21 (DE3) *str*-pET28a or *E. coli* BL21 (DE3) *pspE*-pET28a (section 2.2.2) and incubated overnight at 37°C, 180 rpm.

The 10 ml seeder culture was then used to inoculate a 1 L culture of LB broth supplemented with 50 µg.ml^{-1} kanamycin. The 1 L culture was incubated at 37 °C, 180 rpm and protein expression induced with 1 ml 0.75 M IPTG (final concentration 0.75 mM) when the optical density at 600 nm was between 0.4 and 0.6. The cultures were then transferred to 22 °C and incubated overnight at 180 rpm. The 1 L culture was then centrifuged at 4 600 rpm at 4 °C for 20 min to pellet cells. The supernatant was discarded followed by resuspension of the cell pellet in 25 ml Lysis buffer (50 mM KPO_4 pH 8, 200 mM NaCl, 20 mM imidazole) and transferred to a 50 ml sterile falcon tube. This was then centrifuged a final time at 4 600 rpm at 4 °C for 20 min, the supernatant was then discarded, and the cell pellets stored at -80 °C.

2.2.4 Purification of Str and PspE

Str and PspE were isolated and purified by immobilised metal affinity chromatography (IMAC) and size exclusion chromatography (SEC) purification methods. SDS-PAGE gel electrophoresis was used to visualise purified protein and determine solubility.

2.2.4.1 IMAC purification

Cell pellets (section 2.2.3) were thawed at room temperature and resuspended in 25 ml Lysis buffer (50 mM KPO_4 pH 8, 200 mM NaCl, 20 mM imidazole). One EDTA-free protease inhibitor tablet (Roche) was added prior to lysis via sonication on ice using a 5-50 ml microtip (Q700 sonicator) with the following pulse settings: 1.0 s burst followed by a 1.0 s rest for a total of 1.30 min with an amplitude of 12. The sonicate was centrifuged at 9 000 rpm, 4 °C for 20 min to separate soluble and insoluble fractions. The resulting supernatant was filtered through 1.2, 0.45 and 0.2 µm Minisart filters and loaded onto a 5 ml nickel column (HisTrap, GE) pre equilibrated with Lysis buffer via the sample pump at a flow rate of 1 ml.min^{-1} using

a BioRad NGC FPLC system. The column was then washed with 10 ml 96 % lysis buffer, 4% elution buffer (50mM KPO_4 pH 8, 200mM NaCl, 1M imidazole) at 2 $ml.min^{-1}$ to remove any unbound proteins. Bound proteins were eluted into collection tubes with a gradient of 4-50% elution buffer at a flow rate of 2 $ml.min^{-1}$. Fractions (2 ml) were collected across the gradient and those corresponding to the elution peak on the 280 nm chromatogram were collected and stored at 4 °C. Eluted protein (peak fractions) was assessed by SDS-PAGE gel electrophoresis (section 2.2.4.3) alongside samples of the pellet (insoluble) and supernatant (column load). Fractions containing protein were then pooled and concentrated via centrifugation in a 10 000 Da MWCO Amicon spin concentrator at 3300 rpm at 4 °C until a volume of 5 ml reached. Concentrated protein was stored at 4 °C for up to 1 day prior to further purification by size exclusion chromatography (SEC).

2.2.4.2 SEC purification

For purification of Str and PspE via size exclusion chromatography a S75 16/60 SEC column (GE) was pre-equilibrated one column volume (125 ml) of water followed by one column volume (125 ml) of SEC buffer (50mM Tris pH 8, 200mM NaCl). The 5 ml of concentrated protein from the IMAC purification (section 2.2.4.1.) was manually loaded into a 5 ml injection loop through a 0.2 µm filter on the Bio-Rad NGC FPLC system. Injection of protein onto the column proceeded at 0.5 $ml.min^{-1}$ followed by 130 ml SEC buffer at 0.5 $ml.min^{-1}$, collecting 2 ml fractions for the entire run. Fractions corresponding to the peak(s) in the resulting 280 nm chromatogram were collected, assessed by SDS-PAGE gel electrophoresis, pooled together, and either stored at 4 °C for immediate use (up to 3 days) or stored as frozen stocks (section 2.2.4.5).

2.2.4.3 SDS-PAGE gel electrophoresis

15% SDS-PAGE gels were used to visualise proteins post IMAC and size exclusion purification (section 2.2.4.1 and 2.2.4.2). All gels were made in-house using a multi-gel caster (Hoefer) capable of making either 5 or 10 mini gels. The resolving gel layer was made by adding together the components listed in Table 2.1 under "resolving layer", mixed by inverting and poured into the gel caster, leaving a 3 cm gap from the top. Isopropanol was gently placed on top of the resolving layer (3 ml) and left until the resolving layer had set (approximately one hour). Once set, the

isopropanol was carefully tipped off, leaving behind the resolving layer. The stacking layer solution was combined by adding the "stacking layer" components together listed in Table 2.1, mixed by inverting, and used to fill the gel caster to the top edge. A ten or fifteen well comb was inserted into the top of each gel and left to set at room temperature for approximately one hour. Gels were stored at 4 °C and stored for up to four weeks.

Table 2.1 Components for five 15% SDS-PAGE gels.

Component	Resolving layer (ml)	Stacking layer (ml)
MQ H_2O	7.05	8.5
30% acrylamide	15.00	2.125
Resolving buffer (1.5 M Tris, pH 8.8)	7.50	-
Stacking buffer (1.0 M Tris, pH 6.8)	-	1.6
10% (w/v) SDS	0.30	0.125
10% (w/v) APS*	0.15	0.063
TEMED	0.015	0.00063

* Fresh ammonium persulfate (APS) stock solution prepared weekly.

Protein samples were prepared for SDS-PAGE by addition of 5 µl 4 × SDS loading dye with 15 µl of protein sample. Pellet and supernatant samples from the IMAC purification were prepared by adding 5 µl of 4 × SDS loading dye to 3 µl of sample and 12 µl of lysis buffer. All samples were heated to 95 °C for five min prior to gel-loading. Precision Plus Protein™ ladder (Bio-Rad Laboratories) (10 µl) was loaded in the first well of each gel. Gels were run in 1 × Tris-Glycine SDS-PAGE running buffer (Appendix B.1) at 100 V until the dye band had migrated to the end of the stacking layer (approximately 15 min). Voltage was then increased to 120 V until migration of the dye band to the end of the gel (approximately 80 min).

Protein bands were visualised by covering the gel in Commassie Fairbanks stain A staining solution (0.05% Coomassie Blue, 25% isopropanol, 10% acetic acid),

heating for 30 s in a microwave, and incubating at room temperature with agitation (120 rpm) for 10 minutes. Stained gels were carefully rinsed with water and covered with de-staining solution (10% acetic acid), heated for 30 s in a microwave, and incubated at room temperature with agitation (120 rpm) until background stain was removed. An iBright imager (Invitrogen) was used to visualise and image the gels.

2.2.4.4 Determining protein concentration

Purified protein concentration was determined by absorbance at 280 nm using a NanoDrop^{TM} 2000. Protein concentration of Str and PspE was calculated by dividing the NanoDrop^{TM} reading by the molar absorption co-efficient of the Str protein (1.4 $M^{-1}.cm^{-1}$) and PspE (0.883 $M^{-1}.cm^{-1}$) as determined by ProtParam (Gasteiger et al., 2005).

2.2.4.5 Long-term storage of sulfurtransferase

Excess protein was stored by adding glycerol (50% (v/v) final concentration) to the protein solution. Aliquots of 500 µl were placed in sterile 1.5 ml tubes, flash frozen with liquid nitrogen and stored at -80 °C.

2.2.5 Sulfurtransferase activity asssys

Str and PspE was purified by IMAC purification and size exclusion chromatography as per sections 2.2.4.1 and 2.2.4.2, respectively. Protein concentration was determined by NanoDrop^{TM} as per section 2.2.4.4. For the duration of all assays, Str and PspE working stocks were kept on ice until required. Two different assays were used to test the sulfurtransferase activity in the presence of thiosulfate and an array of thiol acceptor substrates glutathione (GSH), cysteine (Cys), homocysteine (HMCYS), and cyanide (CN)).

2.2.5.1 Thiosulfate-thiol sulfurtransferase activity

The sulfurtransferase activity of Str and PspE in the presence of thiosulfate and an array of thiols as the acceptor substrate (GSH, Cys or HMCYS) was assessed by monitoring the formation of hydrogen sulfide using a modified version of previously described lead acetate colorimetric assay (Chiku et al., 2009). Hydrogen sulfide produced as a result sulfurtransferase activity converts lead acetate to lead sulfide. The formation of lead sulfide is measured by spectrophotometry at 390 nm.

The following assay was performed in a Stopped flow spectrophotometer (KinetAsyst^{TM}/SF-61SX2, TgK Scientific), pre-equilibrated in assay buffer (200 mM sodium phosphate buffer, pH 7.4). For each thiosulfate and thiol acceptor pair, data were collected in triplicate for both a thiosulfate (thiol donor) concentration gradient and a thiol acceptor gradient, except for homocysteine due to a lack of resources.

2.2.5.1.1 Substrate and assay component preparation

Master stocks of thiosulfate (200 mM) and lead acetate (10 mM) were prepared and stored at room temperature. Master stocks of glutathione (250 mM) were prepared as 1 ml aliquots and stored at -20 °C. When required, GSH aliquots were thawed and kept short-term on ice to mitigate the oxidation of glutathione at room temperature. Cysteine (250 mM) and homocysteine (250 mM) stocks were prepared immediately prior to the assays and kept on ice for the duration of the assays to minimise oxidation. All substrates were made up in MQ H_2O.

2.2.5.1.2 Stopped-Flow assay protocol

For thiosulfate concentration gradients, the reaction mixture contained 1 µg or 0.4 µg of enzyme, 0.4 mM lead acetate, and either GSH or cysteine (50 mM) in assay buffer to a total volume of 1 ml (Table 2.2). The reaction mixtures for the thiol acceptor concentration gradients were the same except for varying glutathione, cysteine, or homocysteine concentrations (0.25-50 mM). All reactions were carried out in the Stopped flow spectrophotometer at 37 °C and were initiated by the addition of thiosulfate (0.25-0 mM) for thiosulfate concentration gradients and 50 mM thiosulfate for the thiol acceptor concentration gradients.

Table 2.2: Thiosulfate-thiol sulfurtransferase activity assay set up.

	Thiosulfate gradient	Thiol acceptor gradient
Component	Volume (µl)	Volume (µl)
Syringe One: Reaction Mix		
Thiol acceptor substrate (GSH, Cys or HMCYS)	200	1-250
Lead acetate	40	40
Enzyme	25	25
Buffer	735	685-959
Syringe Two: Thiosulfate		
Thiosulfate	2.5-250	250
Buffer	750-997.5	750

Data were collected in triplicates in an 18-shot sequence where each reaction proceeded for 50, 90, or 120 seconds with five 0.2 s second dummy shots occurring prior to each reaction. Each reaction contained 40 µl of reaction mix (Table 2.2) and 40 µl of thiosulfate (Table 2.2). The change in absorbance at 390 nm was measured continuously.

Raw data were analysed using Kinetic Studio Analysis. A linear regression model was fitted to the initial velocity of the reaction to determine rate ($\Delta Ab.s^{-1}$). The molar extinction coefficient of 5,500 $M^{-1}.cm^{-1}$ for lead sulfide was used to calculate the rate of reaction as H_2S produced ($mM.s^{-1}$).

2.2.5.2 Preliminary enzyme mechanism assessment

Data were collected to investigate enzyme mechanism as per section 2.2.5.1. The rates at various thiosulfate concentrations (0.5-50 mM) were determined with constant glutathione concentrations of 10 and 50 mM. The initial rate at each thiosulfate concentration was determined. Rate and substrate concentrations values

were transformed by inverting the values to generate a double reciprocal plot (1/velocity on the y-axis and 1/substrate concentration on the x-axis).

2.2.5.3 Cyanide detoxification assay

The cyanide detoxification activity of Str was measured in a modified version of a stopped colorimetric assay as previously described (Sorbo et al., 1953). The formation of a ferric-thiocyanate complex was used to measure thiocyanate production at 460 nm. Data were collected for both a thiosulfate concentration gradient and a cyanide concentration gradient to determine Michaelis-Menten kinetics.

2.2.5.3.1 Substrate and assay components preparation

Thiosulfate (200 mM) was pre-prepared and stored at room temperature. The potassium cyanide (KCN) (250 mM) working stock was prepared and stored at -20 °C. When required, the KCN stock was placed at room temperature for the duration of the assay. Formaldehyde (15%) and ferric nitrate (165 mM ferric nitrate nonahydrate, 13.3% (v/v) nitric acid) stocks were prepared daily and stored at room temperature for the duration of the assay. All substrates and components were made up in MQ H_2O.

2.2.5.3.2 Assay protocol

For thiosulfate concentration gradients, the reaction mixture contained 1 µg of sulfurtransferase, 0.25–50 mM thiosulfate, 50 mM KCN and assay buffer (200 mM sodium phosphate buffer, pH 7.4) to a total volume of 330 µl (Table 2.3). The reaction mixture for KCN concentration gradients were the same, except for varying KCN concentrations (0.25-50 mM) and a constant thiosulfate concentration (50 mM). Buffer, cyanide, and enzyme were added to 1.5 ml tube and placed at 37 °C in a thermomixer. Reactions were initiated with the addition of 100 µl thiosulfate and incubated for 30 or 60 seconds. 100 µl of 15% formaldehyde was added to stop the reaction. The reaction mixture was then placed at room temperature followed by addition of 500 µl ferric nitrate solution. The absorbance of the resulting ferric-thiocyanate complex was measured via spectrophotometry at 460 nm.

Table 2.3: Thiosulfate:cyanide sulfurtransferase activity assay set-up.
Concentrations of substrates were varied by diluting the substrate master stocks in assay buffer to ensure volumes added were consistent across substrate concentrations, thereby minimising pipetting errors at very low concentrations. The enzyme working stock was consistent for all reactions (total 1 µg per reaction).

	Thiosulfate gradient	Cyanide gradient
Component	Volume (µl)	Volume (µl)
Cyanide	66	100
Thiosulfate	100	100
Str (Enzyme)	10	10
Buffer	154	120

The reaction mix without the addition of enzyme was used as the blank. Data were collected in triplicates for each substrate concentration and time points. The concentration of thiocyanate formed was determined using a standard curve (Appendix B.2).

The standard curve was generated to reflect the cyanide detoxification assay. Potassium thiocyanate concentrations, 0.01, 0.05, 0.1, 0.5, 1, and 2 mM, were made up to a final volume of 330 µl, diluted when required with assay buffer. As per the cyanide assay reaction mix, 100 µl of 15% formaldehyde was added following by of 500 µl ferric nitrate solution to form the ferric-thiocyanate complex. Absorbance at each thiocyanate concentration was measured at 460 nm via spectrophotometry. The gradient of the resulting linear plot (y-axis, absorbance; x-axis thiocyanate concentration) was determined to be 0.7553.

Raw data were analysed using Microsoft Excel. Using a linear regression model, initial velocity ($mM.s^{-1}$) was calculated by converting change in absorbance into thiocyanate concentration (mM) (absorbance value divided by 0.7553). The change in concentration values were divided by the change in time (30 s).

2.2.6 Michaelis-Menten kinetics

The kinetic parameters, K_M and V_{max}, were calculated for substrate(s) of interest by varying the concentration of the substrate in question (0.5-50 mM) whilst keeping the other substrate constant at saturating conditions (50 mM) as to not limit the reaction. The steady-state rate at each substrate concentration was determined via a linear regression model and plotted as rate ($mM.s^{-1}$) as a function of substrate concentration (0.5-50 mM). V_{max}, the theoretical maximum rate of the enzyme and K_M, the measure of enzyme affinity for the substrate as defined by the substrate concentration at which the rate is half of V_{max}, was determined by non-linear regression fit of the Michaelis-Menten equation using GraphPad Prism (version 9.1.0).

Equation 2.1: The Michaelis-Menten equation. V, velocity (or rate); S, substrates; K_M, Michaelis constant; V_{max}, theoretical maximum rate

$$v = \frac{v_{max}[S]}{K_M + [S]}$$

The catalytic efficiency of Str was determined by calculating the catalytic constant and specificity constant, k_{cat} and K_m/k_{cat}, respectively. k_{cat} (s^{-1}), the number of product produced per unit of time, was calculated by dividing the V_{max} by the molar concentration of the Str monomer ($mol.L^{-1}$). The k_{cat} value was subsequently used to determine the specificity constant by dividing the k_{cat} by the K_M (M) value for each substrate.

2.2.7 Crystallisation of Str

2.2.7.1 Protein preparation

Sulfurtransferase was purified by IMAC and size exclusion chromatography purification as per sections 2.2.4.1 and 2.2.4.2, respectively. Protein concentration was determined by NanoDrop™ as per section 2.2.4.4. Protein was stored at 4 °C for a maximum of two days post-purification for use in crystal screens.

2.2.7.2 High-throughput crystallisation screens- sitting drop method

To identify promising conditions suitable for sulfurtransferase crystallisation, high throughput crystallisation screens were set up. Index^{TM}-HR2-144, PEGRxHT^{TM}-HR2-086, CrystalHT^{TM}-HR2-130 and the SaltRxHT^{TM}–HR2-136 (Hampton Research) screens were used for this purpose. Screens were set up in low profile 96 well Intelli-plate using the Mosquito crystallisation robot (TTP LabTech Ltd). Each crystallisation screen was pipetted into the reservoirs of an Intelli-plate. Each crystallisation condition has a reservoir solution of 100 µl and a 200 nl sitting drop of 200 nl. Protein drops consisted of a 1:1 ratio (100 nl: 100 nl) of concentrated protein and reservoir solution. Screens were initially checked within three to five days for crystal formation, then periodically afterwards using a dissection microscope.

Further crystallisation attempts included the addition of Str substrates, thiosulfate, glutathione, or cysteine, at saturating concentrations (final concentrations of 10 mM) to the concentrated protein stocks.

2.2.7.3 Crystallisation fine screens– hanging drop method

Promising crystallisation conditions from high throughput screens were optimised via hanging drop fine screens. For each condition, 24 well VDX trays were set up with 1000 µl of crystallisation solution which varied in pH and precipitant concentration relative to the original high throughput condition. Hanging drops were prepared by mixing a 1:1 ratio (1:1 µl) of reservoir solution and concentrated protein (containing substrates in concentrations as per 2.2.7.2) onto a siliconised coverslip. The coverslip was inverted (drop side down) over a well pre-lined with silicone grease. Crystallisation drops were monitored for crystal growth under a dissection microscope within the first five days and periodically thereafter.

2.2.7.4 Crystal preparation for X-ray diffraction

Using a cryo-loop, crystals were removed from the hanging drop, and flash cooled in liquid nitrogen. Crystals were stored in liquid nitrogen short-term prior to data collection.

2.2.7.5 Data collection

Crystal candidates were sent to the Australian Synchrotron (Melbourne, Victoria) to collect X-ray diffraction data on the MX2 beamline (McPhillips et al., 2002), equipped with an EIGER x 16M detector (Dectris, Switzerland).

2.3 Results and Discussion

2.3.1 Purification of Str

To biochemically characterise the activity of Str from *N. gonorrhoeae,* we first need to purify soluble and active protein. Purification of Str was optimised by Annmaree Warrender in the Hicks lab prior to this project commencing.

Str was successfully purified by IMAC and size exclusion chromatography (section 2.2.4) The chromatogram (280 nm) for the IMAC purification shows Str elutes at approximately 22-28 % elution buffer, corresponding to 220-280 mM imidazole (Figure 2.1a). Non-specific unbound proteins elute early in the elution gradient (flow-through). SDS-PAGE analysis (Figure 2.1b) indicates that the majority of Str was successfully removed from the cell pellet during sonication as there was little Str present in the pellet sample and the majority of *E. coli* proteins present in the supernatant were successfully removed during IMAC purification. As a result, the Str protein sequestered was relatively pure and was shown to be approximately 15 kDa (indicated by a black arrow in Figure 2.1b) via SDS gel assessment, consistent with the predicted molecular weight of the Str monomer (with His-tag) (14.29 kDa).

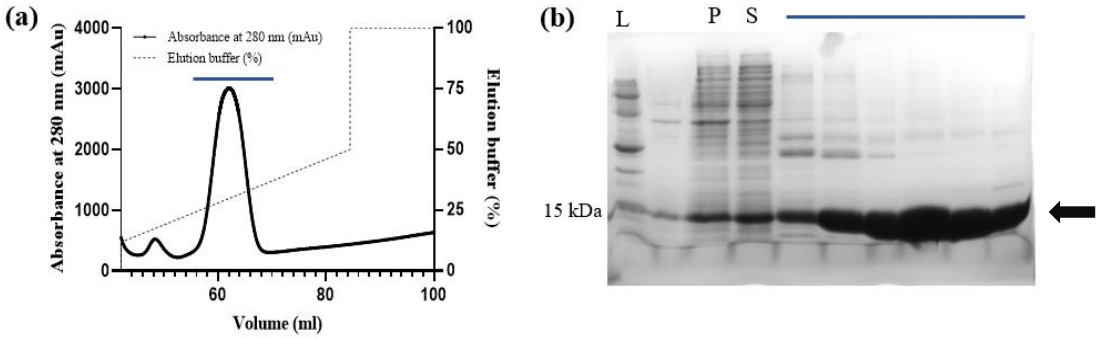

Figure 2.1: IMAC purification of Str at room temperature. (a) IMAC chromatogram of A_{280} nm, volume (x axis) and elution buffer concentration (%B, right axis). Data from 0-50 ml has been omitted for scaling purposes. (b) 15% SDS-PAGE gel of Str IMAC purification. Str protein labelled with a black arrow which is present in peak fractions (blue bar), the insoluble pellet (P), and the soluble supernatant (S). The Precision Plus Protein Standard (L) was used to identify Str by molecular weight.

Fractions containing IMAC purified Str (Figure 2.1, blue bar) were concentrated and underwent a second purification step via size exclusion chromatography as per section 2.2.4.2. Str elutes from a S75 16/60 size exclusion column as a single peak with an elution volume of 72 ml (Figure 2.2a), successfully yielding Str of high concentration and purity. Corresponding SDS-PAGE analysis demonstrates contaminating proteins present in the IMAC purified Str have been removed resulting in highly pure Str protein (Figure 2.2b).

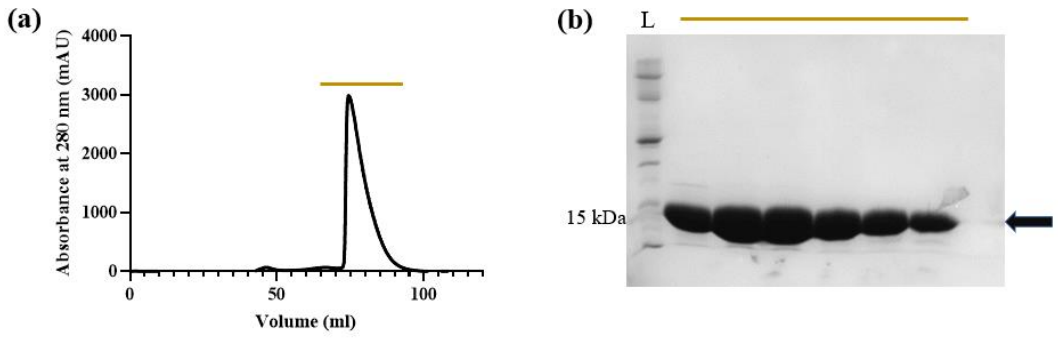

Figure 2.2: Size exclusion purification of Str at room temperature. (a) S75 16/60 size exclusion chromatogram showing the elution of a single, large peak at 72 ml. (b) 15% SDS-PAGE gel analysis of size exclusion peak fractions (yellow bar) showing a high yield and successfully isolated Str (black arrow). The Precision Plus Protein ladder (L) was used as the standard.

2.3.2 Purification of PspE

To conduct preliminary activity assessment of PspE from *N. gonorrhoeae*, we first needed to purify soluble and active protein. Purification of PspE was achieved using the IMAC and SEC protocols established for Str. However, the purification process revealed that expression of PspE in *E. coli* was extremely poor. As the aim of PspE purification herein was to conduct a preliminary analysis of PspE activity, a high enough yield was achieved for this purpose by combining three cell pellets from 1 L expression cultures (section 2.2.3) for purification.

The chromatogram for the IMAC purification of PspE demonstrates PspE elutes at approximately 25-31% elution buffer, corresponding to 250–310 mM imidazole (Figure 2.3a). Non-specific, unbound proteins elute early in the elution gradient (flow-through). SDS-PAGE analysis (Figure 2.3b) indicates that the majority of PspE was successfully removed from the cell pellet during sonication and the majority of *E. coli* proteins present in the supernatant were successfully removed during IMAC purification. As a result, the PspE protein sequestered was relatively pure and was shown to be approximately 15 kDa (indicated by a red arrow in Figure 2.3b), consistent with the predicted molecular weight of the PspE monomer (with His-tag) (15.279 kDa).

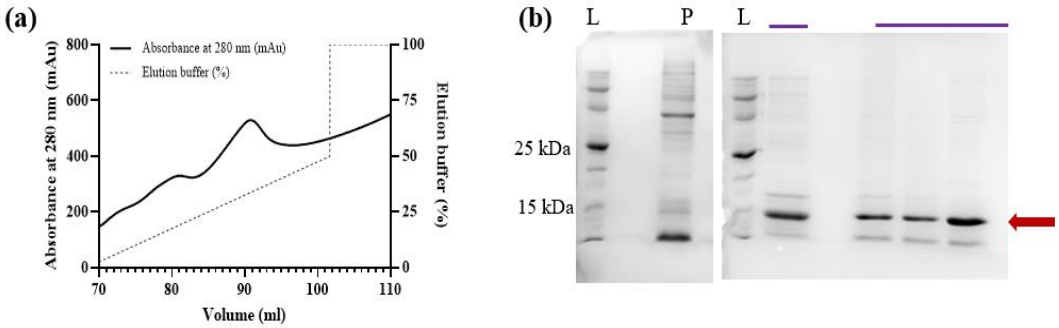

Figure 2.3: IMAC purification of PspE at room temperature. (a) IMAC chromatogram of A_{280} nm, volume (x axis) and elution buffer concentration (%B, right axis). Data from 0-70 ml has been omitted for scaling purposes. (b) 15% SDS-PAGE gel of PspE IMAC purification. PspE protein labelled with a red arrow which is present in peak fractions (purple bar) and absent in the insoluble pellet (P). The Precision Plus Protein Standard (L) was used to identify PspE by molecular weight.

Fractions containing IMAC purified PspE (Figure 2.3a, purple bar) were concentrated and underwent a second purification step via size exclusion purification as per section 2.2.4.2. PspE eluted from the S75 16/60 size exculsion column as two, small peaks at 44-52 and 73-83 ml (Figure2.4a), which was observed on both attempts for PspE purification. Fractions corresponding to each peak were run on a 15% SDS-PAGE gel for visual assessment. Curiously, both peaks produced a protein band at the expected size (~15 kDa). As the second peak eluted at ~74-80 ml, similar to the elution volume of Str (72 ml) (Figure 2.2b) which is very similar molecular weight (15.279 kDa and 14.29 kDa respectively), it's therefore likely that the second peak corresponds to the PspE monomer. However, the earlier peak, which suggests a slightly larger molecular weight (as it eluted earlier in the elution profile), is yet to be determined although could correspond to PspE being in a persulfide form as previously described (Cheng, 2003; Cheng et al., 2008).

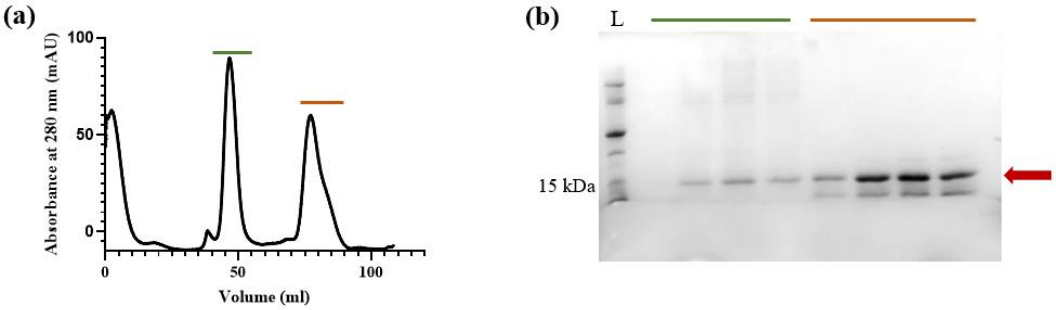

Figure 2.4: Size exclusion purification of PspE at room temperature. (a) S75 16/60 size exclusion chromatogram showing the elution of a two small peaks, the first at 44-50 ml and the second at 72-80 ml. (b) 15% SDS-PAGE gel analysis of the two SEC peak fractions (peak one represented by green bar and peak two represented by an orange bar), showing a low yield and successful isolation of PspE (red arrow). The Precision Plus Protein ladder (L) was used as the standard.

2.3.3 Conservation of active site amino acids in PspE and Str

Many single domain sulfurtransferases have the active site motif CRXGX[R/T], with the catalytic cysteine highly conserved. PspE from *N. gonorrhoeae* has the sequence CRSGRR, and Str from *N. gonorrhoeae* has the active site motif CHHGIR, with a histidine and position two instead of an arginine. To investigate

conservation of the active site motif across single domain sulfurtransferases from bacteria we downloaded 500 sulfurtransferase sequences (most annotated as either GlpE or PspE). A ClustalW multiple sequence alignment of the 500 sequences demonstrates there is little sequence conservation across the family (Figure 2.5). The active site motif is in fact more variable than predicted active site motif, with positions one (cysteine) and four (glycine) highly conserved. There are other highly conserved amino acids in this family of proteins, although the function of these at this point is unknown.

The Str sulfurtransferase from *N. gonorrhoeae* clusters with the GlpE sulfurtransferase family members and has 26.2% identity to the GlpE protein from *E. coli*. Whereas the PspE sulfurtransferase from *N. gonorrhoeae* clusters with PspE sulfurtransferase family members. This is consistent with many bacteria species having two sulfurtransferases belonging to the GlpE and PspE families and is interesting as the two sulfurtransferases from *N. gonorrhoeae* have 27.7% sequence identity.

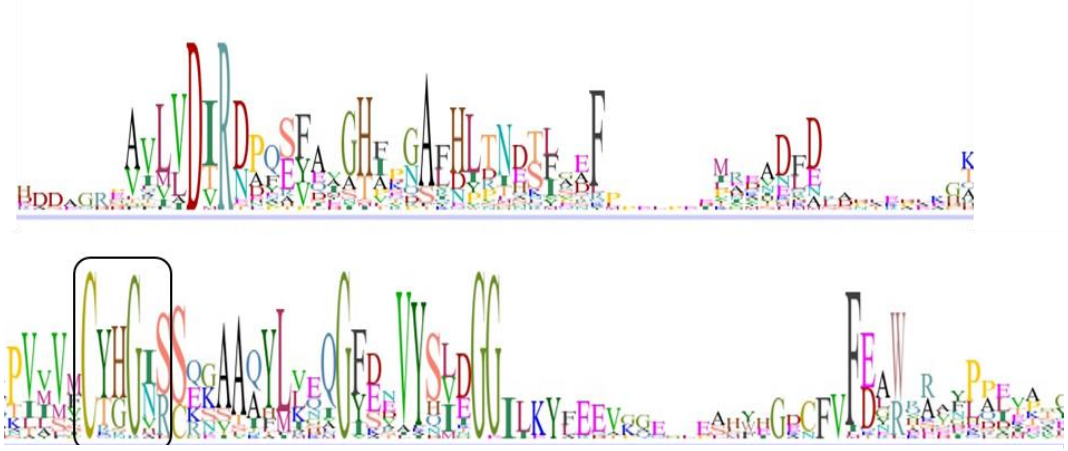

Figure 2.5: Sequence logo of sulfurtransferase sequence alignment. The sequence logo was generated by ClustalW alignment of 500 sulfurtransferase sequences from bacteria using Geneious Version 7.1.9 (Biomatters). The height and width of letters (corresponding to amino acids) in the sequence logo represents the presence of the amino acid at that position. Black box indicates active site motif.

Both Str and PspE sulfurtransferase from *N. gonorrhoeae* contain the highly conserved catalytic cysteine and the highly conserved glycine in position four. We subsequently investigated enzyme activity of these enzymes from *N. gonorrhoeae*.

2.3.4 Assay optimisation

2.3.4.1 Thiosulfate-thiol sulfurtransferase activity assay optimisation

The lead acetate assay has previously been used in numerous studies to determine thiosulfate-thiol sulfurtransferase activity by monitoring the formation of lead sulfide at 390 nm. Herein we performed the assay in an automated stopped flow spectrophotometer which mitigates the drawbacks of manual operation, including imprecise time control and inconsistencies in substrate or product concentration measurements at the initial stage of the reaction (Hartwell & Grudpan, 2012). We first embarked to optimise this assay in the stopped flow spectrophotometer. We adopted the stopped flow sequence protocol previously optimised and established by Emma Walker (University of Waikato) which includes five 0.2 s dummy shots between each reaction which eliminates residual components in the reaction chamber from the previous reaction. All optimisation trials were performed for varying thiosulfate concentrations and constant glutathione concentration of 50 mM.

The first thing to note about this assay is that it is relatively complicated as lead sulfide (the measured product) forms as the product of three sequential reactions. Firstly, glutathione is converted to glutathione persulfide catalysed by the sulfurtransferase, which then reacts spontaneously with a second glutathione molecule to form oxidised glutathione and hydrogen sulfide which in turn reacts with lead acetate to form lead sulfide, the colourimetric product (reaction 5).

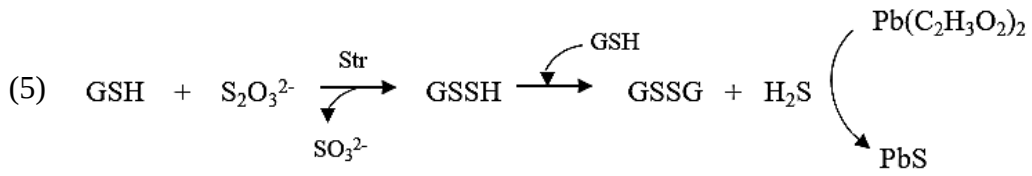

Initial trials were conducted by initiating the reaction with 10 µg of Str with the reactions proceeding for 50 s. In the resulting raw data, at low thiosulfate concentrations the profile is reminiscent of burst phase kinetics (Figure 2.6a). Whereas a peculiar shape was observed for thiosulfate concentrations upward of 5 mM (Figure 2.6b).

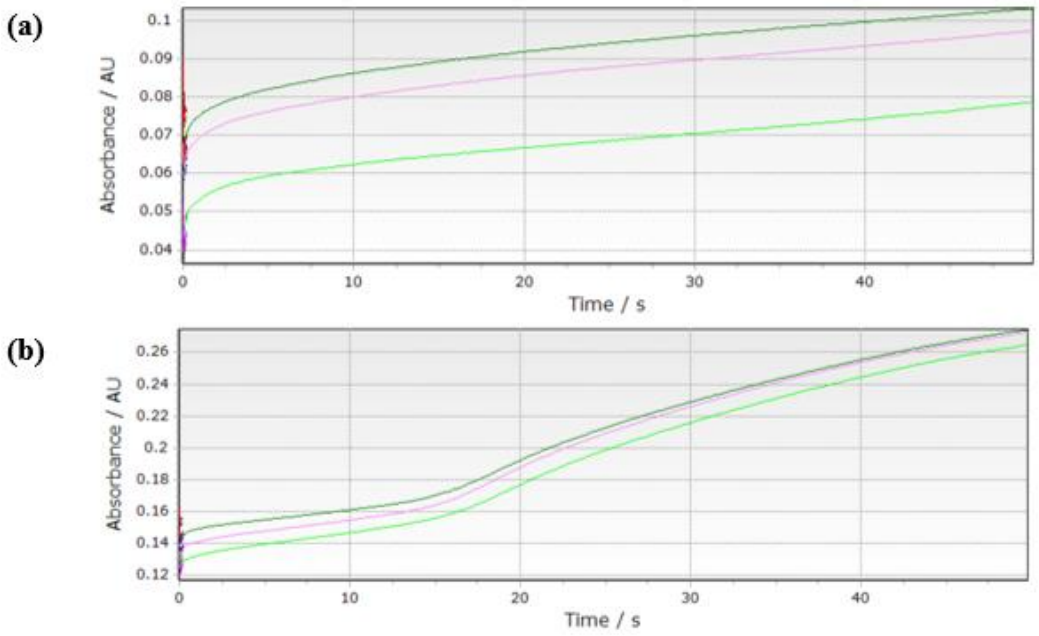

Figure 2.6: Raw stopped flow data reaction example for 50 s. The reactions depicted were carried out in the stopped flow at 37 °C. Absorbance (y axis) was monitored at 390 nm for 50 s (x axis). For both reactions, glutathione concentration was constant at 50 mM. (a) reaction contains 0.5 mM thiosulfate and resembles burst phase kinetics. (b) Reaction contains 15 mM and shows the peculiar shape observed.

We first ruled out any unaccounted-for spontaneous reactions occurring in the assay system as contributing to this effect by testing the reaction mix without enzyme and with sulfite (a product of the enzymatically catalysed step) in lieu of thiosulfate which resulted in no change in absorbance and therefore no reaction occurring (data not shown). Following this, the reaction time was increased to 90 s to get a better visual on what was occurring at the later phase of the reaction. The same shape was subsequently observed and formed a 'bump' like shape where an initial 'lag' phase precedes the first linear phase (slope (i) in Figure 2.7) which begins to plateau followed by a second linear phase (slope (ii) in Figure 2.7).

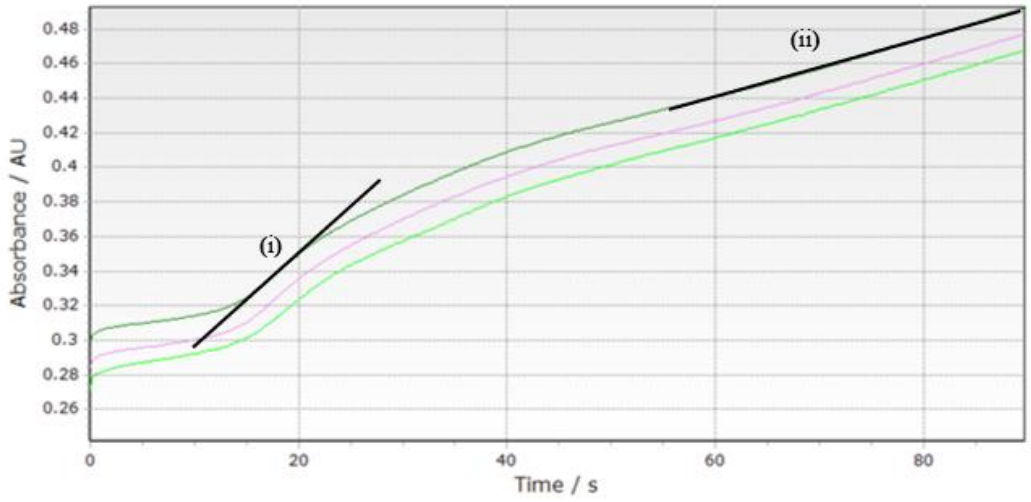

Figure 2.7: Raw stopped flow data reaction example for 90 s. The reaction depicted is at 15 and 50 mM for thiosulfate and glutathione, respectively. The reaction was performed at 37 °C and proceeded for 90 s (x-axis), monitoring the absorbance (y-axis) at 390 nm. (i) Line showing the first slope (or enzymatic phase) and the second line (ii) showing the second linear phase (or chemical phase).

The two gradients observed in the raw data (Figure 2.7 i and ii) were analysed separately by plotting rate ($mM.s^{-1}$) of slope over each substrate concentration ($[S_2O_3^{2-}]$ 0.25-60 mM) to investigate the 'bump-like' observation in the raw data. Data were not collected for thiosulfate concentrations from 0.25-4 mM for the second gradient analysis as at these concentrations the second slope was not present.

Analysis of the first slope across different thiosulfate concentrations (Figure 2.7 i) resulted in a Michaelis-Menten curve (Figure 2.8a) while the second slope (Figure 2.7 ii) yields a straight line (Figure 2.8b) indicative of a chemical reaction, named the enzymatic phase and chemical phase, respectively.

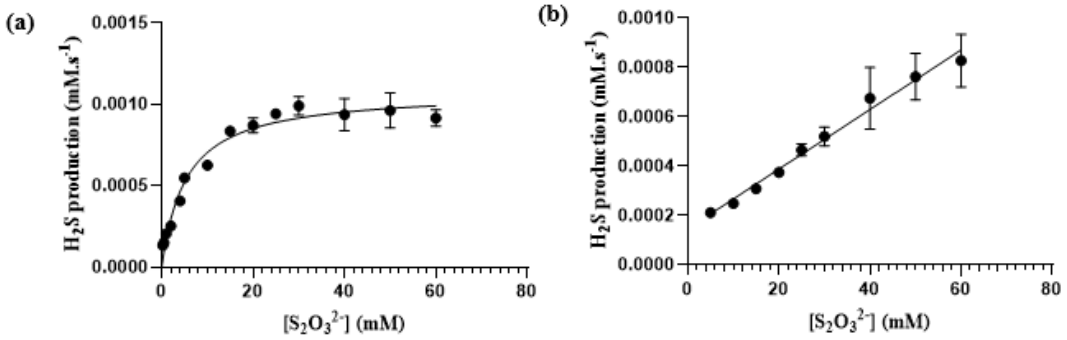

Figure 2.8: Analysis of the raw data gradients. The velocity of two gradients (y-axis) for the raw date reactions for each concentration of thiosulfate (0.6-60 mM, x-axis) were determined separately and plotted. Reactions were carried out in the stopped flow at 37°C and proceeded for 90 s. All data points are averages with standard deviations (error bars) from three replicate. Both model fits had an R^2 value greater the 0.92. (a) Plot of the first slope (Figure 2.7 i) resulting in a Michaelis-Menten curve. (b) Plot of the second slope (Figure 2.7 ii) resulting in a linear regression indicative of a chemical reaction.

One explanation for what might be occurring in the assay system is that the initial (or pre-enzymatic) phase of the reaction represents a burst-phase or system equilibrium phase. The second (or enzymatic) phase is governed by the enzymatic step of the reaction which begins to plateau due to depleting thiosulfate concentrations. As glutathione is saturating, in the final (or chemical) phase, the chemical reaction of unreacted GSSH build up to H_2S, and subsequently H_2S to PbS, is observed. In support of this, the chemical phase is absent in reactions when glutathione is less saturating (10 mM), however, modelling of the assay system is required to confirm this hypothesis.

Attempts were made to reduce the confounding effects present within the reaction system by trialling reduced enzyme concentrations of 1 µg and 0.4 µg with the aim to reduce the build-up of reaction intermediates such as GSSH which may contribute to altering the flux of the assay system through to the chemical phase. Additionally, the reaction set-up was altered to initiate the reaction with thiosulfate as opposed to enzyme (reasoning in section 2.3.4.1). Together, these changes mitigated the 'bump-like' formation except at very high thiosulfate concentration (30 mM and 50 mM) and hence established the protocol used to determine Michaelis-Menten kinetics.

2.3.4.2 Cyanide detoxification assay optimisation

As the cyanide detoxification assay is a stopped assay, prior to collecting initial velocity data for Michaelis-Menten kinetics, we first needed to establish an appropriate enzyme concentration coupled with appropriate reaction times to ensure the linear velocity stage of the reaction was captured. This was accomplished by conducting time trials at low (1 mM) and high (50 mM) thiosulfate concentrations with the cyanide concentration kept constant at 50 mM. Data were collected in triplicates at the following time points; 10, 30, 60 and 120 seconds. Assays were carried out as per section 2.2.5.3 at 37 °C.

Enzyme concentrations of 15 µg and 1 µg were trailed, initially with substrate concentrations 50 mM thiosulfate and 50 mM glutathione. The resulting plot of absorbance versus time was unsuccessful in capturing initial velocity when the enzyme concentration was 15 µg (data not shown) while the 1 µg enzyme condition plot was linear, indicating that a combination of any time points would suffice to capture initial velocity. This was consistent for low substrate concentration (1 mM thiosulfate) (Figure 2.9), thus, thirty and sixty seconds, or zero and thirty seconds, was chosen for practical reasons as ten seconds was practically challenging and prone to a greater margin of human error.

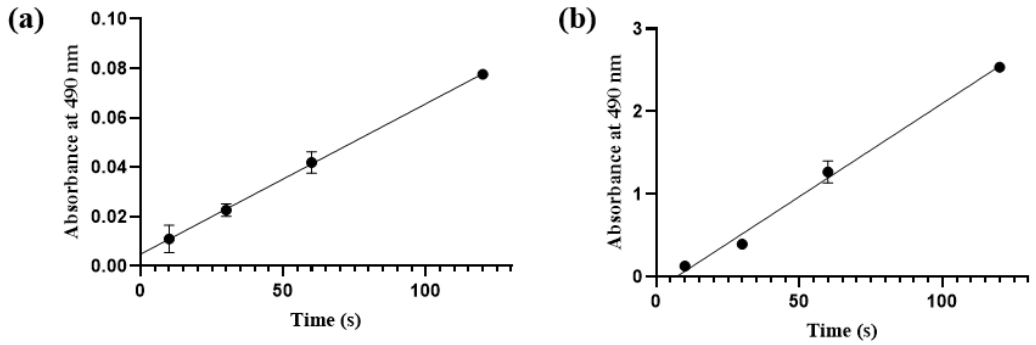

Figure 2.9: Cyanide detoxification assay time trials. Absorbance (y axis) of thiocyanate formation was monitored at 460 nm for 120 s (x axis). All data points are averages with standard deviations (error bars) from three replicates. Both time trials had a cyanide concentration of 50 mM. Time trials were performed for (a) low thiosulfate concentration (1 mM) and (b) high thiosulfate concentrations (50 mM) to ensure time points chosen would suffice for the concentration range 1-50 mM substrate.

2.3.5 Investigation of enzyme mechanism

Enzyme mechanism was considered early in our biochemical characterisation investigation due to the unusual behaviour observed in the raw thiosulfate-thiol sulfurtransferase activity assay data. This information was required to inform the optimisation of this assay protocol in the stopped flow.

The formal enzymatic mechanism of rhodanese activity with thiosulfate and cyanide is known to proceed via an ordered double-displacement mechanism in which the literature is endowed with evidence for numerous rhodaneses (Cheng, 2003; Cheng et al., 2008; Adams et al., 2002; Westley et al., 1983). Thiosulfate enters the active site and donates a sulfur atom to the catalytic cysteine residue, forming a covalently substituted sulfur-enzyme persulfide intermediate and discharging sulfite. The enzyme persulfide is subsequently attacked by cyanide, forming, and releasing thiocyanate thereby regenerating the free enzyme (Westley et al., 1983; Cheng et al., 2008). In comparison, the formal mechanism of thiosulfate-thiol sulfurtransferases (transfer of sulfur from thiosulfate to thiols) is distinct from rhodaneses and proceeds via an ordered single displacement mechanism, whereby both substrates form a ternary complex with the enzyme, with the thiol acceptor being the leading substrate (Chauncey & Wesley, 1983). The products are released from the ternary complex in an unspecified (as not yet proven) order. Notably, in this mechanism the attacking sulfhydryl nucleophile that cleaves the sulfur-sulfur bond of thiosulfate belongs to the thiol acceptor substrate in contrast to the double-displacement mechanism where the nucleophile is supplied by the active site cysteine residue of the enzyme.

As some rhodaneses display both traditional rhodanese activity in addition to thiosulfate-thiol sulfurtransferase activity, the corresponding formal mechanism for the different thiol acceptor substrates has thus far been investigated in one study, to the best of our knowledge. The authors of this analysis show that enzyme mechanism varies with the thiol acceptor substrate employed (Aird, Heinrikson & Westley, 1987). When cyanide is the thiol acceptor substrate, the reaction proceeds as expected for rhodanese. However, in the presence of glutathione the reaction proceeds via an ordered single displacement mechanism, reminiscent of the thiosulfate-thiol sulfurtransferase formal mechanism.

The formal mechanism with glutathione present was briefly investigated for Str as future analysis of the kinetic data intends to model the assay system in Cell ML to aid in explaining the unusual shape we observed within of thiosulfate-thiol sulfurtransferase activity assay, in addition to informing assay optimisation (section 2.3.4.1). Activity assays were carried out as per section 2.2.5.1 for various thiosulfate concentrations (0.25-50 mM) with glutathione held constant at 10 mM or 50 mM. Rates were determined at each thiosulfate concentrations ($mM.s^{-1}$). Data were transformed by inverting thiosulfate substrate concentration and velocity to generate a double-reciprocal plot of the data at each glutathione concentration, producing a Lineweaver-Burk plot. The resulting Lineweaver-Burk plot of this preliminary assessment is indicative of a single displacement mechanism whereby a ternary complex is formed as indicated by converging linear regressions line (Figure 2.10), which also represent the theoretical K_m value for glutathione (approximately 0.64 mM). While this is consistent with the conclusions from (Aird, Heinrikson & Westley, 1987), additional data is required at various other glutathione concentrations to further support this notion.

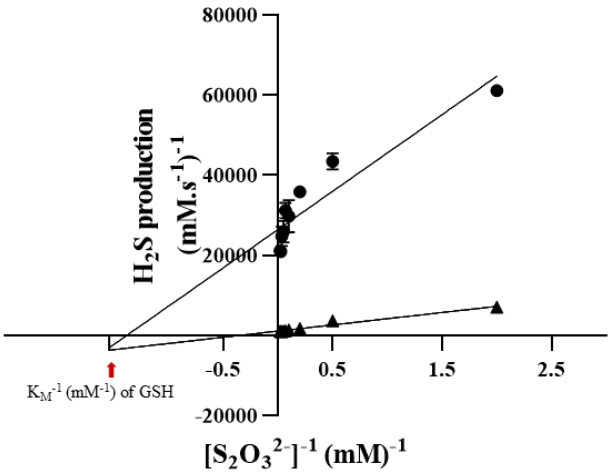

Figure 2.10: Double reciprocal plot of Str with thiosulfate and glutathione. Thiosulfate was varied from 0.5-50 mM at constant glutathione concentrations of 10 mM (●) and 50 mM (▲). The red arrow represents the theoretical K_M value of glutathione as $1/K_M$

2.3.5.1 Effect of enzyme mechanism in thiosulfate-thiol sulfurtransferase activity assays

Assuming that Str activity with thiosulfate and cyanide proceeds via the double-displacement mechanism as per all other rhodaneses, this means, with respect to the thiosulfate-thiol sulfurtransferase activity assays, there are two possibilities of substrate interaction with the enzymatic catalytic site (Figure 2.11). The first possibility is the sulfur transfer from thiosulfate to the catalytic cysteine residue of the enzyme, producing enzyme persulfide and sulfite thereby occupying the active site. Without an available thiol acceptor, the enzyme persulfide and sulfite will be converted back to thiosulfate and free enzyme. The second possibility is the binding of glutathione in the active site of the free enzyme, allowing catalysis of the sulfur transfer from thiosulfate to glutathione. Thus, both thiosulfate and glutathione compete for the active site. While any effect this may be having in the thiosulfate-thiol sulfurtransferase activity assays is minimal when glutathione is saturating and thiosulfate concentrations are low to moderate, the amount of free enzyme available for glutathione to bind may be lessened when thiosulfate is saturating, and glutathione concentrations are low to moderate. As such, the assay set up was altered to initiate with thiosulfate as opposed to enzyme which aimed to mitigate thiosulfate monopolising the enzyme active site. This assay set-up was employed for all substrate concentration gradients for continuity purposes.

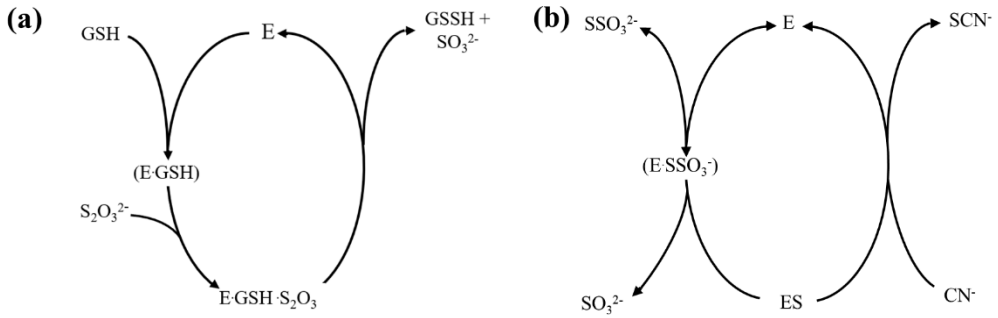

Figure 2.11: Hypothesised reaction scheme for Str catalysis in the presence of different thiol acceptor substrates. (a) ordered single displacement mechanism when glutathione (or other thiols) are the thiol acceptor substrates. (b) ordered double-displacement mechanism when cyanide is the thiol acceptor substrate.

2.3.6 Kinetic characterisation of Str

As the physiologically relevant reactions catalysed by Str are currently unknown, the efficiency of Str to catalyse the sulfur transfer from thiosulfate to an array of thiol acceptor substrates was examined at physiologically relevant conditions (pH 7.4 and 37 °C) with the aim to identify physiological relevant substrates for Str in *N. gonorrhoeae*. Michaelis-Menten analysis was performed for the thiol donor and thiol acceptor pairs by varying one substrate (0.5-50 mM) whilst keeping the other substrate constant (50 mM) (section 2.25 and 2.2.6). The affinity for different substrates was determined from the dependence of the reaction rate on substrate concentration.

2.3.6.1 Thiosulfate-thiol sulfurtransferase activity

The efficiency of Str to catalyse sulfur transfer from thiosulfate to low-molecular weight thiol acceptors (glutathione, cysteine, and homocysteine) was determined by monitoring the formation of H_2S at 390 nm (Figure 2.12).

Rate versus substrate concentration plots, fitted with the Michaelis-Menten model (Equation 2.1), for glutathione (50 mM) with varying thiosulfate concentration (0.5-50 mM) and the inverse; thiosulfate (50 mM) with varying glutathione concentrations (0.5-50 mM), obey Michaelis-Menten kinetics (Figure 2.12a and b), with an R^2 value of 0.98 and 0.84, respectively. From these plots, the following kinetic parameters of thiosulfate:glutathione sulfurtransferase activity were obtained: $K_{M\ (thiosulfate)}$ 6.29 ± 0.6 mM, $K_{M\ (glutathione)}$ 3.731 ± 0.7 mM, and k_{cat} 2.755 s^{-1} (Table 2.5). Given the high intracellular glutathione concentrations within *N. gonorrhoeae* (upward of 15 mM) (Seib et al., 2006), the physiological relevance for glutathione as a substrate for Str is supported based on the high affinity for glutathione (K_M = 3.731 ± 0.7 mM). In addition, the catalytic efficiency determined for thiosulfate:glutathione activity, albeit low, is within the vicinity of those previously reported and of particular interest, comparable to the rhodanese domain of the PRF protein in *Burkholderia. phytofirmans* (k_{cat} = 9.0 s^{-1}) (Table 2.4) for which the physiological relevance of thiosulfate:glutathione sulfurtransferase activity is evidently supported (Motl et al,. 2017).

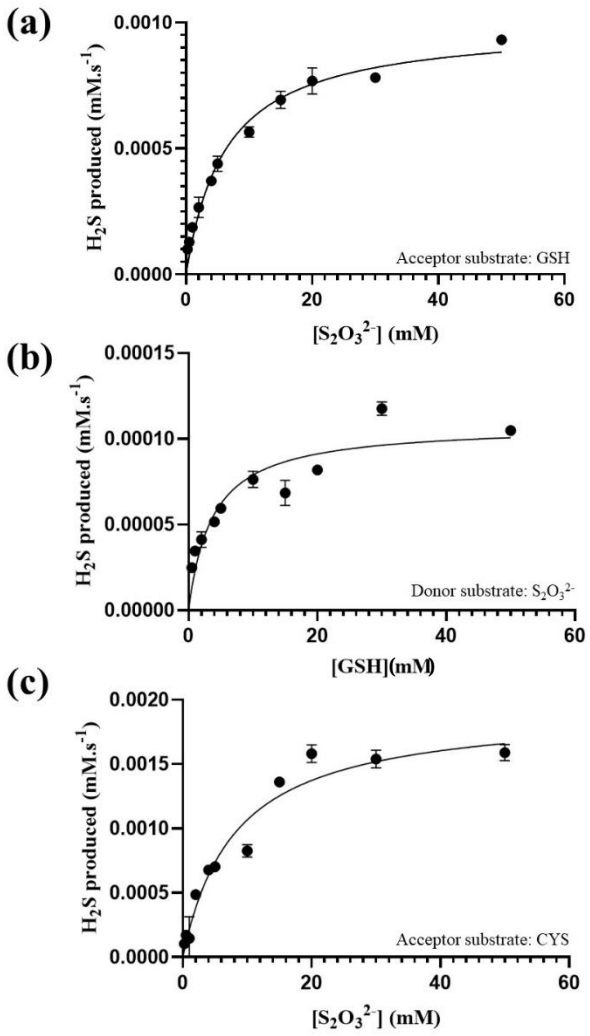

Figure 2.12: Kinetic analysis of Str thiosulfate-thiol sulfurtransferase activity. Str sulfurtransferase activity was determined in the presence of varying thiosulfate concentrations (0.5-50 mM) at constant concentrations (50 mM) of (a) glutathione (GSH) and (c) cysteine. (b) Dependence of the reaction rate on glutathione concentrations (0.5–50 mM) was determined in the presence of 50 mM thiosulfate. All data were fitted with the Michaelis–Menten equation (solid line) The R^2 values for the Michaelis-Menten model are 0.98, 0.84, and 0.95 for (a), (b), and (c), respectively. All data points are averages with standard deviations (error bars) from three replicates.

Rate versus substrate concentration plots for cysteine (50 mM) as a thiol acceptor with varying thiosulfate concentration (0.5-50 mM) also obey Michaelis-Menten kinetics (R^2 = 0.95). The kinetic parameters $K_{M\ (thiosulfate)}$ 8.084 ± 1.2 and k_{cat} 2.013 s^{-1}, where obtained and are comparable to Str thiosulfate:glutathione

sulfurtransferase activity (Table 2.5) and the thiosulfate:cysteine sulfurtransferase activity of the PRF enzyme from *B. phytofirmans*. At least four independent data sets were collected with varying cysteine concentration at a constant thiosulfate concentration (50 mM) to determine Str affinity for cysteine. However, all attempts in analysis, examining rate as a function of cysteine concentration, resulted in non-Michaelis-Menten kinetics (Figure 2.13a). We were, therefore, unable to determine Str substrate affinity for cysteine.

Homocysteine as a thiol acceptor with the substrate thiosulfate was also tested. Rate data were collected at varying homocysteine concentrations (0.5-20 mM), with a constant thiosulfate concentration (50 mM). Due to a limited amount of homocysteine substrate, data were not collected for higher homocysteine concentrations (30-50 mM) as done for the other thiol substrates, nor were we able to collect data for varying thiosulfate concentrations and a constant homocysteine concentration. As was the case for cysteine concentration gradients, we were unable to determine Michaelis-Menten kinetics for homocysteine as the acceptor substrate for the same reasons outlined above (Figure 2.13b). We speculate that the non-Michaelis-Menten behaviour observed for homocysteine and cysteine gradients is due to confounding effects in the thiosulfate-thiol sulfurtransferase activity assay which will require further optimisation to determine the Michaelis-Menten kinetic parameters for these thiol acceptor substrates. As the K_M value for thiosulfate (K_M = 8.08 ± 1.2 mM) in the presence of cysteine was obtained, and saturating conditions typically defined as 2 × K_M, trialling lower thiosulfate concentrations of 16 mM (as opposed to 50 mM) for varying cysteine concentrations (0.5-50 mM) would be a promising place to start.

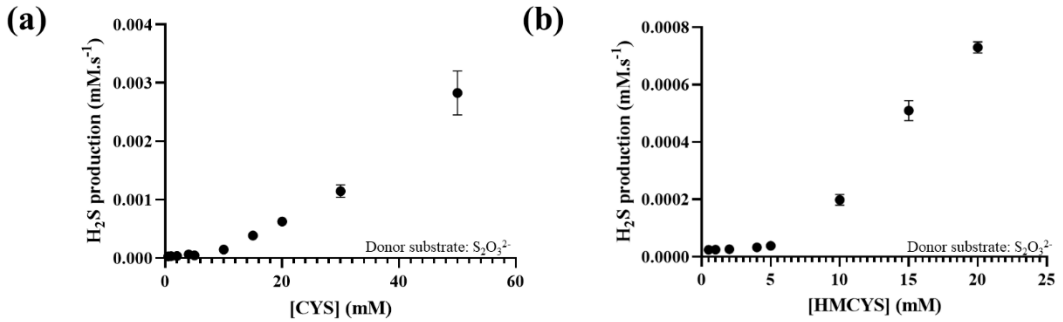

Figure 2.13: Kinetic plots of thiol acceptor substrates cysteine and homocysteine. Str sulfurtransferase activity was determined in the presence of constant thiosulfate concentration (50 mM) and (a) varying cysteine (Cys) concentrations (0.5-50 mM) and (b) varying homocysteine (HMCYS) concentrations (0.5-20 mM). Dependence of the reaction rate on thiol acceptor substrates are plotted showing non-Michaelis-Menten kinetics. All data points are averages with standard deviations (error bars) from three replicate.

Although additional data and assay optimisation is required to determine thiol substrate preference, we show that Str demonstrates substrate ambiguity with respect to thiols as the thiol acceptor substrate, evident by confirmation of thiosulfate-thiol sulfurtransferase activity with cysteine, homocysteine, and glutathione. The kinetic data presented supports the physiological relevance of Str sulfurtransferase activity with substrates thiosulfate and glutathione. While the notion that glutathione is required for sulfur acquisition for the synthesis of cysteine and other downstream important thiol containing compounds such as glutathione, could be counterintuitive, the substrate ambiguity demonstrated by Str with respect to thiols as the acceptor substrates advantageously allows scavenging of available resources for sulfur acquisition (Pandya et al., 2014). It should also be noted that the oxidised glutathione product is regenerated back to two glutathione molecules by glutathione reductase (Gor) in the presence of NADPH, and therefore is not consumed by the reaction, instead, acts as means to liberate sulfide from thiosulfate.

Table 2.4: Comparison of sulfurtransferase kinetic parameters.
[a]PRF is a multidomain protein containing a catalytic rhodanese module. Reported values in this table are for the isolated rhodanese module of this enzyme, which are comparable to the multidomain activity. [b]YrkF is a double domain sulfurtransferase enzyme, with both domains containing a catalytic Cys residue.

Organism (enzyme)	K_m donor *mM*	K_m acceptor *mM*	k_{cat} s^{-1}	k_{cat}/K_m donor $M^{-1}s^{-1}$	k_{cat}/K_m acceptor $M^{-1}s^{-1}$	Reference
Thiol donor substrate: $S_2O_3^{2-}$, thiol acceptor substrate: GSH						
N. gonorrhoeae MS11 (Str)	6.292	3.731 ± 0.7	2.675	4.25×10^3	7.17×10^3	This work
H. sapiens (TSTD1)	17 ± 1	11 ± 1	0.432	25.41	39.27	(Libiad et al., 2018)
B. phytofirmans (PRF*)	3.8 ± 0.5	14.9 ± 0.5	9.0	2.37×10^3	6.04×10^2	(Motl et al., 2017)
Thiol donor substrate: $S_2O_3^{2-}$, thiol acceptor substrate: Cys						
N. gonorrhoeae MS11 (Str)	8.084	ND	2.013	249.01	ND	This work
H. sapiens (TSTD1)	14 ± 2	13.7 ± 1.9	0.7	50	51	(Libiad et al., 2018)
B. phytofirmans (PRF[a])	3.1 ± 0.1	6.1 ± 0.4	0.8	258.06	131.18	(Motl et al., 2017)
Thiol donor substrate: $S_2O_3^{2-}$, thiol acceptor substrate: CN^-						
N. gonorrhoeae MS11 (Str)	17.66	14.3	108.04	6.12×10^3	7.56×10^3	This work
H. sapiens (TSTD1)	22 ± 3	0.27 ± 0.02	0.52	24	1.94×10^3	(Libiad et al., 2018)
B. phytofirmans (PRF*)	9.2 ± 0.8	23 ± 1	4.6	500	200	(Motl et al., 2017)
E. coli (PspE)	2.7	32	64	2.37×10^4	2.0×10^3	(Cheng et al., 2008)
E. coli (GlpE)	78	17	115	1.47×10^3	6.76×10^3	
B. subtilis (YrkF[b])	1	30	81	8.1×10^4	2.7×10^3	(Hunt, 2004)

2.3.6.2 Thiosulfate:cyanide sulfurtransferase activity

The capacity of Str to detoxify cyanide was determined by the formation of thiocyanate at 460 nm (Figure 2.14). Rates versus substrate concentration plots were fitted with the Michaelis-Menten model (Equation 2.1) for varying thiosulfate concentration (0.5-50 mM) with cyanide constant (50 mM) and the inverse; varying cyanide concentrations (0.5-50 mM) with thiosulfate constant (50 mM) also obey Michaelis-Menten kinetics (R^2 = 0.90 and 0.96 for Figure 2.14a and b, respectively). The following kinetic parameters for cyanide detoxification activity of Str was obtained: $K_{M\ (thiosulfate)}$ 17.66 ± 4.5 mM, $K_{M\ (cyanide)}$ 14.3 ± 2.4 mM and k_{cat} 108.04 s^{-1} (Table 2.5).

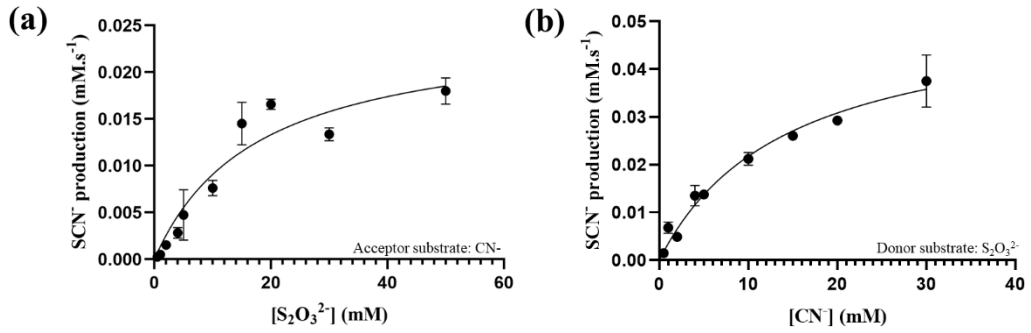

Figure 2.14: Kinetic analysis of Str thiosulfate:cyanide sulfurtransferase activity. Str sulfurtransferase activity was determined in the presence of (a) varying thiosulfate concentrations (0.5-50mM) at constant concentrations of cyanide (50 mM), (b) varying cyanide concentrations (0.5-50 mM) a constant thiosulfate concentration (50 mM). Dependence of rate on substrate concentrations was plotted and fitted with the Michaelis-Menten equation. (R^2 = 0.90 and 0.96 for (a) and (b), respectively) All data points are averages with standard deviations (error bars) from three replicate.

Interestingly, the affinity for the substrate thiosulfate (K_M 17.66 ± 4.5 mM) with cyanide as an acceptor is notably lower than the affinity observed when thiols (glutathione K_M 6.292 ± 0.6 mM and cysteine K_M 8.084 ± 1.2 mM) were the acceptor substrates (Table 2.5). As the interaction of thiosulfate with the active site varies dependent upon the thiol acceptor employed (section 2.3.4), the observation that the affinity for thiosulfate is higher when thiols are present is indicative of preferential binding for the active site when the single displacement mechanism is employed, which is reliant on glutathione (or thiols) binding first versus the double-

displacement mechanism in which thiosulfate enters the active site first. The preference for this mechanism supports the physiological relevance of thiosulfate-thiol sulfurtransferase activity over cyanide detoxification.

Table 2.5: Kinetic parameters for Str.

V_{max} values were determined with an enzyme concentration of 1 µg. ND= not determined

	Thiol donor/thiol acceptor		
Kinetic parameter	$S_2O_3^{2-}$ / GSH	$S_2O_3^{2-}$ / Cys	$S_2O_3^{2-}$ / CN
V_{max} ($mM.s^{-1}$)	$9.0x10^{-4} \pm 2.8\times10^{-5}$ / $9.0x10^{-4} \pm 5.5\times10^{-6}$	$1.9 \times10^{-3} \pm 9.9x10^{-5}$ / ND	0.025±0.03 / 0.05 ± 0.004
K_M (mM)	6.292 ± 0.6 / 3.731 ± 0.7	8.084 ± 1.2 / ND	17.66 ± 4.5 / 14.3 ± 2.4
k_{cat} (s^{-1})	2.675	2.013	108.04
k_{cat}/K_M ($M^{-1}.s^{-1}$)	4.25×10^3 / 7.17×10^3	2.49×10^2 / ND	6.12×10^3 / 7.56×10^3

Offering additional support to this notion, Str affinity for cyanide is particularly low (K_M =14.3 ± 2.4 mM) consistent with previous reports for single domain rhodaneses (Table 2.5), making the physiological relevance of this reaction dubious. Of the thiol acceptors examined, reaction with thiosulfate and cyanide does, however, have the highest catalytic efficiency (k_{cat}=108.04 s^{-1}), comparable to those determined for bacterial single domain rhodaneses, PspE (k_{cat} = 64 s^{-1}) and GlpE (k_{cat} = 115 s^{-1}) from *E. coli* (Table 2.5). However, for both PspE and GlpE in *E. coli*, the catalytic capabilities of cyanide detoxification *in vitro* does not confer cyanide resistance *in vivo* as assessed by phenotypic characterisation of Δ*pspE*, Δ*glpE*, Δ*pspE*Δ*glpE* mutant strains (Cheng et al., 2008). Based on the low affinity of Str for cyanide, and the unlikelihood of *N. gonorrhoeae* encountering cyanide within its primary environmental niche (urogenital tract) under normal conditions, it is unlikely that cyanide detoxification is a relevant physiological role for Str in *N. gonorrhoeae*. It

is more feasible that the *in vitro* activity of Str with cyanide is a promiscuous function, defined as enzyme activity other than for which its evolved that is irrelevant to the organism's physiology (Khersonsky and Tawfik, 2010). Interestingly, it's hypothesised that a physiologically irrelevant promiscuous function of an enzyme represents the divergence point for the evolution of new enzymes (Khersonsky and Tawfik, 2010). Thus, the catalytic capabilities of this reaction can be attributed to an ancestral function, rather than a modern day relevant physiological function.

2.3.7 Preliminary activity assessment of PspE

Thiosulfate-thiol sulfurtransferase activity of PspE was confirmed using assay protocols established for Str (section 2.2.5.1), for the thiol acceptors glutathione and cysteine. As enzyme yield from purification was low, Michaelis-Menten kinetics were not determined, therefore activity was assessed at substrate concentrations 15 mM and 50 mM for thiosulfate and each thiol acceptor respectively, which was determined to be maximum velocity for Str. Moving forward, PspE expression requires optimisation for future inquiry and full biochemical characterisation.

As PspE eluted as two peaks during size exclusion purification (section 2.3.2), thiosulfate-thiol sulfurtransferase activity was assessed for each peak separately. Both PspE peaks (PspE-1 and PspE-2) were found to be functionally active with no significant differences of reaction rate between the two peaks across the substrates tested. PspE exhibited comparable velocity under these substrate concentrations to Str with glutathione as the thiol acceptor substrate, suggesting functional redundancy of thiosulfate-thiol sulfurtransferase activity. In contrast, PspE demonstrates significantly reduced velocity in the presence of cysteine (Figure 2.15), although the reasons for difference this is currently unclear.

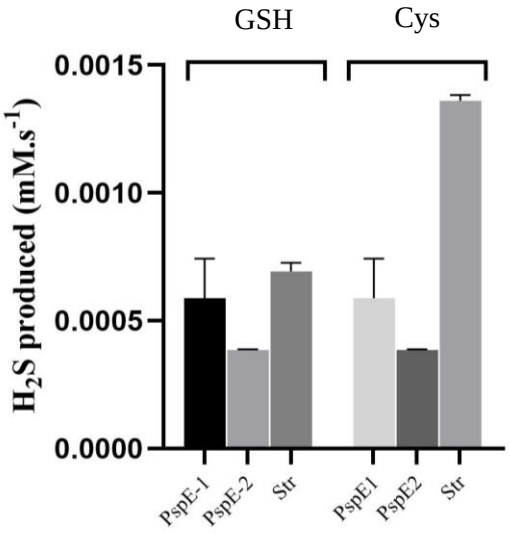

Figure 2.15: Comparison of PspE and Str thiosulfate-thiol sulfurtransferase activity. Initial velocity values reported for reactions containing 15 mM thiosulfate and 50 mM thiol acceptor substrate (glutathione or cysteine) at 37 °C. All data points are averages with standard deviations (error bars) from three replicate.

2.3.8 Crystallisation of Str

Four high throughput crystallisation screens of 96 conditions each were trialled with Str concentrations of 2.5 $mg.ml^{-1}$ 4.252 $mg.ml^{-1}$, 5 $mg.ml^{-1}$, 5.9 $mg.ml^{-1}$, 9.86 $mg.ml^{-1}$, 14.92 $mg.ml^{-1}$, and 18.6 $mg.ml^{-1}$. However, in all cases, no promising crystallisation conditions were observed. This led to co-crystallisation attempts with Str bound with substrate. Initially, co-crystallisation was attempted with Str and with thiosulfate (final concentration of 10 mM). In the resulting crystal screens, only one promising crystallisation condition was observed. This condition (0.2 M calcium chloride, 0.1 M Bis-Tris pH 5.5, 35% (v/v) 2-Methyl-2,4-pentanediol, MPD) was refined by varying pH (4.5-6) and MPD concentration (35-55 % (v/v)) for fine screen via the hanging drop method. In the resulting fine screen, two conditions grew promising crystals (55% MPD, 0.1M Bis-Tris at pH 5 and 6 respectively) within three days.

Crystals were prepared for X-ray diffraction by flash freezing in liquid nitrogen. A cryoprotectant was not added due to the high MPD percentage being sufficient to preserve the crystals. Unfortunately, diffraction data collected from Australian

synchrotron on the MX2 beamline, equipped with an EIGER detector, revealed a diffraction pattern reminiscent of salt crystals and hence co-crystallisation of Str with thiosulfate was also unsuccessful.

Further attempts were made to obtain Str crystals by co-crystallisation with glutathione or cysteine. High throughput crystallisation screens trialled with glutathione (final concentration of 10 mM) showed no promising crystallisation conditions however, numerous promising crystallisation conditions were observed when Str (2.5 $mg.ml^{-1}$ or 5 $mg.ml^{-1}$) was co-crystalised with cysteine (final concentration 10 mM). Crystals grew within three days and the majority of the morphologies observed were hexagonal or rectangular plates (example Figure 2.16). Due to time constraints, the highest priority condition was identified (Figure 2.16b), a rectangular cube displaying the most three-dimensional morphology. Optimisation of this condition (0.1M citric acid pH 3.5, 28% PEG 8000) was attempted by generating fine screens via the hanging drop method, varying pH (3 to 4.5) and PEG 8000 (24-34%). Unfortunately, no well-formed crystals grew.

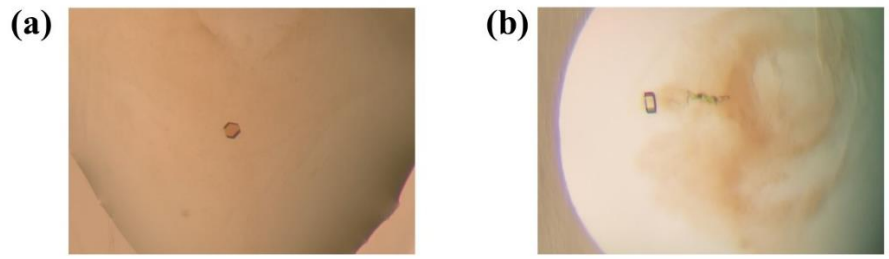

Figure 2.16: High-throughput crystal fine screens examples. Co-crystallisation of Str (5 $mg.ml^{-1}$) with 10 mM cysteine. (a) example of hexagonal plates (condition: 0.1 M sodium acetate trihydrate pH 4.5, 25% w/v PEG 3,350), (b) crystal condition (condition: 0.1M citric acid pH 3.5, 28% PEG 8000) optimised for fine screening via the hanging drop method.

As many low- quality crystals were observed in high throughput crystal screens for Str with cysteine, further optimisation of other promising conditions could potentially grow crystals of sufficient quality for X-ray diffraction. However, due to time constraints, this was unable to be investigated further at this point.

2.4 Conclusions

To elucidate the role of Str in *Neisseria gonorrhoeae*, we first set out to biochemically characterise Str activity with various thiol acceptor substrates to decipher physiologically relevant substrates. We confirm Str activity with cyanide as the acceptor substrate, thereby distinctly classifying Str as a rhodanese. However, based on the low affinity for cyanide and thiosulfate under physiologically relevant conditions, we conclude cyanide detoxification is unlikely to be primary physiological role of Str, instead we hypothesise that cyanide detoxification is a promiscuous function. We identify thiosulfate and glutathione as being physiologically relevant substrates for Str, as determined by mechanism preference and substrate affinity for glutathione, which is within the realms of the intracellular glutathione concentrations found within *N. gonorrhoeae* (>15 mM) (Seib et al., 2006). Additionally, we present that Str demonstrates substrate ambiguity with respect to thiols as the thiol acceptor substrate, capable to utilising glutathione, cysteine and homocysteine, which advantageously allows the scavenging of available resources for sulfur acquisition, however we were unable to determine thiol preference at this point. Furthermore, we demonstrate that Str activity with thiosulfate and thiols is functionally redundant based on the comparable activity of PspE.

The second aim of this chapter was to determine protein structure via protein crystallography. However, crystallisation of Str proved challenging and, despite extensive efforts, obtaining Str protein crystals was unsuccessful. As such, co-crystallisation was pursued with Str substrates thiosulfate, glutathione, and cysteine. While co-crystallisation with glutathione and thiosulfate were also unsuccessful, we have identified numerous promising conditions of co-crystallisation attempts with cysteine that warrant further optimisation.

2.5 Future research

The sulfurtransferase activity assays herein will be subject to further optimization to determine the affinity for thiol acceptor substrates, cysteine and homocysteine. Once established, expression trails for PspE should be conducted to obtain a higher

yield of purified PspE protein that will be used to biochemically characterise PspE, using the same methods established for Str.

Due to the unusual observations in the thiosulfate-thiol sulfurtransferase activity raw data, we intend to model the assay system in Cell ML. To do so, the rate of the chemical reaction of lead acetate to lead sulfide will be determined followed by the enzymatic rate step by using a stopped assay which measures the production of sulfite, eliminating the confounding effects of the assay. This will allow as to deduce the rate of the spontaneous reaction of glutathione persulfide and glutathione. Once all this above information is obtained, the assay system can be modelled to investigate our suspicions of the behaviour observed in the raw data.

Based on the preliminary assessment of formal mechanism we hypothesise that the reaction between thiosulfate and thiols proceed via an ordered single displacement mechanism, in consensus with previous reports. However, additional kinetic data will be collected for Str activity at different constant concentrations of glutathione while varying thiosulfate concentrations to add confidence to this hypothesis. Herein, we have assumed that thiosulfate and cyanide reaction catalysed of Str proceeds via an ordered double-displacement mechanism based on the overwhelming amount of evidence for this within the literature. To confirm this for the case of Str, kinetic data will be collected to generate a Lineweaver-Burk plot.

Promising hight through-put crystallisation conditions of Str with cysteine will be subject to refinement with the aim to obtain X-ray diffraction quality crystals. The achievement of this would be invaluable in confirming thiol substrate interaction with the active site. High-throughput crystallisation screening will also be performed for PspE with the aim to determine the protein structure.

Chapter 3

In vivo Characterisation of the TST Sulfurtransferase in *Neisseria gonorrhoeae*

3.1 Introduction

The recent discovery of the alternative thiosulfate assimilation pathway (CysM independent pathway) elucidates a physiological role of sulfurtransferases in thiosulfate assimilation for cysteine biosynthesis. Thus far, this pathway has been characterised in two prokaryotic organisms, *E. coli* and *S. cerevisiae* (Kawano, Suzuki & Ohtsu, 2018). *Neisseria gonorrhoeae* is one of numerous human pathogens with the inability to assimilate sulfate due to an incomplete sulfate assimilation pathway (Hicks & Mullholland, 2018). However, in many cases the sulfur requirements can fulfilled by thiosulfate *in vitro* (Le Faou, 1983; Lithgow et al., 2004). As thiosulfate is a viable source of sulfur for during infection (due to a high abundance present in the host-pathogen interface) (Lensmire & Hammer, 2019) and sulfurtransferases are ubiquitously found, it is plausible that the CysM independent pathway presents an alternative route for sulfur acquisition in pathogenic bacteria, specifically for those incapable of sulfate assimilation. Thus far, this alternative pathway has not been investigated in pathogens incapable of sulfate assimilation.

N. gonorrhoeae undergoes natural transformation at high frequencies and as such makes it an ideal model to investigate alternative sulfur acquisition pathways in bacterial pathogens due to the ease of genetic manipulation and the evident absence of conventional inorganic sulfate and thiosulfate assimilation pathways. In Chapter Two we demonstrate that the sulfurtransferase enzyme we hypothesise to be involved in thiosulfate assimilation does reduce thiosulfate to sulfide *in vitro*. However, to support this as a physiologically relevant role of Str in *N. gonorrhoeae,* further *in vivo* evidence is required. Herein, we generate a *N. gonorrhoeae* sulfurtransferase deletion strain via homologous recombination and assess its ability to grow in the presence of different sulfur sources, with the aim to determine if Str utilises exogenous inorganic thiosulfate as substrate *in vivo*.

3.2 Methods

The *Neisseria gonorrhoeae* MS11 strain (GenBank accession number NC 022240.1) was used in this study.

3.2.1 Bacteria cell culture

Glycerol stocks of *N. gonorrhoeae* MS11 WT and *N. gonorrhoeae* MS11 Δ*str* (made as per section 3.2.2.5) were stored at -80 °C.

3.2.1.1 *Growth on solid media*

N. gonorrhoeae was cultured on GCB agar plates. GCB plates were made by adding 36.25g GC Medium Base (Difco) to one litre of water according to the method in (Dillard, 2011). The solution was sterilised by autoclaving and cooled to 50-60 °C. Immediately prior to pouring plates, the GCB agar solution was supplemented with 10 ml (per litre) of Iso Vitalex supplement (BD Biosciences). GCB agar to support the growth of *N. gonorrhoeae* Δ*str* (kanamycin resistant) strain was additionally supplemented with 50 $\mu g.ml^{-1}$ kanamycin. Plates were poured with approximately 20 ml agar per plate and set at room temperature. GCB agar plates were stored at 4 °C for up to one month.

A sterile loop of *N. gonorrhoeae* MS11 WT glycerol stock was steaked onto GCB agar plates, and *N. gonorrhoeae* MS11 Δ*str* glycerol stocks were streaked out onto kanamycin supplemented GCB agar places and incubated upside-down at 37 °C with 5% CO_2.

3.2.1.2 *Growth in liquid media*

McCoys medium (Gibco) supplemented with 10% fetal bovine serum (FBS), 1 $\mu g.ml^{-1}$ vancomycin and 2.5 $\mu g.ml^{-1}$ amphotericin B was used to culture *N. gonorrhoeae* MS11 WT in liquid media. 50 $\mu g.ml^{-1}$ kanamycin was added to the McCoys medium to support the growth of *N. gonorrhoeae* MS11 Δ*str*.

A sterile loop was used to transfer a colony from an agar plate (section 3.2.1.1) to inoculate 3-5 ml of pre-warmed McCoys medium (or McCoys plus 50 $\mu g.ml^{-1}$

kanamycin for Δ*str*) in a vented cell culture flask and incubated at 37 °C with 5% CO_2.

3.2.1.3 *Chemically defined liquid media for growth experiments*

A chemically defined medium as described by (Catlin, 1973) was used to phenotypically characterise the Δ*str* strain. The chemically defined medium was comprised of all the components listed in Appendix C.1. Stock solution #1, 3a, 3b, 5, 6, were sterilised by autoclaving and the remainder was sterilised by filtration through a 0.2 µm filter. All stock solutions and components were stored at 4 °C for up to one month except for stock solutions #6 and 7 which were stored at -20 °C. All stock solutions and components were made up prior to preparing the medium except for cysteine, tyrosine, hypoxanthine and stock solution #7 which were made the day of assembling. For preparation of one litre of the complete medium, the components were added in the order and volumes listed in Appendix C.1. into a sterilised Schott bottle. After the addition of oxalacetic acid the medium was neutralised by the addition of approximately 2 ml of 1 M NaOH. Finally, after adding the final component, MQ H_2O, the medium was adjusted to a final pH of 7.45. Two versions of the chemically defined medium were constructed, one that contained the organosulfur sources cysteine, cystine and methionine and the other that omitted these sulfur sources and was substituted with sodium thiosulfate to a final concentration of 1.5 mM in one litre. All chemical components were ordered from Sigma.

3.2.2 Construction of a *Neisseria gonorrhoeae* sulfurtransferase deletion strain

Two DNA constructs were developed in attempt to create a sulfurtransferase deletion strain, (1) a markerless construct (without selection marker) and (2) a marked construct (introducing a kanamycin resistant gene in lieu of the sulfurtransferase gene). The sulfurtransferase deletion strain was created using the (Dillard 2011) spot transformation protocol, tested by colony PCR and sequenced for confirmation.

3.2.2.1 *DNA construct design and primer design*

3.2.2.1.1 *Construct design*

The marked and markerless constructs were designed by Dr. Joanna Hicks and contained the 10-bp long DNA uptake sequence (DUS) required for homologous recombination. The markerless construct consists of only the 5' and 3' flanks for the *str* gene (Figure 3.1a) while the marked construct includes a kanamycin resistant gene between the two flanks in lieu of the sulfurtransferase gene (Figure 3.1b). The sulfurtransferase deletion DNA constructs were ordered as a geneblock from Twist Bioscience. Lyophilised DNA was suspended in 20 µl MQ H_2O.

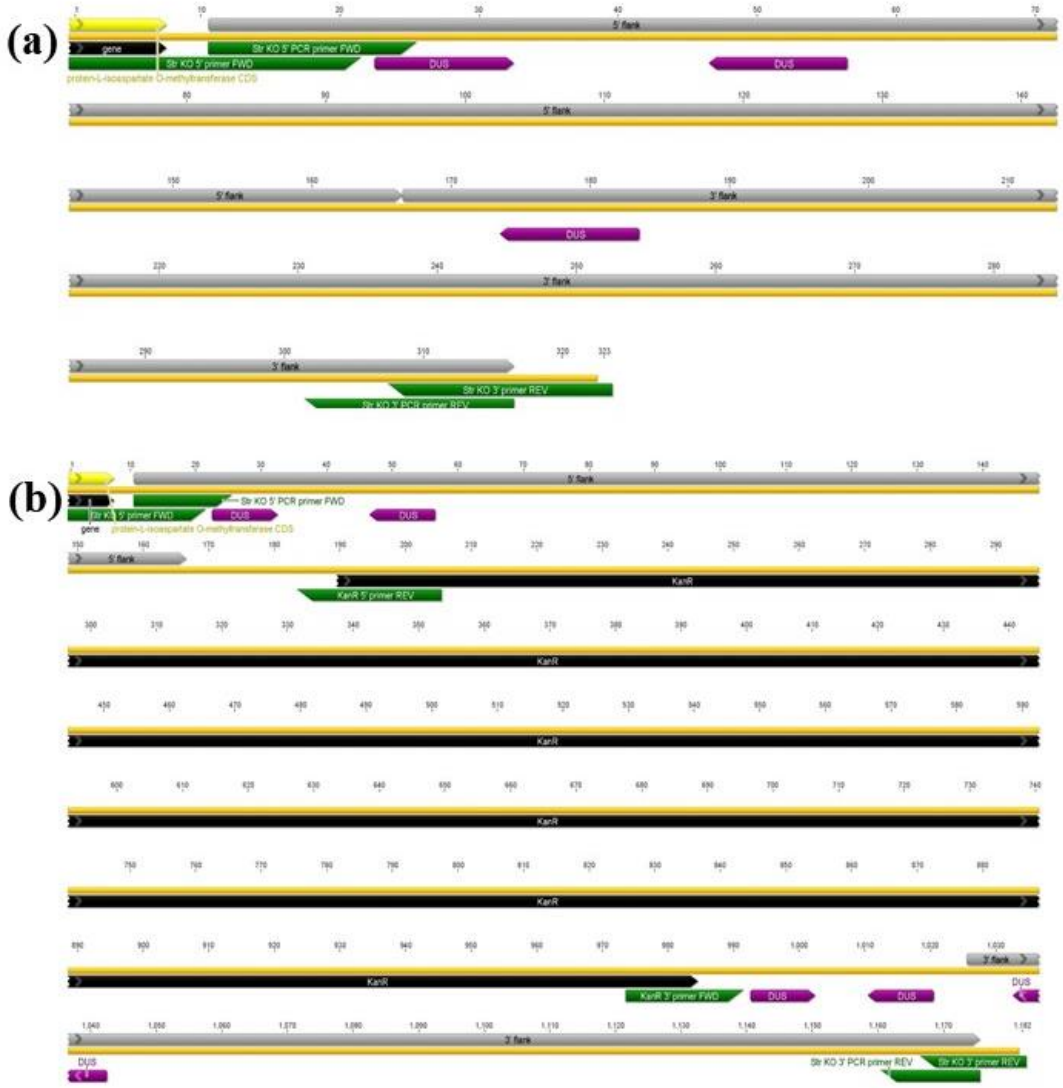

Figure 3.1: Sulfurtransferase deletion strain constructs with primer sequences annotated. (a) The markerless DNA construct which omits the *str* gene, (b) the marked DNA construct containing the kanamycin resistant gene in lieu of the *str* gene. Flanking sequences for homologous recombination are shown in grey, kanamycin resistance gene (*kanR*) shown in black. DNA uptake sequences (DUS) shown in purple and primers are shown in green.

3.2.2.1.2 *Primer design*

Primers for construct amplification were designed by Dr. Joanna Hicks to cover the entire construct (annotated as Str KO 5' PCR primer FWD and Str KO 3' PCR

primer REV, on Figure 3.1). Primers for colony PCR were fitted on the outer region of the 5' and 3' flanks (annotated as Str KO 5' FWD and Str KO 3' REV, on Figure 3.1). Primers for DNA sequencing were mapped within the kanamycin resistant gene and over the integration site of the construct, spanning the outer genomic regions and flanks (annotated as: strKO seq FWD, strKO seq REV, KanR FWD seq and KanR REV seq, on Figure 3.1b). All primers used in this study are listed in Appendix C.2.

All primers were supplied by IDT and resuspended in 1 × TE.

3.2.2.2 *Preparation of DNA construct via polymerase chain reaction (PCR)*

PCR reactions to generate DNA for spot-transformations were set up using HOT FIREPol® DNA polymerase Blend Master mix with the DNA constructs in section 3.2.2.1.1 used as the DNA template. Reactions were set up as in Table 3.1 using the Str KO 5' PCR primer FWD and Str KO 3' PCR primer REV, primer sequences (sequences in Appendix C.2.).

Table 3.1: PCR reaction conditions for DNA construct amplification.

Component	Volume (µl)
5 × HOT FIREPol® Blend	4
10 µM forward primer	0.6
10 µM reverse primer	0.6
10 ng/µl DNA template	1.0
MQ H_2O	14.8

The PCR reactions were performed in replicates of four with one negative control in which case the DNA template was omitted and replaced with 1 µl of MQ H_2O. PCR cycling conditions were as per Table 3.2.

Table 3.2: PCR cycling conditions.

Step	Temperature (°C)	Time (min)	PCR Cycles
Initial denaturation	95	15:00	1
Denature	95	0:20	
Anneal	57	0:30	29
Extension	72	0:30/1:20*	
Final extension	72	10:00	1
Hold	12	-	-

* Extension time was dependent on the DNA construct used based on the difference in construct size. For the markerless construct an extension time of 30 seconds was required whereas the marked constructs had an extension time of 1:20 min.

Following PCR amplification, all 20 µl reactions were combined (except for the negative control which was used for an agarose gel sample), 2 µl was removed for an agarose gel sample and the remainder was purified using the High Pure PCR Clean-Up Micro Kit (Roche) as per manufacturer's instructions. Post purification, 2 µl of the purified PCR product was removed for an agarose gel sample. DNA concentration was determined by absorbance at 260 nm by NanoDrop^{TM} using the purification elution buffer as the blank. Purified PCR product was stored at -20 °C. The negative control, pre, and post purification DNA samples were prepared for agarose gel electrophoresis by addition of 2 µl 10 × DNA loading dye to 2 µl of DNA sample. Samples were loaded onto a 1.5% TAE agarose gel pre-stained with 1 × SYBR Safe DNA gel stain (Invitrogen) with 7 µl of 1 kb plus ladder (Thermo Fischer) in the first well of each gel. Agarose gels were run for 40 min at 100 V. Gels were visualised on an iBright imager (Invitrogen).

3.2.2.3 *Spot-transformation protocol*

N. gonorrhoeae MS11 WT was cultured onto a GCB plate as per 3.2.1.1 and incubated for 24 hours. On a new GCB plate, two circles were drawn 90° apart. In each circle, 10-20 µl of DNA (10-20 ng.µl^{-1}) construct (section 3.2.2.1.1) was pipetted onto the GCB plate within the drawn circles and left to absorb into the plate for approximately 10 minutes. For DNA transformation to be successful *N. gonorrhoeae* requires the expression of Type IV pili (Giltner, Nguyen &

Burrows, 2017). Potentially pilated WT colonies were identified under the microscope as those having a smaller morphology accompanied by a darker circumference. These were then selected to be used for transformation. A single piliated WT colony was selected with a sterile wire loop from a fresh *N. gonorrhoeae* MS11 plate and streaked through the DNA spots, sterilising the wire loop between each spot. The spot transformation plate was incubated overnight at 37 °C, 5% CO_2. For the markerless construct, colonies that grew within the DNA spots were directly subjected to colony PCR. For the kanamycin marked construct, colonies that grew within the DNA spots were scraped using a sterile wire loop and streaked out onto a fresh GCB plate containing 50 $\mu g.ml^{-1}$ kanamycin and incubated overnight at 37 °C, 5% CO_2. Colonies that grew on the kanamycin supplemented GCB plates were then subject to colony PCR.

All GCB agar plates used were prewarmed to 37 °C prior to culturing.

3.2.2.4 Colony PCR diagnostic of Δstr transformants

Colonies from the spot-transformation plates as previously described (section 3.2.2.3) were screened for successful transformation by colony PCR using the Str KO 5' FWD and Str KO 3' REV primers (Appendix C.2.). A PCR reaction was set up for each colony using the components in (Table 3.3) and carried out using an Eppendorf PCR machine with the cycle conditions as per (Table 3.2), with extension time dependent on the DNA construct. In all colony PCRs performed, a wild type colony was added to one reaction mix to serve as a positive control, and one reaction mix, void of a DNA template, served as a negative control.

Table 3.3: PCR reaction conditions for colony PCR diagnostic.

Component	Volume (µl)
5 × HOT FIREPol® Blend	4
10 µM forward primer	0.6
10 µM reverse primer	0.6
MQ H_2O	14.8

PCR products were directly loaded onto a 1.5 % agarose gel for visual assessment as previously described. Transformants with the desired PCR product size were passaged onto a fresh GCB or GCB kanamycin plate, incubated overnight at 37 °C, 5% CO_2, and subject to a second round of colony PCR in pursuit of a completely homogeneous transformant colony. Successful homogeneous colonies were streaked out onto a new GCB plate (or GCB kanamycin plate) and incubated overnight to make glycerol stocks.

3.2.2.5 *Glycerol stocks of Δstr strain*

Plates from section 3.2.2.4 were used to make 3 ml liquid cultures as per section 3.2.1.2 and incubated for 48 hours at 37 °C, 5% CO_2. Liquid cultures were centrifuged for 5 min at 4000 rpm. The supernatant was discarded leaving 0.5 ml to resuspend the cell pellet. The resuspended pellet was transferred to a sterile 1.5 ml cryo vial containing 0.5 ml of sterile 50% (v/v) glycerol and mixed well. Glycerol stocks were stored at -80 °C.

3.2.2.6 *DNA sequencing of transformants*

Successfully transformed *N. gonorrhoeae* isolates were subject to DNA sequencing to confirm integration of the construct at the correct site in the genome and absent of mutation. *N. gonorrhoeae* MS11 Δ*str* (kanamycin resistant) glycerol stocks were streaked out onto 50 $\mu g.ml^{-1}$ kanamycin supplemented GCB agar as per section 3.2.2.1 and incubated for 48 hours. Colony PCR was performed for each successful culture and visualised on 1.5% agarose gel as previously described in section 3.2.2.4. DNA was purified and quantified as previously described in section 3.2.2.2. Purified DNA was used as the template for the sequencing reactions. Four sequencing reactions were set up for each promising transformed culture using a different primer sequences that were mapped over the integration site and onto the DNA construct (Figure 3.1b). Sequencing was performed by the Massey Genome Sequencing Service.

3.2.3 Growth rate experiment

Liquid cultures were set up as per section 3.2.1.2 for *N. gonorrhoeae* MS11 WT and Δ*str* strains and incubated for 48 hours. Liquid cultures were used to inoculate

seeder cultures for each strain in two conditions, (1) McCoys medium supplemented with 10% FBS and (2) chemically defined medium (section 3.2.1.3). Each seeder culture was comprised of 4 ml media and 40 µl of liquid culture. Seeder cultures to support the growth of Δ*str* was additionally supplemented with 50 $\mu g.ml^{-1}$ kanamycin. Seeder cultures were incubated for 24 hours at 37 °C and 5% CO_2. The seeder cultures were used for a 1:100 inoculation of 25 ml cultures, of which there was three conditions, (1) McCoys medium supplemented with 10% FBS, (2) chemically defined medium containing organic sulfur sources cysteine, cystine and methionine and (3), chemically defined medium containing thiosulfate as the sole sulfur source, for each strain (WT and Δ*str*). McCoys medium seeder cultures were used to inoculate the culture in McCoys medium while the chemically defined medium seeder cultures were used to inoculate the two chemically defined media conditions. An initial optical density (OD) reading at 600 nm was taken followed by incubation of the cultures at 37 °C, 5% CO_2. The next OD_{600} reading was taken 4.5 hours post-inoculation and then every two hours thereafter until 12 hours post-inoculation. OD readings continued the following day, at 22.5, 25, 28.5, 30.5, 34, 36, and 47 hours post-inoculation. The experiment was performed in triplicate. All media was pre-warmed to 37 °C prior to inoculation.

Differences in growth rates between strains and culture conditions were analysed by unpaired t-test in GraphPad Prism using the Holm-Šídák method with the P value set at 0.05.

3.3 Results and Discussion

To investigate the physiological role of the sulfurtransferase enzyme, Str, in *N. gonorrhoeae*, a sulfurtransferase deletion strain (Δ*str*) was generated. The deletion strain was used to examine the ability of *N. gonorrhoeae* MS11 to grow in the presence of different sulfur sources (compared to wild type) to determine the involvement of Str in inorganic thiosulfate assimilation *in vivo.*

3.3.1 *Neisseria gonorrhoeae* MS11 Δ*str* deletion strain generation

Briefly, the deletion strain was generated following the spot transformation protocol from (Dillard, 2011) and confirmed by colony PCR diagnostics using primers that

overlay the 5' and 3' flanks of the *str* gene. PCR products were visualised on a 1.5% agarose gel and successful transformants were identified by the PCR product band size of 306 bp (for the markerless construct) or 1,163 bp (for the marked construct). Colonies that produced a PCR product size of ~630 bp represented unsuccessful transformation (WT).

Initial attempts to generate a sulfurtransferase deletion strain involved the use of a markerless construct which aimed to eliminate any survival bias introduced by the addition of an antibiotic resistant selection marker. The markerless Δ*str* construct contained the 10-bp DUS required for homologous recombination and omitted the sulfurtransferase gene (Figure 3.1a). After performing numerous spot-transformations with varying DNA concentrations and testing over a thousand colonies via colony PCR, all but one colony tested negative for successful transformation. One candidate appeared to be a mixed colony of transformants and WT as indicated by the two DNA products sizes, ~300 bp (transformant) and ~600 bp (WT) on the corresponding agarose gel (Figure 3.2a; circled in red). This colony was streaked onto a fresh GCB agar plate in attempt to isolate a transformed colony. From the plate, one hundred and six colonies were tested for transformation via colony PCR which revealed all to be unsuccessful (example Figure 3.2b).

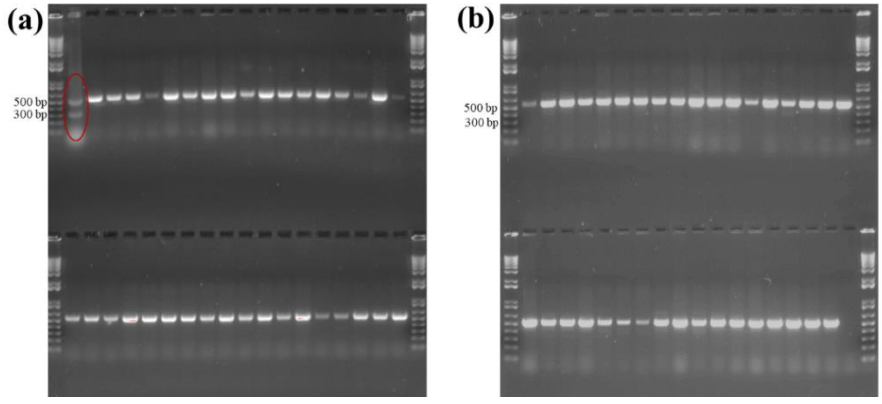

Figure 3.2: Colony PCR diagnostic of markerless deletion strain attempt. Agarose gel of colony PCR post spot-transformation attempt using the markerless sulfurtransferase deletion construct. (a) Initially observed mixed colony by the band sized of ~300 bp which indicates transformant and ~500-600 bp which indicated WT. (b) Further testing of 'mixed' colony post passaging showing isolating a transformant was unsuccessful as indicated by band size of 500-600 bp (WT).

The failure to generate a sulfurtransferase deletion strain using the markerless construct led to the decision to use kanamycin resistance as a selection marker.

The kanamycin Δ*str* construct contained the 10-bp DUS and a kanamycin resistance gene in lieu of the sulfurtransferase gene (Figure 31.b). A spot-transformation using 20 µl of 10 ng.µl^{-1} DNA construct was successful in generating transformants in all twenty-nine colonies tested as indicated by a PCR product size 1,165 bp, although most of the colonies were a mix of transformants and wild type (Figure 3.2a) as indicated by two bands on the agarose gel.

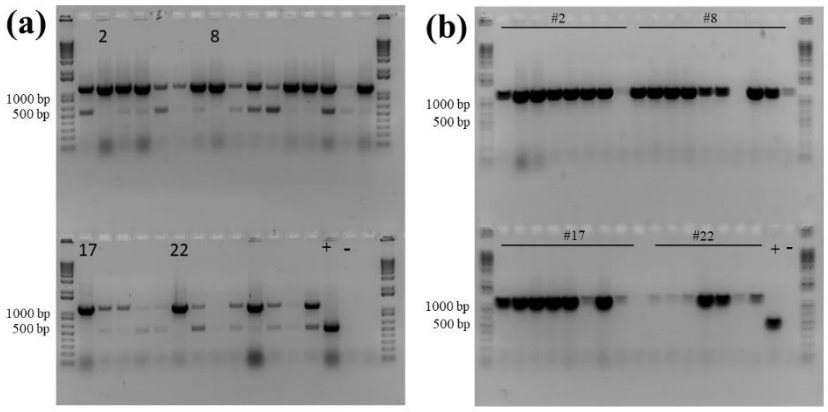

Figure 3.3: Colony PCR diagnostic of kanamycin marked deletion strain. Agarose gel of colony PCR showing successful sulfurtransferase deletion transformants using the kanamycin resistance marked construct. Bands at ~500-600 bp indicate WT and bands at ~1500 bp indicate successful transformants. + indicates WT (positive control) and – indicates the negative control. (a) Lanes labelled 2, 8, 17 and 22 were identified as showing the most homology. (b) Second round of colony PCR. Bars and numbers indicate the original colony from (a).

Four colonies, labelled 2, 8, 17 and 22 on Figure 3.3a showed complete deletion of the *str* gene (were not mixed colonies) and therefore were selected and passaged onto GCB agar supplemented with 50 µg.ml^{-1} kanamycin for a second round of colony PCR to ensure the presence of the kanamycin resistance gene in every chromosome. All colonies tested showed complete integration of the kanamycin resistance gene into the *str* locus in all chromosomes (Figure 3.3b). A single colony from each was subsequently passaged to generate glycerol stocks. Upon culturing from these glycerol stocks, two grew successfully while two failed to grown upon

thawing. The two glycerol stocks that grew (named 2 and 8 as were initially from colony #2 & 8 in Figure 3.3) were subject to colony PCR to obtain a DNA template for sequencing by Massey Genome Sequencing Service. The primers used for sequencing covered the genomic regions outside of the 5' and 3' flanks to ensure integration of the construct into the correct site of the genome. Sequencing results provides confirmation that the construct was integrated in the appropriate genome site in both cases. However, for one sample (#2) an insertion mutation was detected (Figure 3.4) whilst the other (#8) showed complete homology with the expected integration construct (Figure 3.5a). Furthermore, the sequencing reads show good coverage over the entire sequence, thereby providing confidence for the consensus and correct integration (Figure 3.5b and c).

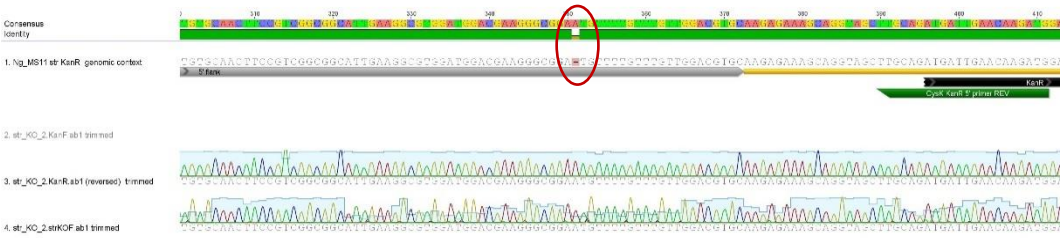

Figure 3.4: Sequencing results showing an insertion mutation. Sequencing results are from the colony PCR products from colony #2. Only the alignment from nucleotide 300-412 is shown. The sequence chromatogram shows signal intensities for the nucleotides, (G, yellow; C, blue; T, green; A red). The insertion mutation of an adenine nucleotide is circled in red. Green bar indicates consensus identity.

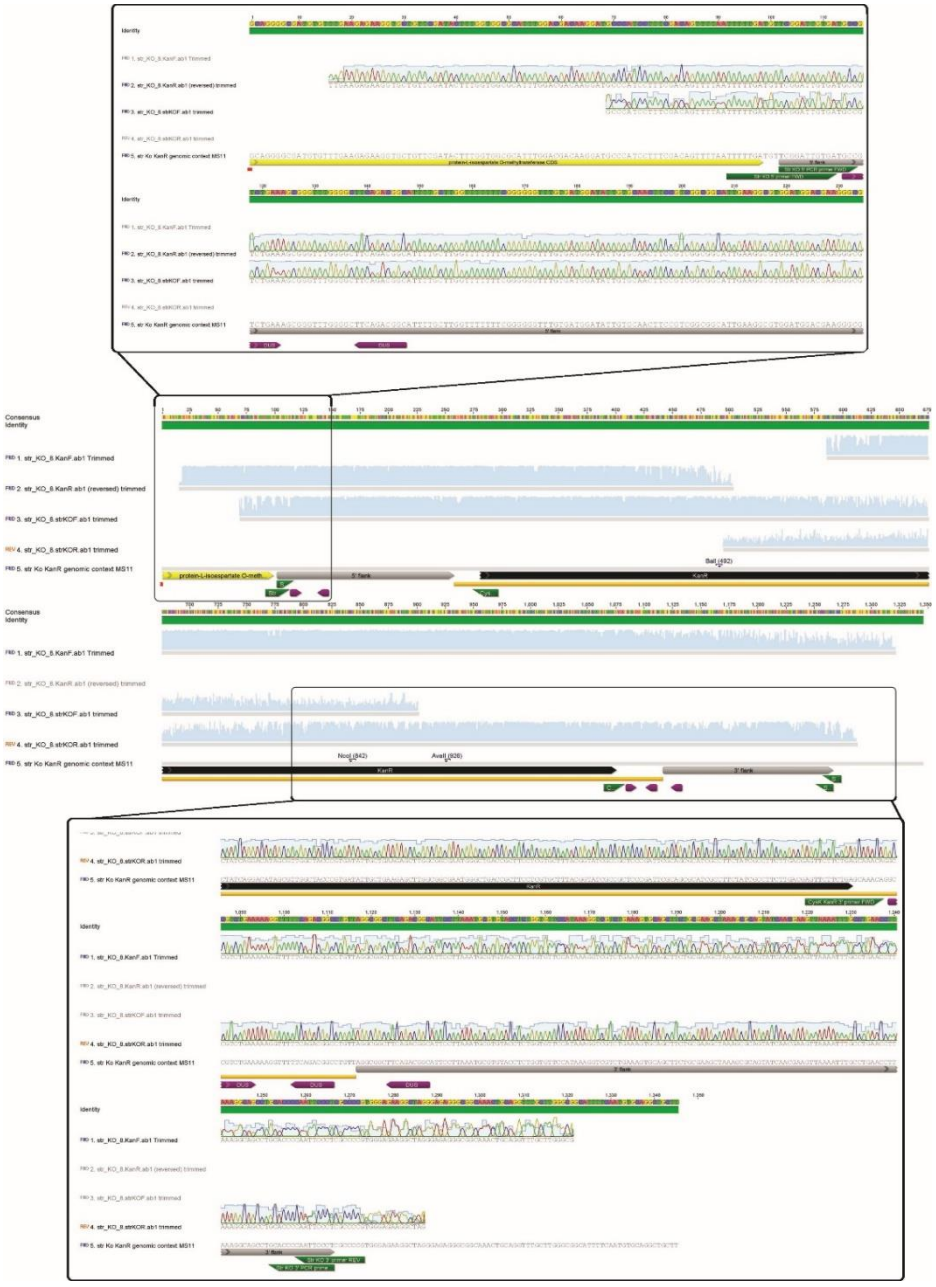

Figure 3.5: Sequencing results confirming the integration of the *str* marked deletion construct. Sequence results are from the colony PCR products from colony #8. The green bar represents identity between the expected integration product and sequencing results. The sequence chromatograms show signal intensities for the nucleotides, (G, yellow; C, blue; T, green; A red). Middle panel: Sequencing results of the entire sequence showing complete homologous integration of the sulfurtransferase deletion construct (green bars), and good coverage reads over the entire sequence (light blue bars). Upper panel: Zoomed image for the 5' integration end. Only the alignment from nucleotide 1-350 is shown. Lower panel: Zoomed image for the 3' integration end. Only the alignment from nucleotide 996-1345 is shown.

3.3.2 Development of chemically defined liquid medium to support the growth of *N. gonorrhoeae* MS11 WT and Δ*str*

To conduct phenotypic characterisation of the Δ*str* strain we first required a culture medium in which we could manipulate the components and that supported the growth of *N. gonorrhoeae* MS11. Within the literature, two chemically defined media were identified to support the growth of *Neisseria* species (Catlin, 1973; Wong, Shockley & Johnston, 1980). Both media were found to support the growth of many *N. gonorrhoeae* strains however, neither study evaluated the growth of *N. gonorrhoeae* MS11 strain. The Catlin (1973) medium was therefore selected as it was more comprehensive, providing a better chance of success.

The medium was comprised of the components listed in the appendix as per section 3.2.1.3. The medium was trialled for *N. gonorrhoeae* WT and Δ*str* strains by monitoring the growth of each strain in the chemically defined liquid medium. A negative control was included to ensure no un-accounted for growth was occurring in the chemically defined medium. OD_{600} readings for WT and Δ*str* strains at 6.5 hours post-inoculation were 0.25 and 0.28, respectively. An additional OD_{600} reading was taken at 17.25 hours post inoculation which was 0.78 and 0.85 for WT and Δ*str* strains, respectively. At both time points, the OD_{600} of the negative control was 0.0 ± 0.01 indicating the absence of contamination. Thus, the chemically defined liquid medium effectively supported the growth of *N. gonorrhoeae* MS11 strains used in this study.

The chemically defined liquid medium was found to be relatively unstable, precipitating after two weeks of storage at 4 °C or room temperature. As such, fresh media was prepared the day before growth experiments.

3.3.3 *In vivo* phenotypic characterisation of *N. gonorrhoeae* Δ*str*

To investigate if the deletion of *str* from the *N. gonorrhoeae* chromosome influences growth rate in the presence of varying sulfur sources, the deletion strain was cultured alongside WT under three conditions, (1) McCoys cell culture medium supplemented with 10% FBS (rich media), (2) a chemically defined medium containing the organic sulfur sources; methionine, cysteine, and cystine, and (3) a

chemically defined medium with thiosulfate as the only available source of sulfur. Cultures were set up in triplicate and OD_{600} readings were taken over the course of 47 hours. Differences in growth rates were analysed via unpaired t-tests and statistically significant differences were identified by an adjusted P value of <0.05.

N. gonorrhoeae WT and Δ*str* strains demonstrate an increased growth rate in McCoys medium compared to both versions of the chemically defined media (Figure 3.6b) as expected due to the McCoys medium containing FBS being a much richer, more complex medium.

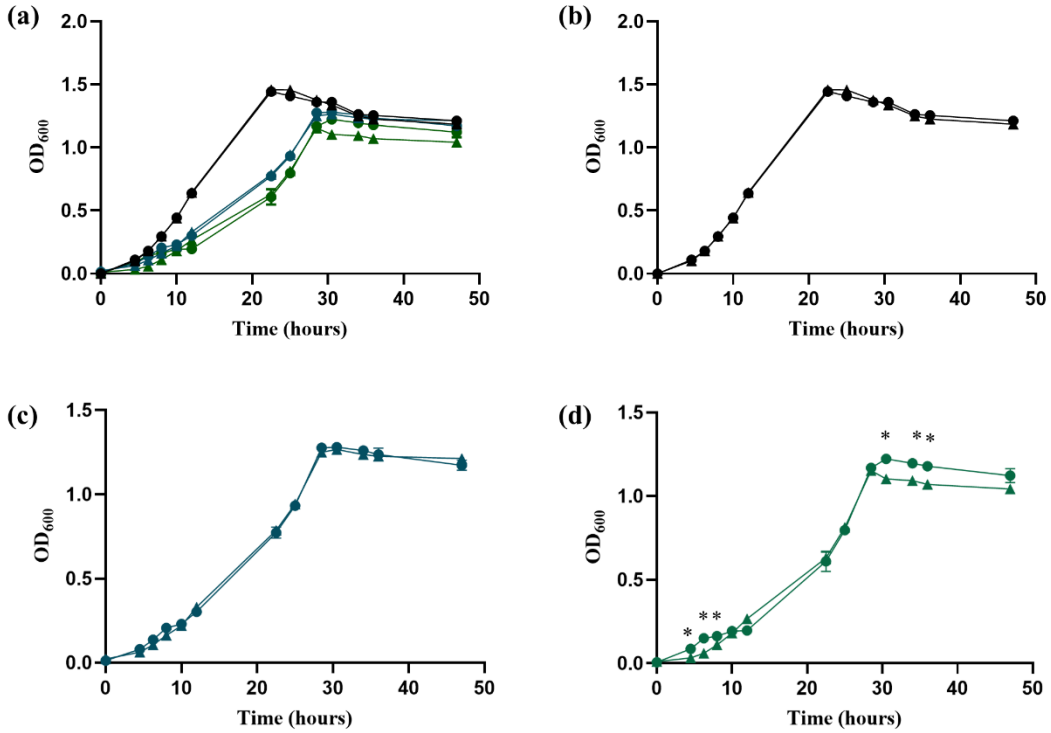

Figure 3.6: Growth curves of *N. gonorrhoeae* MS11 WT and Δ*str* cultured in different sulfur sources. (a) *N. gonorrhoeae* wild type (●) and Δ*str* (▲) grown in McCoys medium supplemented with 10% FBS (black lines), chemically defined medium containing organic sulfur sources (blue lines) and chemically defined medium containing thiosulfate as the sole source of sulfur (green lines). (b) Comparison of *N. gonorrhoeae* wild type (●) and Δ*str* (▲) in McCoys medium, (c) Comparison of *N. gonorrhoeae* wild type (●) and Δ*str* (▲) in chemically defined medium with organic sulfur sources (d) Comparison of *N. gonorrhoeae* wild type (●) and Δ*str* (▲) in chemically defined medium in the absence of organic sulfur sources with thiosulfate as the sole source of sulfur. * Indicates statistical significance (adjusted p= <0.05). Data plotted are the average of three replicates with standard deviation shown as error.

Comparison of WT compared to Δ*str* showed no differences in growth in McCoys medium (Figure 3.6b), and likewise with growth in the chemically defined medium containing only organic sulfur sources (Figure 3.6c). On the other hand, significant differences between growth in WT and Δ*str* was observed when thiosulfate was the sole source of sulfur. *N. gonorrhoeae* Δ*str* exhibited slower growth in both the lag and stationary growth phases of growth compared to wild type as indicated in Figure 3. 6d.

When thiosulfate was the sole source of sulfur, *N. gonorrhoeae* MS11 WT showed slower growth at 12, 25, 28.5 and 34 hrs corresponding mostly to late exponential and stationary phase of growth when compared to the chemically defined medium containing the organic sulfur sources (Figure 3.7a). This effect was exacerbated in the Δ*str* strain (Figure 3.7b) which shows slower growth across the entire growth curve, despite the starting inoculum and first OD_{600} readings being the same between the two strains. Taken together, the phenotypic differences observed as a result of sulfurtransferase deletion in the presence of thiosulfate compared to wild type and compared to growth in organosulfur sources supports the notion that exogenous inorganic thiosulfate is a physiological relevant substrate for this sulfurtransferase in *N. gonorrhoeae*.

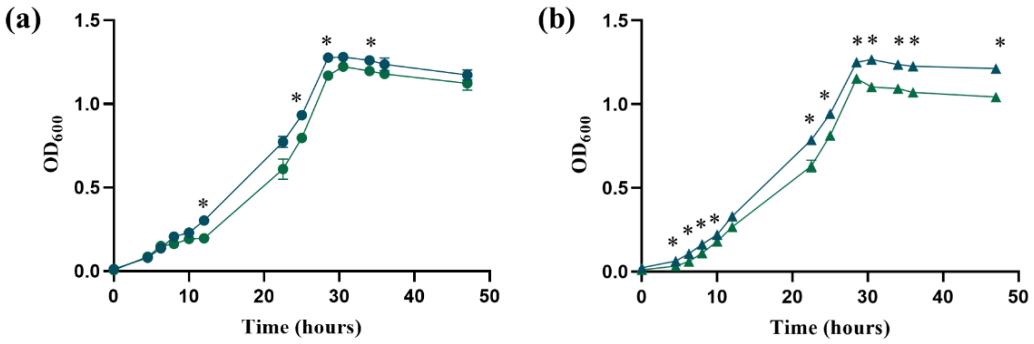

Figure 3.7: Comparison of growth curves in the presence of different sulfur sources. Differences in growth between organic sulfur (blue) and thiosulfate conditions (green) for *N. gonorrhoeae* wild type (●) and Δ*str* (▲) strains. (a) *N. gonorrhoeae* wild type grown in the presence of organic sulfur sources (blue) and thiosulfate (green) conditions, (b) *N. gonorrhoeae* Δ*str* grown in the presence of organic sulfur sources (blue) and thiosulfate (green). * Indicates statistical significance (adjusted p= <0.05). All data are averages with standard deviations (error bars) from three replicates.

Significantly, sulfurtransferase deletion in *N. gonorrhoeae* does exhibit a distinct phenotypic growth effect when thiosulfate is the sole source of sulfur compared to wild type. This is in contrast to other bacterial species such as *E. coli* and *S. typhimurium* where Δ*pspE*Δ*glpE* strains exhibit no growth phenotypic effect when grown in the presence of thiosulfate (Cheng et al., 2008; Wallrodt et al., 2013). This difference can be attributed to the fact that *E. coli* and *S. typhimurium* both have functional CysM enzymes and therefore are capable of assimilating thiosulfate via the CysM dependent pathway, which is absent in *N. gonorrhoeae*.

The observation that *N. gonorrhoeae* Δ*str* is still capable of growth when thiosulfate is the only available sulfur source can be explained by the functional redundancy exhibited by the presence of the second sulfurtransferase, PspE, found in *N. gonorrhoeae*. The biochemical characterisation investigation in Chapter Two demonstrates that Str and PspE display similar sulfurtransferase activity in the presence of glutathione and thiosulfate. Based on this, it is feasible that *pspE* can replace the role of *str*, however to what extent is yet to be investigated. In support of this, deletion of two sulfurtransferase genes, *rdh1* and *rdl2*, in *S. cerevisiae* resulted in a more drastic phenotypic effect when grown in the presence of thiosulfate as the sole source of sulfur, than the single deletions alone. The authors demonstrate that both Rdh1 and Rdh2 reduce thiosulfate to sulfide *in vitro* and that while Rhd1 is primarily involved in thiosulfate utilisation *in vivo*, this role can be in partially fulfilled by Rdh2 (Chen et al., 2018). From the observation that growth of Δ*str* is significantly reduced in the lag phase of growth in the thiosulfate supplemented condition, compared to WT, we hypothesise that exogenous thiosulfate utilisation is the primary role for Str which can partially fulfilled by PspE, as if thiosulfate utilisation was a secondary physiological role for Str, we would expect to see no significant differences in growth rate across the entire growth curve and in all conditions.

3.3.4 Conclusion

Due to a large genomic deletion and pseudogenes, *N. gonorrhoeae* is incapable of sulfate assimilation and therefore cannot grow when sulfate is the sole sulfur source. However, *N. gonorrhoeae* can grow in the presence of thiosulfate, yet lacks the

ability to reduce thiosulfate via the conventional CysM dependent pathway. Recently, an alternative thiosulfate assimilation pathway has been identified, named the CysM independent pathway. This pathway relies on thiosulfate, glutathione and a sulfurtransferase enzyme to reduce thiosulfate to bisulfide which can subsequently be incorporated into *O*-acetylserine to form cysteine. We hypothesise this pathway to be functional within *N. gonorrhoeae*. We propose that Str has a physiological role in this pathway and utilises exogenous inorganic thiosulfate for sulfur acquisition for the purpose of cysteine biosynthesis.

Biochemical characterisation of Str performed in Chapter Two confirms Str activity with thiosulfate and glutathione to form bisulfide *in vitro.* To investigate this hypothesis *in vivo,* in the current chapter we successfully generated a sulfurtransferase deletion strain in *N. gonorrhoeae* MS11 via homologous recombination using a kanamycin resistant selective marker. We show that the *N. gonorrhoeae* Δ*str* strain demonstrated distinct phenotypic differences with regards to growth rate compared to wild type, which offers support to our hypothesis that Str is involved in exogenous inorganic thiosulfate assimilation. We reason that, the presence of the second sulfurtransferase in *N. gonorrhoeae*, PspE, offers a viable explanation as to why our deletion strain grows in the presence of thiosulfate and as such, expect that a double deletion of these genes will exacerbate growth defects when thiosulfate is the only available source of sulfur.

While demonstrating that Str utilises exogenous inorganic thiosulfate as a substrate is an important and promising first step in elucidating the role of sulfurtransferases within *N. gonorrhoeae,* further investigation is required to support the role of Str in *de novo* cysteine biosynthesis and assess the importance of thiosulfate assimilation during the pathogenicity of *N. gonorrhoeae.*

3.4 Future Research

The sulfurtransferase deletion strain generated in this chapter will be subject to further *in vivo* experiments. Moving forward, a *N. gonorrhoeae* Δ*pspE* strain will first need to be generated followed by a double deletion (Δ*str*Δ*pspE*) due to the functional redundancy exhibited by the presence of both these enzymes as

concluded in Chapter Two. Complement strains for each deletion strain will also be generated, by adding back the deleted gene into the *iga/trpB* complementation locus (Dillard, 2011). The three deletion strains (Δ*str*, Δ*pspE*, and Δ*str*Δ*pspE*) will undergo a series of experiments in unison to achieve a more detailed understanding of the overall and relative importance of these two proteins with respect cysteine biosynthesis, pathogenesis and resistance to stress conditions.

Firstly, the growth rate experiment in chemically defined media with different sulfur sources should be conducted for the other two deletion strains and complement strains. This will aid in elucidating the relative involvement of Str versus PspE in pathogenic growth and determine which sulfurtransferase is primarily involved in thiosulfate utilisation. At the same time, intracellular glutathione levels of the deletion strains grown with different sulfur sources should be evaluated using a glutathione quantification kit to determine the effects of thiosulfate assimilation on downstream glutathione production, given that synthesis of glutathione is contingent upon *de novo* cysteine biosynthesis.

Following this, the ability of the three deletion strains to survive under various stress conditions (compared to wild type) will be tested to determine if, or under what conditions, these genes are essential. This will be achieved by a hydrogen peroxide assay which will determine the ability of the deletion strains to survive under oxidative stress conditions and whether or not the deletion of Str and PspE has downstream effects on protection systems against oxidative stress. As Str demonstrated *in vitro* cyanide detoxification, a cyanide toxicity assay will be performed to determine if Str offers protection against cyanide toxicity *in vivo.*

Furthermore, given that cysteine biosynthesis is upregulated during infection, the effectiveness deletion strains to infect endocervical cells will be assessed via host association assays. This will aid in elucidating the role of Str in cysteine biosynthesis and determine the importance of sulfurtransferases during pathogenesis.

Lastly, metabolic profiles of the deletion and wild type strains both *in vitro* (in culture) and *in vivo* (during infection of host cells) should be analysed to compare

the abundance of important sulfur metabolites (specifically sulfite, the by-product of the sulfurtransferase reaction) which will aid in explaining the sulfite accumulation observed in *N. gonorrhoeae*.

Chapter Four

Conclusions

Neisseria gonorrhoeae is an obligate human pathogen which predominantly infects the lower urogenital tract, causing the sexually transmitted infection, gonorrhoea. *N. gonorrhoeae* has demonstrated an extraordinary ability to develop resistance to antimicrobial treatments, facilitated by a high rate of transmission and the often-asymptomatic nature of infection leading to prevailing, undiagnosed, and untreated infection. The success of *N. gonorrhoeae* as a human pathogen is attributed to sophisticated mechanisms evolved to evade the host immune response and persist within human tissues. Like all *Neisseria* species, *N. gonorrhoeae* is exceptionally adapted to its mucosal niche which is supported by a high frequency of natural transformation. Unravelling key pathways essential for pathogenicity, growth and persistence of *N. gonorrhoeae* infection is crucial for identifying suitable and novel therapeutic targets to combat the emergence of antibiotic resistance.

N. gonorrhoeae harbours robust defence mechanisms to combat oxidative stress inflicted by the host upon infection. Reduced sulfur compounds such as glutathione, cysteine and methionine are essential for pathogenic growth and provide protection against oxidative stress. In contrast to mammals, who require essential methionine for cysteine production, bacteria are capable of *de novo* cysteine biosynthesis. To achieve this, bacteria must first acquire the essential element, sulfur. This is traditionally accomplished by the reduction of inorganic sulfate to bisulfide via an energetically expensive pathway. Due to large genomic deletions, *N. gonorrhoeae* is incapable of sulfur acquisition via the sulfate reduction pathway and therefore cannot grow on sulfate as the source of sulfur. *N. gonorrhoeae* can, however, grow on thiosulfate as the sole sulfur source and yet, lacks the ability to reduce thiosulfate via the conventional thiosulfate reduction pathway. This poses the question of how *N. gonorrhoeae* acquires essential sulfur for *de novo* cysteine biosynthesis.

The identification of two novel, single domain sulfurtransferases (rhodaneses), Str and PspE, within the *N. gonorrhoeae* genome has led to the hypothesis of an alternative thiosulfate assimilation pathway in *N. gonorrhoeae*. We hypothesise that

these sulfurtransferases in *N. gonorrhoeae* catalyse the sulfur transfer from thiosulfate to glutathione, ultimately releasing sulfide in the form required for cysteine biosynthesis. This pathway of sulfur acquisition has thus far has been characterised in just two prokaryotic organisms (Kawano, Suzuki & Ohtsu, 2018). Elucidating the role of these sulfurtransferases in *N. gonorrhoeae* is pivotal in advancing our understanding on sulfur acquisition in bacterial pathogens.

The thiosulfate sulfurtransferases, or rhodaneses, are ubiquitous enzymes yet despite this are relatively understudied and often functionally ambiguous. Rhodaneses, like all sulfurtransferases, catalyse the transfer of sulfur from a thiol donor substrate (thiosulfate for rhodaneses) to a thiol acceptor substrate. Rhodaneses are most renowned for catalysing the sulfuration of cyanide to produce the less toxic metabolite, thiocyanate which has led to the long withstanding proposed physiological function as cyanide detoxifiers. Alternatively, rhodaneses display catalytic activity with thiols as the acceptor substrate, namely glutathione, forming oxidised disulfide and bisulfide. We propose this reaction to be physiologically relevant for Str in *N. gonorrhoeae*, with thiosulfate being acquired exogenously and reduced to bisulfide for incorporation into cysteine.

In this research phenotypic characterisation of the *N. gonorrhoeae* MS11 Δ*str* strain (generated as part of this research) and biochemical characterisation of the recombinant sulfurtransferase enzyme are combined to investigate the proposed role of Str in *N. gonorrhoeae.* Through a cyanide detoxification assay, we confirm Str activity with cyanide *in vitro,* thereby distinctly classifying Str as a rhodanese. However, kinetic analysis reveals that Str's affinity for cyanide is low, making it unlikely that cyanide is a physiologically relevant substrate for Str. As such, we hypothesise cyanide detoxification to be an irrelevant promiscuous function, attributing catalytic activity to an ancestral function. To explore this hypothesis in future research, we will examine the ability of the *N. gonorrhoeae* MS11 Δ*str* strain to offer protection against cyanide toxicity compared to wild type.

With respect to thiosulfate-thiol sulfurtransferase activity, Str demonstrates substrate ambiguity, as evident by the production of hydrogen sulfide in the presence of glutathione, cysteine and homocysteine, which advantageously allows

the scavenging of available resources for sulfur acquisition. While we are unable to infer thiol substrate preference at this stage, kinetic analysis of thiosulfate: glutathione activity supports the physiological relevance of this reaction within *N. gonorrhoeae*, as Str has a high affinity for glutathione, which is within the realm of intracellular glutathione concentrations in *N. gonorrhoeae*. Although Str displays moderate affinity for thiosulfate, *in vitro*, phenotypic characterisation of the *N. gonorrhoeae* Δ*str* strain supports the use of exogenous inorganic thiosulfate as a viable substrate for Str as the *N. gonorrhoeae* Δ*str* strain exhibits a significant reduction in the lag and stationary phases of growth compared to wild type when thiosulfate was the sole source of sulfur. Furthermore, thiosulfate:glutathione sulfurtransferase activity was found to be functionally redundant as demonstrated by comparable activity of Str and PspE *in vitro*, indicative of an important functional role of this reaction. Thus, a *N. gonorrhoeae* Δ*str*Δ*pspE* strain is essential in understanding the full effect of these sulfurtransferases in relation to pathogenic growth. The *N. gonorrhoeae* Δ*str* strain generated herein will be subject to further phenotypic characterisation studies to assess the importance of thiosulfate assimilation during the pathogenicity of *N. gonorrhoeae* to further support our proposed pathway.

Despite extensive efforts, crystallisation attempts of Str (isolated or bound with thiosulfate or glutathione) was unsuccessful. Numerous promising crystallisation conditions have been identified for Str bound with cysteine that warrant refinement to obtain quality crystals. This structure would provide crucial information regarding the interaction of thiols with the Str active site.

To date, there remains large gaps in our knowledge of how pathogens fulfil their sulfur requirements. The energetically favourable pathway of thiosulfate reduction via sulfurtransferase enzymes could be pivotal in advancing our understanding in this field. This thesis offers insight into the versatility and function of sulfurtransferases within *N. gonorrhoeae*, contributing to the limited knowledge of sulfurtransferases in prokaryotes and identifying a viable physiological function that is feasibly applicable to pathogens beyond *N. gonorrhoeae*, given that sulfurtransferase are ubiquitously encountered and exogenous inorganic thiosulfate is an abundant source of sulfur for pathogens during infection.

Appendices

Appendix A: Protein information

NGFG_00156 Str

MDIVQLPSAALKAWMDEGRMFCLLDVRTDEEAAVCSLPNALHIPMNLIP
LRQNELPDDVPLVVYCHHGIRSLHTAMYLAEAGFENLYNLQGGIDAWAV
EV DAEMARY*

Amino acids: 107
Molecular weight: 11.99 kDa
Isoelectric point: 4.24

NGFG_00156 Str + N-terminal His-Tag

MGSSHHHHHHSSGLVPRGSHMMDIVQLPSAALKAWMDEGRMFCLLDVR
TDEEAAVCSLPNALHIPMNLIPLRQNELPDDVPLVVYCHHGIRSLHTAMY
LAEAGFENLYNLQGGIDAWAVEVDAEMARY*

Amino acids: 128
Molecular weight: 14.29 kDa
Isoelectric point: 5.9

NGFG_00520 PspE

MNIKQLITAALIASAAFATQAAPQKPVSAAQTAQHSAVWIDVRSEQEFSE
GHLHNAVNIPVDQIVRRIYEAAPDKDTPVNLYCRSGRRAEAALQELKKAG
YTNVANHGGYEDLLKKGMK*

Amino acids: 119
Molecular weight: 12.96 kDa
Isoelectric point: 9.06

NGFG_00520 PspE + N-terminal His-tag

MGSSHHHHHHSSGLVPRGSHMMNIKQLITAALIASAAFATQAAPQKPVSA
AQTAQHSAVWIDVRSEQEFSEGHLHNAVNIPVDQIVRRIYEAAPDKDTPV
NLYCRSGRRAEAALQELKKAGYTNVANHGGYEDLLKKGMK*

Amino acids: 140
Molecular weight: 15.279 kDa
Isoelectric point: 9.51

Appendix B: Protein purification and kinetic data

B.1. Recipes for protein expression and purification

LB Broth

5 g Peptone

10 g NaCl

5 g Yeast extract

1 L of Distilled water

Tris-glycine SDS buffer

25 mM Tris (pH8.5)

250 mM glycine

0.1% SDS (w/v)

B.2. Standard curve used to determine thiocyanate concentration

Absorbance (460 nm) readings were taken for thiocyanate concentrations 0.01, 0.05, 0.1, 0.5, 1 and 2 mM

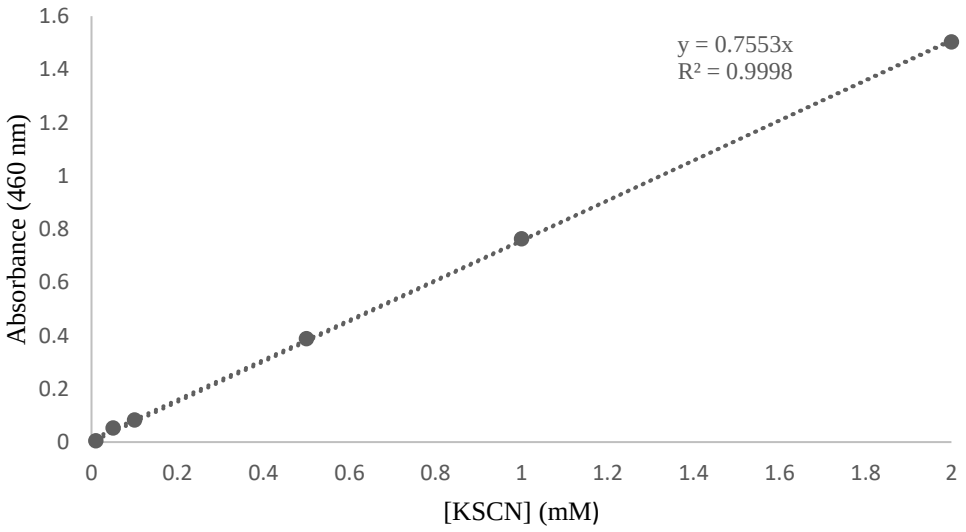

Appendix C: Construct and characterisation of *N. gonorrhoeae* MS11 WT and Δ*str*

C.1. Chemically defined growth medium

Component	Concentration in stock solution ($mg.ml^{-1}$)	Volume of stock solution (ml)	Volume of stock solution (ml) for 1L	pH
Stock Solution 1			**100**	7.3
L-Aspartic Acid	5			
L-Glutamic Acid	13			
NaCl	58			
K2SO4	10			
$MgCl_2.6H_2O$	4.1			
NH_4Cl	2.2			
Ethylenediamine-tetraacetate (EDTA)	0.037			
MQ H_2O		100		
Stock Solution 2a			**10**	
L-Arginine hydrochloride	15			
Glycine	2.5			
L-Serine	5			
MQ H_2O		10		
Stock Solution 2b			**10**	
L-Leucine	9			
L-Isoleucine	3			
L-Vaine	6			
MQ H_2O		9.5		
L-Tyrosine (dissolved in HCl)	10	0.5		
Stock Solution 3			**5**	7.4
Sodium Lactate	50			
Glycerin	184			
Polyvinyl Alcohol	1			
Tween 80, 0.5% (vol/vol)				
Uracil (dissolved in 0.1 $_N$ NaOH)	2	0.5		
Hypoxanthine (dissolved in HCl)	0.8	0.5		
MQ H_2O		4		
Stock Solution 5			**200**	
K_2HPO4	17.4			

KH_2PO4	13.6		
MQ H_2O		200	
L-Cysteine.HCL.H_2O (dissolved in HCL)	17.5		
L-Cystine (Dissolved in HCL)	12		
Oxalacetic Acid	2		**100**
Stock Solution 8			**10**
L-Alanine	10		
L-Lysine.HCl	5		
L-Proline	5		
L-Tryptophan	8		
L-Threonine	5		
MQ H_2O			
Solution 9			**5**
L-Phenylalanine	5		
L-Asparagine.H_2O	5		
MQ H_2O		5	
L-Glutamine	10		**5**
L-Hisidine	7.76		**2**
L-Methionine	14.9		**1**
Glutathione (reduced)	15.36		**3**
Spermine	10.117		**5**
$NaHCO_3$	84		**0.5**
Glucose	200		**25**
Sodium acetate ($NaC_2H_2O.3H_2O$)	340		**10**
Solution 6			**2**
Hemin	1		
L-Histidine	1		
2,2',2"-Nitrilotri-ethanol, 4% (vol/vol)			
Solution 7			**0.2**
Nicotinamide adenine dinucleotide	10		
Thiamine hydrochloride	10		
Calcium pantothenate	10		
MQ H_2O		0.2	
Solution 10			**0.2**
Choline chloride	7		
Myo-Inositol	1.8		
MQ H_2O		0.2	
Biotin	Saturated		**1**
Thiamine pyrophosphate	4.25		**0.1**
MQ H_2O			**500**
$CaCl_2.2H_2O$	37		**1**

$Fe(NO_3)3.9H_2O$	4	**1**

C.2. Primer sequences

For amplification of DNA construct for transformation:

Str KO 5’ PCR primer FWD Sequence: TCGGATTGTGATGCC

Name: Str KO 3’ PCR primer REV Sequence: AGGGAATTGGGGTGC

For colony PCR:

Str KO 5’ primer FWD Sequence: TTTTTGATGTTCGGATTGTGA

Str KO 3’ primer REVSequence: CGGGGCGAGGGAATTG

For sequencing:

strKO seq FWD Sequence (5’ to 3’): GGCGATGTGTTTGAAGAG

strKO seq REV Sequence (5’ to 3’): CACATTGAAAATGCCGCCCA

KanR FWD seq Sequence (5’ to 3’): TTGTCACTGAAGCGGGAAGG

KanR REV Seq Sequence (5’ to 3’): CCTTCCCGCTTCAGTGACAA

References

Adams, H., Teertstra, W., Koster, M., & Tommassen, J. (2002). PspE (phage-shock protein E) of Escherichia coli is a rhodanese. *FEBS Letters*, *518*(1–3), 173–176. https://doi.org/10.1016/S0014-5793(02)02695-9

Adamson, P. C., & Klausner, J. D. (2021). The Staying Power of Pharyngeal Gonorrhea: Implications for Public Health and Antimicrobial Resistance. *Clinical Infectious Diseases*, *9239*(Xx), 1–3. https://doi.org/10.1093/cid/ciab074

Aird, B. A., Heinrikson, R. L., & Westley, J. (1987). Isolation and characterization of a prokaryotic sulfurtransferase. *Journal of Biological Chemistry*, *262*(36), 17327–17335. https://doi.org/10.1016/s0021-9258(18)45381-1

Alkhuder, K., Meibom, K. L., Dubail, I., Dupuis, M., & Charbit, A. (2009). Glutathione provides a source of cysteine essential for intracellular multiplication of Francisella tularensis. *PLoS Pathogens*, *5*(1). https://doi.org/10.1371/journal.ppat.1000284

Bauer, M., & Papenbrock, J. (2002). Identification and characterization of single-domain thiosulfate sulfurtransferases from Arabidopsis thaliana. *FEBS Letters*, *532*(3), 427–431. https://doi.org/10.1016/S0014-5793(02)03723-7

Benoni, R., Pertinhez, T. A., Spyrakis, F., Davalli, S., Pellegrino, S., Paredi, G., … Mozzarelli, A. (2016). Structural insight into the interaction of O-acetylserine sulfhydrylase with competitive, peptidic inhibitors by saturation transfer difference-NMR. *FEBS Letters*, *590*(7), 943–953. https://doi.org/10.1002/1873-3468.12126

Brissette, J. L., Russel, M., Weiner, L., & Model, P. (1990). Phage shock protein, a stress protein of Escherichia coli (filamentous phage/heat shock protein/o32-independent transcription/membrane protein/Psp protein). *Proc. Nati. Acad. Sci. USA*, *87*(February), 862–866. Retrieved from https://www.pnas.org/content/pnas/87/3/862.full.pdf

Brissette, J. L., Weiner, L., Ripmaster, T. L., & Model, P. (1991). Characterization and sequence of the Escherichia coli stress-induced psp operon. *Journal of Molecular Biology*, *220*(1), 35–48. https://doi.org/10.1016/0022-2836(91)90379-K

Bulut, H., Moniot, S., Licht, A., Scheffel, F., Gathmann, S., Saenger, W., & Schneider, E. (2012). Crystal structures of two solute receptors for l-cystine and l-cysteine, respectively, of the human pathogen Neisseria gonorrhoeae. *Journal of Molecular Biology*, *415*(3), 560–572. https://doi.org/10.1016/j.jmb.2011.11.030

Campanini, B., Pieroni, M., Raboni, S., Bettati, S., Benoni, R., Pecchini, C., … Mozzarelli, A. (2015). Inhibitors of the Sulfur Assimilation Pathway in

Bacterial Pathogens as Enhancers of Antibiotic Therapy. *Current Medicinal Chemistry*, *22*, 187–213.

Chauncey, T. R., & Westley, J. (1983). The catalytic mechanism of yeast thiosulfate reductase. *Journal of Biological Chemistry*, *258*(24), 15037–15045.

Chen, Z., Zhang, X., Li, H., Liu, H., Xia, Y., & Xun, L. (2018). The complete pathway for thiosulfate utilization in Saccharomyces cerevisiae. *Applied and Environmental Microbiology*, *84*(22), 1–15. https://doi.org/10.1128/AEM.01241-18

Cheng, H., Donahue, J. L., Battle, S. E., Ray, W. K., & Larson, T. J. (2008). Biochemical and Genetic Characterization of PspE and GlpE, Two Single domain Sulfurtransferases of Escherichia coli. *The Open Microbiology Journal*, *2*(1), 18–28. https://doi.org/10.2174/1874285800802010018

Chiku, T., Padovani, D., Zhu, W., Singh, S., Vitvitsky, V., & Banerjee, R. (2009). H2S biogenesis by human cystathionine γ-lyase leads to the novel sulfur metabolites lanthionine and homolanthionine and is responsive to the grade of hyperhomocysteinemia. *Journal of Biological Chemistry*, *284*(17), 11601–11612. https://doi.org/10.1074/jbc.M808026200

Cipollone, R., Ascenzi, P., & Visca, P. (2007). Common themes and variations in the rhodanese superfamily. *IUBMB Life*, *59*(2), 51–59. https://doi.org/10.1080/15216540701206859

Cipollone, R., Ascenzi, P., Frangipani, E., & Visca, P. (2006). Cyanide detoxification by recombinant bacterial rhodanese. *Chemosphere*, *63*(6), 942–949. https://doi.org/10.1016/j.chemosphere.2005.09.048

Cipollone, R., Frangipani, E., Tiburzi, F., Imperi, F., Ascenzi, P., & Visca, P. (2007). Involvement of Pseudomonas aeruginosa rhodanese in protection from cyanide toxicity. *Applied and Environmental Microbiology*, *73*(2), 390–398. https://doi.org/10.1128/AEM.02143-06

Cowie, D. B., Bolton, E. T., & Sands, M. K. (1951). Sulfur metabolism in Escherichia coli. II. Competitive utilization of labeled and nonlabeled sulfur compounds. *J Bacteriol*, 62:63-74.

Dillard, J. P. (2011). Genetic Manipulation of Neisseria gonorrhoeae. In *Current Protocols in Microbiology* (Vol. 176). https://doi.org/10.1016/j.physbeh.2017.03.040

Dillard, J. P. (2011). HHS Public Access. In *Current Protocols in Microbiology* (Vol. 176). https://doi.org/10.1016/j.physbeh.2017.03.040

Donadio, S., Shafiee, A., & Hutchinson, C. R. (1989). Disruption of a rhodaneselike gene results in cysteine auxotrophy in Saccharopolyspora erythraea. *Journal*

of Bacteriology, *172*(1), 350–360. https://doi.org/10.1128/jb.172.1.350-360.1990

Dubois, T., Dancer-Thibonnier, M., Monot, M., Hamiot, A., Bouillaut, L., Soutourina, O., … Dupuy, B. (2016). Control of Clostridium difficile physiopathology in response to cysteine availability. *Infection and Immunity*, *84*(8), 2389–2405. https://doi.org/10.1128/IAI.00121-16

Edwards, J. L., & Apicella, M. A. (2004). The molecular mechanisms used by Neisseria gonorrhoeae to initiate infection differ between men and women. *Clinical Microbiology Reviews*, *17*(4), 965–981. https://doi.org/10.1128/CMR.17.4.965-981.2004

El-Benna, J., Hurtado-Nedelec, M., Marzaioli, V., Marie, J. C., Gougerot-Pocidalo, M. A., & Dang, P. M. (2016). Priming of the neutrophil respiratory burst: role in host defense and inflammation. *Immunol Rev, 273*(1), 180-93.

Gasteiger, E., Hoogland, C., Gattiker, A., & Duvaud, S. (2005). Protein Identification and Analysis Tools in the ExPASy Server. In *The Proteomics Protocols Handbook* (pp. 571-607). Totowa, NJ: Humana Press.

Gebhardt, M. J., Gallagher, L. A., Jacobson, R. K., Usacheva, E. A., Peterson, L. R., Zurawski, D. V., & Shuman, H. A. (2015). Joint transcriptional control of virulence and resistance to antibiotic and environmental stress in acinetobacter baumannii. *MBio*, *6*(6). https://doi.org/10.1128/mBio.01660-15

Giltner, C. L., Nguyen, Y., & Burrows, L. L. (2012). Type IV Pilin Proteins: Versatile Molecular Modules. *Microbiology and Molecular Biology Reviews*, *76*(4), 740–772. https://doi.org/10.1128/mmbr.00035-12

Guédon, E., & Martin-Verstraete, I. (2006). Cysteine Metabolism and Its Regulation in Bacteria. *Microbiol. Monogr.* https://doi.org/10.1007/7171

Guédon, E., & Martin-Verstraete, I. (2007). *Cysteine Metabolism and Its Regulation in Bacteria BT - Amino Acid Biosynthesis ~ Pathways, Regulation and Metabolic Engineering*. Retrieved from https://doi.org/10.1007/7171_2006_060

Hartwell, S. K., & Grudpan, K. (2012). Flow-based systems for rapid and high-precision enzyme kinetics studies. *Journal of Analytical Methods in Chemistry*, *1*(1). https://doi.org/10.1155/2012/450716

Hatzios, S. K., & Bertozzi, C. R. (2011). The regulation of sulfur metabolism in mycobacterium tuberculosis. *PLoS Pathogens*, *7*(7), 1–8. https://doi.org/10.1371/journal.ppat.1002036

Henne, M., König, N., Triulzi, T., Baroni, S., Forlani, F., Scheibe, R., & Papenbrock, J. (2015). Sulfurtransferase and thioredoxin specifically interact as demonstrated by bimolecular fluorescence complementation analysis and

biochemical tests. *FEBS Open Bio*, *5*, 832–843. https://doi.org/10.1016/j.fob.2015.10.001

Hicks, J. L., & Mullholland, C. V. (2018). Cysteine biosynthesis in Neisseria species. *Microbiology (United Kingdom)*, *164*(12), 1471–1480. https://doi.org/10.1099/mic.0.000728

Kawano, Y., Onishi, F., Shiroyama, M., Miura, M., Tanaka, N., Oshiro, S., … Ohtsu, I. (2017). Improved fermentative l-cysteine overproduction by enhancing a newly identified thiosulfate assimilation pathway in Escherichia coli. *Applied Microbiology and Biotechnology*, *101*(18), 6879–6889. https://doi.org/10.1007/s00253-017-8420-4

Kawano, Y., Suzuki, K., & Ohtsu, I. (2018). Current understanding of sulfur assimilation metabolism to biosynthesize l-cysteine and recent progress of its fermentative overproduction in microorganisms. *Applied Microbiology and Biotechnology*, *102*(19), 8203–8211. https://doi.org/10.1007/s00253-018-9246-4

Kertesz, M. A., & Wietek, C. (2001). Desulfurization and desulfonation: Applications of sulfur-controlled gene expression in bacteria. *Applied Microbiology and Biotechnology*, *57*(4), 460–466. https://doi.org/10.1007/s002530100800

Kim, J., Senadheera, D. B., Lévesque, C. M., & Cvitkovitch, D. G. (2012). TcyR regulates l-cystine uptake via the TcyABC transporter in Streptococcus mutans. *FEMS Microbiology Letters*, *328*(2), 114–121. https://doi.org/10.1111/j.1574-6968.2011.02492.x

Kirkcaldy, R. D., Weston, E., Sequrado, A., & Hughes, G. (2018). Epidemiology of Gonorrhea: A Global Perspective Robert. *Sex Health*, *16*(5), 401–411. https://doi.org/10.1071/SH19061.Epidemiology

Le Faou, A. (1984). Sulphur nutrition and metabolism in various species of Neisseria. Annales de l'Institut Pasteur / Microbiologie, 135(1, Supplement B), 3-11.

Lensmire, J. M., & Hammer, N. D. (2019). Nutrient sulfur acquisition strategies employed by bacterial pathogens. *Current Opinion in Microbiology*, *47*(Table 1), 52–58. https://doi.org/10.1016/j.mib.2018.11.002

Libiad, M., Motl, N., Akey, D. L., Sakamoto, N., Fearon, E. R., Smith, J. L., & Banerjee, R. (2018). Thiosulfate sulfurtransferase-like domain-containing 1 protein interacts with thioredoxin. *Journal of Biological Chemistry*, *293*(8), 2675–2686. https://doi.org/10.1074/jbc.RA117.000826

Lithgow, J. K., Hayhurst, E. J., Cohen, G., Aharonowitz, Y., & Foster, S. J. (2004). Role of a Cysteine Synthase in Staphylococcus aureus. *Journal of*

Bacteriology, *186*(6), 1579–1590. https://doi.org/10.1128/JB.186.6.1579-1590.2004

Masi, A. T., & Eisenstein, B. I. (1981). Disseminated gonococcal infection (DGI) and gonococcal arthritis (GCA): II. Clinical manifestations, diagnosis, complications, treatment, and prevention. *Seminars in Arthritis and Rheumatism*, *10*(3), 173–197. https://doi.org/10.1016/S0049-0172(81)80002-9

McClure, R., Nudel, K., Massari, P., Tjaden, B., Su, X., Rice, P. A., & Genco, C. A. (2015). The gonococcal transcriptome during infection of the lower genital tract in women. *PLoS ONE*, *10*(8). https://doi.org/10.1371/journal.pone.0133982

McPhillips, T. M., McPhillips, S. E., Chiu, H.-J., Cohen, A. E., Deacon, A. M., Ellis, P. J., Garman, E., Gonzalez, A., Sauter, N. K., Phizackerley, R. P., Soltis, S. M., & Kuhn, P. (2002). Blu-Ice and the Distributed Control System: software for data acquisition and instrument control at macromolecular crystallography beamlines. *Journal of Synchrotron Radiation*, *9*(6), 401-406.

Meza, A. N., Cambui, C. C. N., Moreno, A. C. R., Fessel, M. R., & Balan, A. (2019). Mycobacterium tuberculosis CysA2 is a dual sulfurtransferase with activity against thiosulfate and 3-mercaptopyruvate and interacts with mammalian cells. *Scientific Reports*, *9*(1), 1–13. https://doi.org/10.1038/s41598-019-53069-6

Ministry of Health. (2020). *Gonorrhoea rate in New Zealand*. https://www.esr.cri.nz/our-services/consultancy/public-health/sti/

Motl, N., Skiba, M. A., Kabil, O., Smith, J. L., & Banerjee, R. (2017). Structural and biochemical analyses indicate that a bacterial persulfide dioxygenase-rhodanese fusion protein functions in sulfur assimilation. *Journal of Biological Chemistry*, *292*(34), 14026–14038. https://doi.org/10.1074/jbc.M117.790170

Nagahara, N., Okazaki, T., & Nishino, T. (1995). Cytosolic mercaptopyruvate sulfurtransferase is evolutionarily related to mitochondrial rhodanese: Striking similarity in active site amino acid sequence and the increase in the mercaptopyruvate sulfurtransferase activity of rhodanese by site-directed mutagenesis. *Journal of Biological Chemistry*, *270*(27), 16230–16235. https://doi.org/10.1074/jbc.270.27.16230

Nandi, D. L., & Westley, J. (1998). Reduced thioredoxin as a sulfur-acceptor substrate for rhodanese. *The International Journal of Biochemistry & Cell Biology*, *30*(9), 973–977. Retrieved from http://www.ncbi.nlm.nih.gov/pubmed/9785461

Ostrowski, J., & Kredich, N. M. (1990). In vitro interactions of CysB protein with the cysJIH promoter of Salmonella typhimurium: Inhibitory effects of sulfide.

Journal of Bacteriology, *172*(2), 779–785. https://doi.org/10.1128/jb.172.2.779-785.1990

Palde, P. B., Bhaskar, A., Pedró Rosa, Laura E. Madoux, F., Chase, P., Gupta, V., Spicer, T., … Carroll, K. S. (2016). First-in-Class Inhibitors of Sulfur Metabolism with Bactericidal Activity against Non-Replicating M. tuberculosis. *ACS Chem Biol*, *11*(1), 172–184. https://doi.org/doi:10.1021/acschembio.5b00517

Papenbrock, J., & Schmidt, A. (2000). Characterization of a sulfurtransferase from Arabidopsis thaliana. *European Journal of Biochemistry*, *267*(1), 145–154. https://doi.org/10.1046/j.1432-1327.2000.00980.x

Papenbrock, J., Guretzki, S., & Henne, M. (2011). Latest news about the sulfurtransferase protein family of higher plants. *Amino Acids*, *41*(1), 43–57. https://doi.org/10.1007/s00726-010-0478-6

Pedre, B., & Dick, T. P. (2021). 3-Mercaptopyruvate sulfurtransferase: An enzyme at the crossroads of sulfane sulfur trafficking. *Biological Chemistry*, *402*(3), 223–237. https://doi.org/10.1515/hsz-2020-0249

Pinto, R., Leotta, L., Shanahan, E. R., West, N. P., Leyh, T. S., Britton, W., & Triccas, J. A. (2013). *Host Cell – Induced Components of the Sulfate Assimilation Pathway Are Major Protective Antigens of Mycobacterium tuberculosis*. *207*. https://doi.org/10.1093/infdis/jis751

Ploegman, J. H., Drent, G., Kalk, K. H., Hol, W. G. J., Heinrikson, R. L., Keim, P., … Russell, J. (1978). The covalent and tertiary structure of bovine liver rhodanese. *Nature*, *273*(5658), 124–129. https://doi.org/10.1038/273124a0

Potter, A. J., Trappetti, C., & Paton, J. C. (2012). Streptococcus pneumoniae uses glutathione to defend against oxidative stress and metal ion toxicity. *Journal of Bacteriology*, *194*(22), 6248–6254. https://doi.org/10.1128/JB.01393-12

Quillin, S. J., & Seifert, H. S. (2018). Neisseria gonorrhoeae host adaptation and pathogenesis. *Nature Reviews Microbiology*, *16*(4), 226–240. https://doi.org/10.1038/nrmicro.2017.169

Ray, W. K., Zeng, G., Potters, M. B., Mansuri, A. M., & Larson, T. J. (2000). Characterization of a 12-kilodalton rhodanese encoded by glpE of Escherichia coli and its interaction with thioredoxin. *Journal of Bacteriology*, *182*(8), 2277–2284. https://doi.org/10.1128/JB.182.8.2277-2284.2000

Remmele, C. W., Xian, Y., Albrecht, M., Faulstich, M., Fraunholz, M., Heinrichs, E., … Rudel, T. (2014). Transcriptional landscape and essential genes of Neisseria gonorrhoeae. *Nucleic Acids Research*, *42*(16), 10579–10595. https://doi.org/10.1093/nar/gku762

Ren, X., Eccles, D. A., Greig, G. A., Clapham, J., Wheeler, N. E., Lindgreen, Stinus Gardner, P. P., & MacKichanc, J. K. (2017). *Genomic, Transcriptomic, and Phenotypic Analyses of Neisseria meningitidis Isolates from Disease Patients and Their Household Contacts Xiaoyun*. *2*(6), 1–22.

Rusniok, C., Vallenet, D., Floquet, S., Ewles, H., Mouzé-Soulama, C., Brown, D., … Pelicic, V. (2009). NeMeSys: A biological resource for narrowing the gap between sequence and function in the human pathogen Neisseria meningitidis. *Genome Biology*, *10*(10). https://doi.org/10.1186/gb-2009-10-10-r110

Schnell, R., Sriram, D., & Schneider, G. (2015). Pyridoxal-phosphate dependent mycobacterial cysteine synthases: Structure, mechanism and potential as drug targets. *Biochimica et Biophysica Acta - Proteins and Proteomics*, *1854*(9), 1175–1183. https://doi.org/10.1016/j.bbapap.2014.11.010

Seib, K. L., Wu, H.-J., Kidd, S. P., Apicella, M. A., Jennings, M. P., & McEwan, A. G. (2006). Defenses against Oxidative Stress in Neisseria gonorrhoeae: a System Tailored for a Challenging Environment. *Microbiology and Molecular Biology Reviews*, *70*(2), 344–361. https://doi.org/10.1128/mmbr.00044-05

Semchenko, E. A., Day, C. J., & Seib, K. L. (2017). MetQ of Neisseria gonorrhoeae is a surfaceexpressed antigen that elicits bactericidal and functional blocking antibodies. *Infection and Immunity*, *85*(2), 1–17. https://doi.org/10.1128/IAI.00898-16

Shatalin, K., Shatalina, E., Mironov, A., & Nudler, E. (2011). H2S: A Universal Defense Against Antibiotics in Bacteria. *Science*, *334*(November), 986–991. https://doi.org/10.5040/9780755621101.0007

Shibuya, N., Tanaka, M., Yoshida, M., Ogasawara, Y., Togawa, T., Ishii, K., & Kimura, H. (2009). 3-Mercaptopyruvate sulfurtransferase produces hydrogen sulfide and bound sulfane sulfur in the brain. *Antioxidants and Redox Signaling*, *11*(4), 703–714. https://doi.org/10.1089/ars.2008.2253

Sörbo, B. H., Lagerkvist, U., Pesola, R., Virtanen, A. I., & Sörensen, N. A. (1953). Crystalline Rhodanese. II. The Enzyme Catalyzed Reaction. *Acta Chemica Scandinavica*, Vol. 7, pp. 1137–1145. https://doi.org/10.3891/acta.chem.scand.07-1137

Spallarossa, A., Donahue, J. L., Larson, T. J., Bolognesi, M., & Bordo, D. (2001). Escherichia coli GlpE is a prototype sulfurtransferase for the single-domain rhodanese homology superfamily. *Structure*, *9*(11), 1117–1125. https://doi.org/10.1016/S0969-2126(01)00666-9

Spyrakis, F., Singh, R., Cozzini, P., Campanini, B., Salsi, E., Felici, P., … Mozzarelli, A. (2013). Isozyme-Specific Ligands for O-acetylserine sulfhydrylase, a Novel Antibiotic Target. *PLoS ONE*, *8*(10). https://doi.org/10.1371/journal.pone.0077558

Stenson, T. H., Patton, A. K., & Weiss, A. A. (2003). Reduced glutathione is required for pertussis toxin secretion by Bordetella pertussis. *Infection and Immunity*, *71*(3), 1316–1320. https://doi.org/10.1128/IAI.71.3.1316-1320.2003

Suay-García, B., & Pérez-Gracia, M. T. (2017). Drug-resistant Neisseria gonorrhoeae: latest developments. *European Journal of Clinical Microbiology and Infectious Diseases*, *36*(7), 1065–1071. https://doi.org/10.1007/s10096-017-2931-x

Suzuki, H., Koyanagi, T., Izuka, S., Onishi, A., & Kumagai, H. (2005). The yliA, -B, -C, and -D genes of Escherichia coli K-12 encode a novel glutathione importer with an ATP-binding cassette. *Journal of Bacteriology*, *187*(17), 5861–5867. https://doi.org/10.1128/JB.187.17.5861-5867.2005

Takahashi, H., Hirose, K., & Watanabe, H. (2004). Necessity of Meningococcal γ-Glutamyl Aminopeptidase for Neisseria meningitidis Growth in Rat Cerebrospinal Fluid (CSF) and CSF-Like Medium. *Journal of Bacteriology*, *186*(1), 244–247. https://doi.org/10.1128/JB.186.1.244-247.2004

Toohey, J. I., & Cooper, A. J. L. (2014). Thiosulfoxide (Sulfane) sulfur: New chemistry and new regulatory roles in biology. *Molecules*, *19*(8), 12789–12813. https://doi.org/10.3390/molecules190812789

Vergauwen, B., Elegheert, J., Dansercoer, A., Devreese, B., & Savvides, S. N. (2010). Glutathione import in Haemophilus influenzae Rd is primed by the periplasmic heme-binding protein HbpA. *Proceedings of the National Academy of Sciences of the United States of America*, *107*(30), 13270–13275. https://doi.org/10.1073/pnas.1005198107

Vergauwen, B., Verstraete, K., Senadheera, D. B., Dansercoer, A., Cvitkovitch, D. G., Guédon, E., & Savvides, S. N. (2013). Molecular and structural basis of glutathione import in Gram-positive bacteria via GshT and the cystine ABC importer TcyBC of Streptococcus mutans. *Molecular Microbiology*, *89*(2), 288–303. https://doi.org/10.1111/mmi.12274

Vorwerk, H., Mohr, J., Huber, C., Wensel, O., Schmidt-Hohagen, K., Gripp, E., … Hofreuter, D. (2014). Utilization of host-derived cysteine-containing peptides overcomes the restricted sulphur metabolism of Campylobacter jejuni. *Molecular Microbiology*, *93*(6), 1224–1245. https://doi.org/10.1111/mmi.12732

Walker, C. K., & Sweet, R. L. (2011). Gonorrhea infection in women: Prevalence, effects, screening, and management. *International Journal of Women's Health*, *3*(1), 197–206.

Wallrodt, I., Jelsbak, L., Thorndahl, L., Thomsen, L. E., Lemire, S., & Olsen, J. E. (2013). The Putative Thiosulfate Sulfurtransferases PspE and GlpE Contribute

to Virulence of Salmonella Typhimurium in the Mouse Model of Systemic Disease. *PLoS ONE*, *8*(8). https://doi.org/10.1371/journal.pone.0070829

Wang, Z., Zhang, M., Shi, X., & Xiang, Q. (2017). Purification and Characterization of an ATPase GsiA from Salmonella enterica. *BioMed Research International*, *2017*. https://doi.org/10.1155/2017/3076091

Wesley Catlin, B. (1973). Nutritional profiles of neisseria gonorrhoeae, neisseria meningitidis, and neisseria lactamica in chemically defined media and the use of growth requirements for gonococcal typing. *Journal of Infectious Diseases*, *128*(2), 178–194. https://doi.org/10.1093/infdis/128.2.178

Westley, J., Adler, H., Westley, L., & Nishida, C. (1983). The sulfurtransferases. *Toxicological Sciences*, *3*(5), 377–382. https://doi.org/10.1093/toxsci/3.5.377

Williams, R. A. M., Kelly, S. M., Mottram, J. C., & Coombs, G. H. (2003). 3-Mercaptopyruvate sulfurtransferase of Leishmania contains an unusual C-terminal extension and is involved in thioredoxin and antioxidant metabolism. *Journal of Biological Chemistry*, *278*(3), 1480–1486. https://doi.org/10.1074/jbc.M209395200

Wong, T. P., Shockley, R. K., & Johnston, K. H. (1980). WSJM, a simple chemically defined medium for growth of Neisseria gonorrhoeae. *Journal of Clinical Microbiology*, *11*(4), 363–369. https://doi.org/10.1128/jcm.11.4.363-369.1980

World Health Organization. (2019). *World Health Organization Global adult estimates of chlamydia , gonorrhoea , trichomoniasis and syphilis including maternal and congenital syphilis , 2016 Sexually transmitted infections (STI)*. (March).

Xayarath, B., Marquis, H., Port, G. C., & Freitag, N. E. (2009). Listeria monocytogenes CtaP is a multifunctional cysteine transport-associated protein required for bacterial pathogenesis. *Molecular Microbiology*, *74*(4), 956–973. https://doi.org/10.1111/j.1365-2958.2009.06910.x